Invited Review to Journal of Quaternary Science

Biomarker proxies for reconstructing Quaternary climate and environmental change

(short running title: **Biomarker proxy review**)

Erin L. McClymont*, Helen Mackay*, Mark A. Stevenson, Thale Damm-Johnsen, Eleanor Maedhbh Honan, Claire E. Penny, Yasmin A. Cole

*these authors contributed equally to this work and should be considered joint first authors.

All authors: Department of Geography, Durham University, Durham, DH1 3LE, UK.

Author information required for the submission process:

ORCID IDs: ELM (0000-0003-1562-8768), HM (0000-0002-8705-8330), MAS (0000-0002-8955-0855), TDJ (0000-0003-4836-2775), EMH (0000-0003-4163-1610), CEP (0000-0001-9879-9006), YC (0000-0003-3784-7873)

Emails: erin.mcclymont@durham.ac.uk; helen.mackay@durham.ac.uk; mark.stevenson@durham.ac.uk; thale.damm-johnsen@durham.ac.uk; eleanor.m.honan@durham.ac.uk; claire.e.penny@durham.ac.uk; yasmin.cole@durham.ac.uk

Data availability statement: Only published data and materials are referred to in this manuscript.

Funding statement: Funding support has been provided by the Leverhulme Trust (Research Leadership Award 2019-023, ELM, TDJ, CP) and the European Research Council H2020 (ANTSIE, grant no. 864637, ELM, MS, EMH, YC).

Conflict of interest disclosure: ELM declares membership of the Journal of Quaternary Science Editorial Board. No other conflicts of interest are declared by the authors.

Ethics approval statement: No ethical approvals were requested as this manuscript reviews existing published data.

Patient consent statement: Not applicable.

Permission to reproduce material from other sources: we have applied to the publisher for permission to present the maps we adapted in Figure 5.

Clinical trial registration: not applicable.

Abstract

To reconstruct past environmental changes, a range of indirect or proxy approaches can be applied to Quaternary archives. Here, we review the complementary and novel insights which have been provided by the analysis of chemical fossils (biomarkers). Biomarkers have a biological source that can be highly specific (e.g., produced by a small group of organisms) or more general. We show that biomarkers are able to quantify key climate variables (particularly water and air temperature) and can provide qualitative evidence for changes in hydrology, vegetation, human-environment interactions and biogeochemical cycling. In many settings, biomarker proxies provide the opportunity to simultaneously reconstruct multiple climate or environmental variables, alongside complementary and long-established approaches to palaeo-environmental reconstruction. Multi-proxy studies have provided rich sets of data to explore both the drivers and impacts of palaeo-environmental change. As new biomarker proxies continue to be developed and refined, there is further potential to answer emerging questions for Quaternary science and environmental change.

up to five keywords

biomarkers, Quaternary, proxies, palaeoclimate, palaeoenvironment

1. Introduction

To reconstruct past environmental and climate changes, indirect physical, chemical or biological signals of environmental variables ("proxies") are recovered from a range of archives (e.g., marine and lake sediments, ice cores, speleothems, peatlands). Biomarker proxies are molecular or chemical fossils with a biological origin (Eglinton and Calvin, 1967), which can be recovered, analysed and identified from palaeo-environmental archives (Peters et al., 2005). Biomarkers have emerged as valuable parts of the Quaternary science toolkit, due to both quantitative and qualitative insights into past environmental changes and because multiple biomarkers (and thus multiple environmental signals) are simultaneously recovered from single samples.

Biomarkers can either be very specific in terms of their environmental signal or biological source (e.g., individual highly branched isoprenoids indicative of sea-ice diatoms), or be more general indicators (e.g., mixtures of *n*-alkanes derived from higher plants) (Figure 1). A key strength of biomarker analysis is that biomarkers from multiple settings can be found in a single sediment sequence, since terrestrial biomarkers (from bedrock, soils or plants) may be transported by wind, rivers or ice into lakes, wetlands, caves or marine environments, allowing both the transport process and changes in different environments to be explored (e.g., Jaffé et al., 2001; Ngugi et al., 2017; Müller et al., 2018). Biomarker transport can also be a disadvantage: advection or bioturbation may influence how biomarkers are incorporated into the sediments and can even lead to age-offsets between different proxies (e.g., Ohkouchi et al., 2002). As organic molecules, biomarkers are subject to degradation processes during transport and deposition (e.g., Madureira et al., 1997; Wakeham et al., 1997; Thomas et al., 2021). However, different classes of organic compounds have varying rates of degradation (Arndt et al., 2013). Some of the most widely applied biomarkers are those which are relatively resistant to alteration (e.g., plant waxes), or where (rapid) transformation of lipids or pigments found in living biomass leaves behind a recognisable chemical signal so that the source organisms or formation processes can be determined (e.g., Harris et al., 1996; Pitcher et al., 2009). Biomarkers may be particularly useful in environments where other proxies (e.g., plant macrofossils) are degraded but their chemical remains can be found (e.g., Ronkainen et al., 2015).

A valuable property of biomarkers is that they can be isolated from the original archive so that isotope analysis can be undertaken on individual components of organic matter with a known origin. This "compound-specific isotope analysis" (CSIA) contrasts with the analysis of bulk samples, where changing isotope ratios could reflect varying contributions of different organic sources through time or space, as well as environmental controls over the contributing isotopic signals (e.g., Holtvoeth et al., 2019; McClymont et al., 2022). By knowing the origin of the biomarker, the relative impact of biological and environmental controls on stable isotope ratios can be determined (Sachse et al., 2012; Holtvoeth et al., 2019). CSIA has enabled, for example, separation of the contributions of C_3 and C_4 plants and isolation of hydrological controls over plant wax deuterium/hydrogen isotopes (Section 4.2).

Our aim in this review is to provide an accessible introduction to the wide range of biomarker applications in Quaternary science. Detailed reviews are also available on both biomarker synthesis and proxy development in marine sediments (Rosell-Melé and McClymont, 2008), lake sediments (Castañeda and Schouten, 2011), peatlands (Naafs et al., 2019), speleothems (Blyth et al., 2016; Meckler et al., 2021) and geoarchaeology (Dubois and Jacob, 2016). Here, we explore a range of studies which have applied biomarker proxies and outline the novel and complementary contributions biomarkers have made to palaeoenvironmental reconstructions across a wide range of geographical regions, timescales, and environments. The review was conducted using methodical keyword literature searches of the Web of Science and Google Scholar

databases. The searches returned thousands of results; therefore, the scope of this review precludes citations of all relevant studies. To address our aim of providing an accessible overview of biomarkers and their applications for all Quaternary scientists, we have prioritised the inclusion of initial foundation studies alongside a diversity of examples that span across different timescales, sedimentary archives, geographical locations, and topics of Quaternary science. Since some biomarker proxies have been applied to multiple archives but reconstruct similar environmental variables (e.g. temperature, salinity), the review is structured according to those variables or research questions, and archive- or proxy-specific considerations are provided. Finally, we reflect on recent developments in biomarker research and consider their future potential in Quaternary science.

2. Introduction to biomarkers: analysis and functions

2.1 An overview of biomarker laboratory methods

Biomarkers used in Quaternary studies include water-insoluble lipids, photosynthetic pigments, and macromolecules including lignin. Biomarkers are often present in very low (trace) concentrations in environmental samples (mg or ng per g of material) and may be components of a complex matrix of organic and minerogenic materials. Isolating the biomarkers of interest requires methods that maximise recovery and minimise contamination. As multiple biomarkers are recovered simultaneously a diverse range of environmental signals can be attained from a single sample.

Lipids and pigments are extracted from environmental or archaeological samples by using a range of organic solvents and approaches, tailored to the chemical properties of the compound(s) of interest. Ultra-sonication, microwave or accelerated solvent extraction methods are most commonly used but may have different efficiencies depending on sample size and composition (e.g. Kornilova and Rosell-Melé, 2003; Nichols, 2010; Kehelpannala et al., 2020; Manley et al., 2020). Lipid biomarkers are typically extracted with dichloromethane and methanol in a ratio aligned with the expected polarity of the target marker, whereas pigments are typically extracted using acetone (e.g. Chen et al., 2001) or a mixture of acetone, methanol and water (Leavitt and Hodgson, 2001). Pigment extractions can include soaking overnight at cold temperatures (e.g. −20°C) to minimise degradation (Jeffrey et al., 1997).

Care is needed, because organic solvents will also extract unwanted compounds and add them to the extract, particularly plasticisers but also oils from the skin/hair of researchers handling the materials (e.g. Blyth et al., 2006). As a result, sub-sampling cores or materials using metal spatulas, storing samples and extracts in glass jars or high-quality (low contaminant) bags, and using foil to separate samples from plastic bags or lids are effective strategies for minimising contamination, alongside using laboratory personal protective equipment (e.g. Nichols, 2010). Inclusion of blanks during sample processing allows for contamination to be detected, monitored and isolated (Blyth et al., 2016). Water can also interfere with lipid extraction efficiency and subsequent clean-up steps, and encourages oxidative degradation; the best approach is to freeze-dry samples (McClymont et al., 2007; Nichols, 2010).

A common approach in palaeo-environmental research is to recover multiple lipid biomarkers in a single extraction procedure to generate an “extract” (Kornilova and Rosell-Melé, 2003; Nichols, 2010). The extract may then be separated into classes of compounds according to their chemistry (e.g. polarity, pH) to isolate the target biomarkers or to remove interfering compounds (Nichols, 2010). Biomarkers are then analysed using liquid (LC) or gas chromatography (GC), whereby a prepared sample is introduced to a capillary column and transferred to a detector by a flow of liquid or gas (Peters et al. 2005). Non-extractable material (e.g., lignins) can be introduced by

158 pyrolysis, whereby high temperatures are used to split the large, refractory, molecules
159 into diagnostic fragments (White et al., 2004). The capillary column (usually 0.20-0.25
160 mm internal diameter) is coated with an internal film called the stationary phase, the
161 chemistry of which determines how compounds are retained and released according to
162 their chemical properties as they travel through the column. The result is a
163 chromatogram of individual compounds separated by their chemical interaction with
164 the column (Figure 2).

165 Biomarker identification usually involves the separated individual compounds being
166 transferred directly to a mass spectrometer (LC-MS, GC-MS), which ionises and
167 fragments them into characteristic patterns (Peters et al., 2005). Semi-quantitative
168 analysis can be achieved by adding internal standards of known mass during the
169 extraction steps, or a calibration curve will be derived using external standards of
170 varying concentrations to enable absolute quantification (e.g., McGowan 2013).
171 However, some analysis remains qualitative where internal standards are not feasible
172 (e.g., McClymont et al., 2011). Ratios between different compounds may be more
173 appropriate for characterising changing biomarker distributions; for several biomarkers
174 these ratios are defined as indices which are specifically linked to, or calibrated
175 against, environmental variables (Tables 1 and 2).

176 Finally, the separation of organic matter also allows for CSIA. Not all samples or
177 compounds are suitable: individual biomarkers need to meet higher detection limits
178 than for GC or LC, and there needs to be excellent baseline separation between
179 peaks. For compound-specific ^{14}C analysis, GC or LC techniques can be used to
180 separate and then collect individual compounds or classes of compounds for
181 subsequent analysis (Eglinton et al., 1996; Yamane et al., 2014; Sun et al., 2020).

182

183 ***2.2 Biological functions of biomarkers***

184 In this section we have selected examples to introduce the biological function of
185 biomarkers and the mechanistic principles behind their palaeoenvironmental proxy
186 applications. The biological function of biomarkers varies between different classes of
187 compounds (Peters et al., 2005; Bianchi and Canuel, 2011; Killops and Killops, 2013).
188 Most lipid biomarkers used within Quaternary research can be classified as leaf wax or
189 cell membrane lipids. Leaf wax lipids, such as such as *n*-alkanoic acids and *n*-alkanes,
190 are synthesised by vegetation to act as waterproof protective barriers against the
191 external environment and to control evaporative water loss and gas exchange
192 (Eglinton and Hamilton, 1967; Post-Beittenmiller, 1996; Jetter et al., 2006). The chain
193 length of leaf wax molecules varies between different plant species and hydrological
194 conditions: aquatic (terrestrial) species are characterised by shorter (longer) chain
195 lengths since they are adapted to wetter (drier) conditions (Cranwell et al., 1987;
196 Ficken et al., 2000; Schefuß et al., 2003; Table 2). Biochemical responses to
197 environmental conditions can occur at fine scales, which should be considered during
198 interpretation of the sedimentary record. For example, *n*-alkane chain lengths
199 (Ronkainen et al., 2013) or concentrations (Huang et al., 2011) have been shown to
200 differ between the leaves and roots of wetland species (Ronkainen et al., 2013;
201 Andersson et al., 2011), and both humidity and timing of leaf growth can impact *n*-
202 alkane distributions even within single plants (e.g., Sachse et al., 2010; Eley and Hren,
203 2018). There is also evidence for loss and transformation of some *n*-alkyl components
204 within soils, although the dominant chain lengths tend to be maintained with depth
205 (Thomas et al., 2021).

206 Cell membrane lipids are synthesized by a range of organisms including fungi, algae,
207 plants and animals (e.g., sterols (e.g. Volkman, 1986), archaea (e.g., isoprenoidal
208 glycerol dialkyl glycerol tetraethers (isoGDGTS) (e.g. Nishihara and Koga, 1987,
209 Sinninghe Damsté et al., 2000) and eubacteria (e.g., hopanoids (e.g. Innes et al. 1997;

Ourisson et al. 1979). Membrane lipids are structural components of cells that provide a stable controlled environment for biogeochemical reactions. Cell membrane lipids regulate the fluidity (or permeability) of the cell membrane by altering structural features such as chain lengths, the placement of unsaturated (double) bonds and cyclic rings (Peters et al., 2005; Bianchi and Canuel; 2011; Killops and Killops, 2013; Figure 3). For example, temperature changes are expressed by the number and position of methyl groups of branched GDGTs (brGDGTs; Weijers et al., 2007) and the number of cyclopentane moieties of isoGDGTs (De Rosa et al., 1980) (Figure 3; Section 3).

The primary functions of some lipids remain unknown or poorly understand. For example, alkenones, synthesised by phytoplankton (Theroux et al., 2010), were originally considered to be fluidity-influencing membrane lipids (e.g., Brassell et al., 1986); however, more recent studies demonstrate that they more likely contribute to energy storage and regulate properties such as melting point and therefore ease of lipid catabolism (e.g., Epstein et al., 2001; Bakku et al., 2018). Regardless of their specific function, differences in alkenone chain lengths and the degree of unsaturation (number of double bonds) can be used to reconstruct palaeotemperature (e.g., Brassell et al., 1986; Figure 3; Section 3.1). Some other types of biomarkers of interest to Quaternary scientists are transformation products that reflect environmental processes. For example, some polyaromatic hydrocarbons (PAHs) and monosaccharide anhydrides are produced during combustion of organic matter and can therefore be used to reconstruct fire histories (Section 8.2).

Pigments can be relatively general biomarkers of photosynthetic processes (e.g. chlorophyll a/b/c and ββ-carotene are general productivity markers) or highly specific (e.g. alloxanthin is only found in cryptophytes; reviewed by McGowan, 2007). Pigment functions also vary: chlorophylls are active sites of photosynthesis, providing energy for the cell, whereas carotenoids can also help absorb light for photosynthesis (Jeffrey et al., 1997) or help protect cells from UV exposure (e.g. scytonemin; McGowan, 2007). The stability of pigments is dependent on specific chemistry, the environment and presence of photoprotection (Leavitt, 1993; Cuddington and Leavitt, 1999). Some pigments are susceptible to oxidative or UV degradation, and even in environments with good preservation there can be as much as 95% degradation in the water column before sedimentation (McGowan, 2007). Pigment analysis is thus often most effective in environments where preservation is facilitated by e.g., anoxic or low light conditions (e.g. Hodgson et al., 2005). Where degradation allows characteristic fragments of the original pigment to be identified, valuable information can be recovered. For example, chlorins represent the preserved central ring structure of the original chlorophyll and are frequently selected as marine productivity biomarkers over glacial-interglacial timescales (Harris et al., 1996) (Section 7.1).

3. Quantifying amplitudes and rates of past temperature change

Air, water and soil temperatures are important for detailing climate system response to radiative forcing, including global climate sensitivity (Masson-Delmotte et al., 2021). Temperatures trace heat transfers through ocean/atmosphere circulation systems and can be informative of local conditions which may influence ecosystems. Quantification of past temperature change has been a key achievement for biomarker proxies and continues to be a frontier of biomarker proxy development. Here, we first outline insights gained from marine and lacustrine settings, before discussing emerging terrestrial records from soils, peats and speleothems.

3.1 Ocean and lake temperature reconstructions

An early biomarker proxy success was the recognition that some aquatic organisms change their cell membrane chemistry in response to water temperature, and that these signals were detectable in sediments (Brassell et al., 1986; Figure 3). Multiple biomarker temperature proxies have subsequently been developed (Table 1). Biomarker temperature indices describe distributions of lipids produced by selected photosynthesising haptophyte algae (alkenone-derived U^{K}_{37}' and U^{K}_{38Me}' indices; Prahl and Wakeham, 1987; Novak et al., 2022), ammonia-oxidising Thaumarchaeota (isoGDGT-derived TEX_{86} index; Schouten et al., 2022), eustigmatophyte algae (long chain alkyl diol-derived LDI; Rampen et al., 2012) and bacteria (hydroxy fatty acid-derived RAN_{13} index and brGDGT derived MBT'_{5Me} index; De Jonge et al., 2014; Yang et al., 2020). As each proxy has different source organisms and controls (Table 1), there is potential to generate detailed water temperature reconstructions which might include seasonality or temperature profiles with water depth. Both the U^{K}_{37}' and TEX_{86} proxies have reconstructed temperatures through the Quaternary and beyond (e.g., Herbert et al., 2010); more recently developed proxies have tended to focus on the Holocene or the last glacial cycle (e.g. Powers et al., 2005; Warnock et al., 2018; Yang et al., 2020).

Biomarker water temperature proxies are calibrated using field sampling, laboratory culture experiments, and sediment core-tops (Table 1). The accuracy and precision of the temperature proxies varies, especially at the upper and lower ends of the calibrations or close to detection limits, and not all proxies are found in all settings. Many of the proxies are calibrated to mean annual surface water temperature (Table 1), but if the producers have preferred seasons or water depths, a seasonal or sub-surface temperature signal may be reconstructed (D'Andrea et al., 2005, 2011; Jaeschke et al., 2017; Tierney and Tingley, 2018; Inglis and Tierney, 2020; Theroux et al., 2020; Spencer-Jones et al., 2021). Although marine biomarkers have global calibrations (Table 1), there can also be local controls over the biomarker-temperature relationship in all aquatic settings (e.g., salinity, sea/lake ice cover, lake size). In some settings a regional temperature calibration may be more appropriate (Table 1) (e.g., Bendle et al., 2005; De Jonge et al., 2014; D'Andrea et al., 2016; Loomis et al., 2014; Longo et al., 2016; De Bar et al., 2020; Sinninghe Damste et al., 2022; Yao et al., 2022).

A key impact of marine SST biomarker proxies has been the generation of quantitative data to calculate amplitudes and rates of change, climate response to changing CO_2, and to facilitate data-model comparisons (e.g., Brassell et al., 1986; MARGO Project Members, 2005; Martrat et al., 2007; Schmittner et al., 2011; Capron et al., 2017; Tierney et al., 2020). Relatively strong mid- and high-latitude SST responses to glacial-interglacial cycles have been demonstrated (Martrat et al., 2007; Naafs et al., 2013), but tropical cooling has also been reconstructed during glacials (MARGO Project Members, 2005; Herbert et al., 2010; McClymont et al., 2013). U^{K}_{37}' records have shown that there are regional and temporal differences in the amplitudes of interglacial warming (MARGO Project Members, 2005; Past Interglacials Working Group, 2016) and that early ocean cooling preceded the evolution of 100-ka glacial-interglacial cycles during the mid-Pleistocene transition (McClymont et al., 2013). Recent calibration of the U^{K}_{38Me}' index shows potential to extend the upper linear calibration limit of the U^{K}_{37}' proxy to ~30°C (Novak et al., 2022), reducing the reconstructed uncertainties at high SSTs (Table 1) and enabling improved reconstructions of interglacial warmth and glacial-interglacial variability in the low latitudes.

Differences in absolute SSTs from U^{K}_{37}' and TEX_{86} or LDI reconstructions from the same sediment sequences have revealed circulation changes on a range of timescales (Figure 4). In the first TEX_{86} reconstruction spanning the last deglaciation from the South China Sea, SSTs aligned well with millennial-scale variability in Hulu Cave stalagmite $\delta^{18}O$, but exceeded and had a different trend to the U^{K}_{37}'-SSTs, which

may in part be explained by different seasons of production (Shintani et al., 2011). In low-latitude upwelling systems, warmer U^{K}_{37}' (surface) and cooler TEX_{86} (sub-surface) temperatures have enabled reconstructions of varying upwelling intensity spanning millennial to million-year timescales (e.g., McClymont et al., 2012; de Bar et al., 2018; Petrick et al., 2018; Erdem et al., 2021). Glacial-interglacial migrations in the latitude of the Subtropical Front in the southern hemisphere have been determined by combining U^{K}_{37}' and TEX_{86} data (Cartagena-Sierra et al., 2021), and seasonally-driven offsets between U^{K}_{37}', TEX_{86} and LDI temperatures identified variable Leeuwin Current strength offshore South-east Australia over the last ~135 ka (Lopes dos Santos et al., 2013a). Although less widely applied, the LDI has isolated Baltic Sea cooling related to the 8.2 ka event, followed by a Holocene Thermal Maximum, and late Holocene cooling with sea-ice expansion (Warnock et al., 2018). On much shorter timescales, an "Atlantification" of waters in the Fram Strait through the 20th century was detected using U^{K}_{37}' and TEX_{86} (Tesi et al., 2021; Figure 4). Here, a multi-biomarker approach, with 5–10 year resolution, enabled interactions between sea ice, ocean mixing, and heat transfer to be better determined than by using the short instrumental record alone.

Lake temperature reconstructions provide valuable climate indicators for continental climate change. Early TEX_{86} records generated new constraints on temperature change in Africa: a ~2°C increase in Lake Malawi surface water temperature occurred during the last ~100 years which exceeded variability in the preceding ~600 years (Powers et al., 2005); coherence between Lake Victoria warming/cooling and rainfall occurred over the last ~14,000 years (Berke et al., 2012a); and both long-term and abrupt temperature changes in Lake Tanganyika were linked to Indian Ocean SSTs across the last deglaciation (Tierney et al., 2008). However, local or regional influences over the biomarker-temperature relationships include lake size and depth (for TEX_{86}; Sinninghe Damste et al., 2022), salinity or alkalinity (for MBT'$_{5Me}$ and alkenones; Pearson et al., 2008; De Jonge et al., 2014; Song et al., 2016; Plancq et al., 2018), nutrient availability (Toney et al., 2010), and inputs of soils containing the same compounds (e.g., Loomis et al., 2012; De Jonge et al., 2015; Russell et al., 2018). GDGT inputs from methanogens and other archaea can also complicate TEX_{86} reconstructions: at Lake Challa (Africa) reliable temperature reconstructions using lacustrine GDGTs were only possible between 25-13 ka, but not in the Holocene section (Sinninghe Damsté et al., 2012).

The brGDGT proxy MBT'$_{5Me}$ (de Jonge et al., 2014), has been used to reconstruct millennial and centennial scale variations in lake temperature, which align with stadial and interstadial events in the Iberian Peninsula (Rodrigo-Gamiz et al., 2022). Although local conditions prevented application of the MBT'$_{5ME}$ index to an Icelandic lake, the combined analysis of brGDGT distributions and U^{K}_{37}' data enabled quantification of temperature change through the Holocene which could be directly compared to reconstructed and modelled ice cap change (Harning et al., 2020). Having quantified early Holocene warmth, the loss of the local ice cap by ~2050 CE was predicted (Harning et al., 2020). A challenge for brGDGT reconstructions is that the calibration uncertainties (up to ~5 °C; Table 1) are of similar magnitude to some reconstructed Quaternary temperature changes. The application of MBT'$_{5Me}$ can be complex since the full range of specific bacterial sources of brGDGTs is unknown: community sequencing of laboratory cultures, environmental samples and micro- and mesocosm studies have identified Acidobacteria as brGDGT producers; however, they currently do not account for the full distributions of brGDGTs found in sedimentary samples (e.g., Weijers et al., 2010; Sinninghe Damsté et al., 2011, 2018; Martinez-Sosa and Tierney, 2019; De Jonge et al., 2021; Halamka et al., 2023).

The uncertainty surrounding the producer organisms (and whether they have changed through time), as well as limited high-latitude samples in global calibrations (Blaga et

al., 2010; De Jonge et al., 2014; Naafs et al., 2017), complicated the interpretation of Greenland lake data which did not align with other biomarker or macrofossil proxies (Kusch et al., 2019). In the high-latitudes of the southern hemisphere, accounting for distinct brGDGT distributions at low temperatures enabled the production of a regional brGDGT calibration with reduced uncertainties; in turn, millennial-scale temperature changes were identified in an Antarctic lake core spanning the last ~4000 years (Foster et al., 2016). In East Africa, a regional MBT'_{5Me} calibration also reduced temperature reconstruction errors to <2.5 °C (Russell et al., 2018). Regional calibrations may therefore need to be considered where strong environmental impacts on lipid synthesis could occur.

Identification of key alkenone producers in North American, Greenland and Alaska lakes, with a preferred spring signal (e.g., D'Andrea et al., 2005; Toney et al., 2010; Wang et al., 2021a), offers the potential to quantify seasonal lake temperature change in the northern high latitudes. Centennial-scale late Holocene winter-spring lake temperature changes have been quantified in Iceland, showing a strong influence from SSTs (Richter et al., 2021). Holocene lake temperature changes linked to ice shelf configuration were reconstructed in North-east Greenland (Smith et al., 2023). With the recent development and calibration of the 3-hydroxy-fatty acid ratios in lakes (Table 1; e.g., Wang et al., 2021a) there is also the potential for new bacteria-derived temperature proxies to be generated, but downcore applications are not yet available.

In aquatic settings where there are inputs of organic matter from the continents, and where the same biomarkers are found onshore, it is important to assess and correct (or remove) temperature data which may incorporate a mixture of both marine and terrestrial inputs, since the two environments have different biomarker-temperature calibrations (e.g., De Jonge et al., 2015; Russell et al., 2018; Martinez-Sosa et al., 2021). For example, samples with high inputs of terrestrial brGDGTs can be flagged and removed using the BIT index (Branched and Isoprenoid Tetraether index; Table 3 and Hopmans et al., 2004), whereas two separate calibrations may be applied if there is sedimentological evidence for a switch from marine to lake environments (Smith et al., 2023). Where a separation between aquatic and terrestrial lipids can be achieved, it is possible to generate terrestrial temperature records using lake/marine sediments (e.g., Blaga et al., 2010; Watson et al., 2018; see Section 3.2).

Finally, on Quaternary timescales, there is potential for evolution to alter the biomarker-temperature relationship. Although the marine U^{K}_{37}'-SST relationship appears robust to evolutionary events in alkenone producers (McClymont et al., 2005), a long-term (million year) warming in TEX_{86} at Lake El'gygytgyn in the Russian Arctic was influenced by archaeal community changes as landscape evolution influenced biogeochemical cycling (Daniels et al., 2021). On shorter timescales, alkenone temperature indices in saline lakes can be impacted by shifts between the dominant haptophytes (Yao et al., 2022). For example, salinity driven changes in the haptophyte assemblage in Lake Van, Turkey are suggested to have complicated the U^{K}_{37}'-temperature reconstructions for the oldest part of the record (~100-270 ka) (Randlett et al., 2014).

3.2 Temperatures reconstructed from soils, peats and speleothems

The calibration of biomarker proxies for continental temperatures using soils, peats and speleothems has been more challenging than for aquatic settings and remains an active area of development (e.g. Weijers et al., 2007; Naafs et al., 2017; Meckler et al., 2021). Quantified temperature data can provide a valuable backdrop to understand the rich environmental information recovered from the same archives (e.g., vegetation and hydrological change, human activity; see Sections 4 and 8).

418 The (acido)bacteria-produced brGDGTs, found in soils, peats and speleothems, have
419 been explored as temperature proxies given their promise in aquatic settings (Section
420 3.1). The uncertainties in the branched GDGT temperature calibrations for peat
421 (~4.7°C, Naafs et al., 2017) and soils (~4.8°C, De Jonge et al., 2014; Yamamoto et al.,
422 2016) make it difficult to reconstruct small amplitude and potentially brief Holocene
423 temperature fluctuations. In the low latitudes, regional calibrations have been
424 developed which have lower uncertainties (Perez-Angel et al., 2020), and
425 loess/palaeosol sequences have required careful interpretation given unusual brGDGT
426 distributions in semi-arid settings (Yang et al., 2014). Conversion of soil or peat
427 temperatures to overlying air temperatures has also been challenging where there are
428 differences between the two (Dearing Crampton-Flood et al., 2020). Nevertheless, in
429 the Great Lakes region (North America) brGDGT-inferred soil/air temperatures from a
430 lake core aligned with pollen-based temperature reconstructions associated with the
431 Bølling-Allerød (B-A) warming, Younger Dryas cooling and Holocene warming (Watson
432 et al., 2018). Importantly, the brGDGT analysis was able to advance understanding
433 beyond pollen-based interpretations by showing that the multi-centennial lag in
434 warming compared to Northern Hemisphere temperature syntheses was due to the
435 effects of continentality and regional influences of ice-sheet extent rather than a
436 delayed vegetation response (Watson et al., 2018). Where soil-derived biomarkers
437 have been transported to different depositional settings, there can be complexity in the
438 signature if the source regions have changed over time: shifting sediment provenance
439 of brGDGT distributions recovered offshore of the Amazon basin over the last
440 deglaciation impacted the reconstructed absolute air temperature time-series, due to
441 the increasing influence of colder, higher-elevation inputs from the Andes into the
442 Holocene (Bendle et al., 2010).

443 In Asia, both isoprenoidal (TEX_{86}) and branched GDGTs have been used in peat,
444 loess and speleothems to explore the drivers and impacts of shifts in the summer
445 monsoon. In peats, the combination of proxies for temperature and hydrology can be
446 effective in considering their different drivers and the potential for (a)synchrony (e.g.
447 Peterse et al., 2014; Wang et al., 2017). A 130,000 year loess-palaeosol sequence
448 yielded high-resolution brGDGT temperature reconstructions: local insolation was the
449 main driver of temperature change, but temperatures led brGDGT inferred precipitation
450 changes with a lag length which was linked to the intensity of northern hemisphere
451 glaciation (Peterse et al., 2014). Rapid brGDGT temperature changes across the
452 Younger Dryas and ~3.2 ka in Southeast China occurred synchronously with pollen
453 assemblage changes over the last ~30,000 years in a peat sequence, and also
454 showed asynchrony between temperature and precipitation proxies during the last
455 deglaciation (Wang et al., 2017). A 4°C increase in mean annual air temperature was
456 recorded by speleothem-TEX_{86} over the last deglaciation: the warming pre-dated
457 Indian Summer Monsoon strengthening but was closely aligned with SST records
458 (Huguet et al., 2018). A pattern of early Holocene warmth followed by cooling towards
459 the present day has been recorded by brGDGTs in peats (NE China; Zheng et al.,
460 2018) and using the more recently developed fatty acid RAN_{15} index in a Chinese
461 speleothem (Wang et al., 2018; Table 1). Given the challenges of recovering
462 biomarkers from low organic carbon archives, and concerns about the relative
463 influence of cave micro-environments on each record (Blyth et al., 2016; Baker et al.,
464 2019), the recovery of both GDGTs and the C_{15} and C_{17} fatty acids from speleothems
465 shows huge potential for generating new terrestrial records of cave or air temperature
466 (e.g., Li et al., 2011; Blyth et al., 2016; Baker et al., 2019). As speleothems can also
467 yield fatty acid, *n*-alkanol and *n*-alkan-2-one distributions, interpreted to reflect
468 changing soil micro-organism responses to Holocene climate change (Xie et al., 2003;
469 Kalpana et al., 2021), there is further potential to consider ecosystem response to
470 temperature change (see also Section 4.1), especially as analytical developments
471 reduce sample sizes (e.g. Meckler et al., 2021).

4. Reconstructing vegetation and hydrological change

Palaeovegetation and palaeohydrology records provide insights into drivers of climate change that impact precipitation/evaporation and terrestrial ecosystem response. Water availability is essential to the functioning of ecosystems and societies; therefore, long-term hydrological records also provide essential context for understanding changes in habitat and landcover, diets, agricultural practises, settlement dynamics and societal structures through the Quaternary. Different vegetation types have characteristic biomarker distributions and stable isotope ratios reflecting their biosynthetic pathways and biological responses to environmental conditions (Table 2, Section 2.2). When the biological source of the biomarkers is well-constrained, compound-specific isotope analysis (CSIA) has enabled the varying biological and environmental influences over $\delta^{13}C$ and δD to be disentangled. CSIA has thus emerged as a powerful tool for reconstructing both past vegetation change and palaeohydrology (Castañeda and Schouten, 2011; Diefendorf and Freimuth, 2017; Holvoeth et al., 2019; Inglis et al., 2022).

4.1 Reconstructing vegetation using biomarker distributions

Plant-derived lipids were among the first to be characterised (Eglinton and Hamilton, 1967), and remain among the most frequently applied biomarker tools owing to their prevalence in Quaternary sequences, their relative resilience to decay, ease of analysis, and the diversity of environmental information that they contain within their distributions and isotopic compositions. Lignin-derived compounds have also been targeted as relatively well-preserved plant remains (e.g. Castaneda et al., 2009b; reviewed in Jex et al., 2014).

Biomarker vegetation reconstructions commonly use distributions of *n*-alkyl compounds such as *n*-alkanes, *n*-alkanols, *n*-alkanoic acids and wax esters, but may also draw upon sterols, phenols and more specific compounds (defined in Table 2). Biomarker vegetation reconstructions are usually made at the family rather than the species level, so the taxonomic detail is lower than other vegetation proxies (pollen, plant macrofossils, and sedimentary ancient DNA (sedaDNA)). However, the relative resistance of *n*-alkyl compounds to decay has enabled vegetation reconstructions in samples with low levels of macro- and micro-fossil preservation, particularly in wetlands (e.g. McClymont et al., 2008a; Ronkainen et al., 2015). Biomarkers are also considered less susceptible to the long range transport processes that can complicate pollen analyses due to the hydrodynamic properties of the leaves they are derived from (Schwark et al., 2002).

Complexity is introduced where some plants produce *n*-alkane distributions that contain peaks in both longer and shorter chain lengths. For example, some *Sphagnum* species produce a dominant *n*-alkane chain length of C_{23}, but also have elevated C_{31}, which complicates the use of the C_{23}/C_{31} ratio as a *Sphagnum* indicator (e.g., Andersson et al., 2011; Bingham et al., 2010; Bush and McInerney, 2013; Table 2). However, the presence of the sphagnum acid product, 4-isopropenylphenol, may offer a complementary assessment of the relative *Sphagnum* inputs to peat cores (e.g. Boon et al., 1986; McClymont et al., 2011). There may also be a bias caused by variable *n*-alkyl lipid production. For example, some conifer groups (e.g. Pinaceae) produce significantly less *n*-alkanes than broad leaf species, whereas others (e.g. Podocarpaceae) are similar (Diefendorf and Freimuth, 2017). As such, in catchments where pollen analyses indicate conifers as being the dominant vegetation type, biomarker interpretations should be part of a multi-proxy assessment: in northern

Poland, this approach enabled subdecadal shifts in vegetation during the last deglaciation to be determined in detail (Aichner et al., 2018).

As different vegetation types have particular moisture preferences, plant biomarkers have been used to assess palaeohydrology by reconstructing the relative contributions of different vegetation types to sedimentary archives including lake sediments (e.g., Meyers, 2003; Castañeda et al., 2009b), marine sediments (Castañeda et al., 2009a), peats (e.g., Pancost et al., 2002; Ortiz et al., 2010; Zhou et al., 2010), and palaeosols (e.g., Zhang et al., 2006) (Table 2). Concurrent changes in the peatland C_{23}/C_{29} *n*-alkane ratio (*Sphagnum*:vascular plants) and solar irradiance highlighted the sensitivity of northeast American hydroclimate to solar forcing, and its amplification by the Arctic/North Atlantic Oscillation since the mid-Holocene (Nichols and Huang, 2012). A key area of research has been the development of multiple records of vegetation change linked to changes in the Asian monsoon. Peatland aquatic:terrestrial vegetation reconstructions using *n*-alkanes identified Holocene intensification of the Indian Summer Monsoon in the Garwhal Himalyas, and in turn, regional heterogeneity in mid-late Holocene monsoonal conditions in the Indian sub-continent (Bhattacharya et al., 2021). Speleothem reconstructions of changing ecosystem dynamics have also been generated using a diverse suite of compounds, including *n*-alkanes (e.g., Xie et al., 2003; Blyth et al., 2007), sterols (e.g., Rousseau et al., 1995), fatty acids (e.g., Wang et al., 2019a) and lignin phenols (e.g., Blyth and Watson, 2009; Heidke et al., 2019). For example, in a Chinese speleothem, ratios of long-chain *n*-alkanes and *n*-alkan-2-ones (from terrestrial vegetation) to shorter chain compounds (from soil organisms) recorded vegetation changes during the Last Glacial Maximum which could be linked to fluctuations in North Atlantic SSTs during the last deglaciation (Xie et al., 2003). However, biomarker distributions (and other proxies) tend to be used as part of the evaluation of biological and/or environmental controls over compound-specific stable carbon and hydrogen isotope ratios, rather than in isolation (e.g. Castañeda et al., 2009a,b).

4.2 Reconstructing vegetation and hydrological change using compound-specific stable isotope analysis

For higher plant biomarkers, stable carbon isotope analysis ($\delta^{13}C$) of individual lipids provides a powerful tool to reconstruct past vegetation changes, because different photosynthetic pathways can be distinguished by their impact on plant tissue $\delta^{13}C$ (Liu et al., 2022). Thus, *n*-alkane $\delta^{13}C$ from trees and shrubs using the C_3 (Calvin-Benson) pathway is on average >10 ppm lower than in *n*-alkane $\delta^{13}C$ from plants using the C_4 (Hatch-Slack) pathway, which are mainly tropical grasses (Castañeda et al., 2009a). A range of additional factors impact fractionation which may need to be considered in interpreting $\delta^{13}C$ records. including moisture availability (for C_3 plants), ecological or physiological changes and past $^{13}CO_2$ values (Diefendorf and Freimuth, 2016). A common nomenclature when presenting stable isotope ratios of individual lipids is $\delta^{13}C_{lipid}$, where "lipid" is the chain-length or the name of the lipid which has been analysed.

The long-term reliability of the leaf wax $\delta^{13}C$ vegetation proxy has been demonstrated through comparisons with pollen records since the late Pleistocene (e.g., Tierney et al., 2010; Huang et al., 2006). Mixing models have successfully used $\delta^{13}C$ differences to reconstruct shifts in the relative abundance of C_3 and C_4 with the caveat that bias may also be introduced by variable *n*-alkyl lipid production (Section 4.1; Garcin et al., 2014). In tropical Africa, $\delta^{13}C_{lipid}$ records have reconstructed variable trees/shrubs (C_3) and grasses (C_4) extending back to the early Pleistocene from both lake and marine sediments (e.g., Castañeda et al., 2007; Schefuß et al., 2003). In Lake Challa, Africa, $\delta^{13}C$ analysis of the C_{31} *n*-alkane ($\delta^{13}C_{31}$) reconstructed a vegetation transition from C_4-

574 dominated plants during the glacial period to a mix of C_3/C_4 plants ~16.5 cal. ka BP,
575 which persisted during the Holocene and reflected the combined influences of
576 increasing atmospheric CO_2 concentrations and increasing monsoon rainfall
577 (Sinninghe Damsté et al., 2011). *N*-alkane, *n*-alkanol and $\delta^{13}C_{31}$ have recorded glacial-
578 interglacial switches between steppe vegetation (C_3) and warm season grasses (C_4) at
579 the Chinese loess plateau over the last 170 ka (Zhang et al., 2006). In Olduvai Gorge,
580 orbitally-paced $\delta^{13}C_{31}$ variations demonstrated rapid and large shifts between closed
581 C_3 woodlands and more open C_4 grasslands ~1.9 Ma, challenging previous
582 reconstructions of relatively stable ecosystems in the early Pleistocene (Magill et al.,
583 2013). The ecosystem variations were likely linked to SST oscillations and monsoon
584 strength, and provide a backdrop for the emergence and dispersal of *Homo* (Magill et
585 al., 2013), as also suggested for more recent hominid migrations (e.g. Castaneda et
586 al., 2009a).

587 By comparing *n*-alkane flux and $\delta^{13}C$ signals across multiple glacial-interglacial
588 timescales offshore of the Angola Basin, a decoupling between enhanced dust
589 deposition ~900 ka and orbital variability in $\delta^{13}C_{31}$ revealed the different impacts of
590 trade wind response to northern hemisphere ice-sheet growth (driving dust) and
591 vegetation responses to regional SST changes (Schefuß et al., 2003). Lignin phenol
592 and *n*-alkane distributions alongside *n*-alkane $\delta^{13}C$ spanning the last 23 ka in Lake
593 Malawi reconstructed millennial-scale variability in vegetation linked to wet conditions
594 in Southeast Africa, and a dominance of higher plant signals in bulk $\delta^{13}C$ was
595 confirmed (Castaneda et al., 2009b). However, caution is required where there may be
596 mixed aquatic/terrestrial or local/regional inputs in the same archive: contributions of
597 aquatic C_{27} and C_{29} *n*-alkanes to a lake sediment resulted in different $\delta^{13}C$ variations
598 compared to the terrestrial leaf wax $\delta^{13}C_{31}$ in the same core (Liu et al., 2015); varying
599 inputs of local and more widely-sourced leaf waxes to an estuarine sequence were
600 identified by different $\delta^{13}C$ signals recorded depending upon the *n*-alkane chain length
601 (Carr et al., 2015).

602 A powerful and direct proxy measurement of hydroclimate comes from $\delta^{2}H$ signatures
603 of lipids derived from plants and algae, which track the $\delta^{2}H$ of their environmental
604 water sources (reviewed by Sachse et al., 2012). D/H fractionation of meteoric water is
605 influenced by temperature, precipitation source and amount, elevation and distance
606 from the ocean, which results in a distinctive geographical pattern of lower $\delta^{2}H_{precipitation}$
607 at increasing latitude (e.g., Craig and Gordon, 1965; Bowen and Revenaugh, 2003).
608 Several environmental and biological processes contribute to further D/H fractionation
609 between the source water and the lipids and can complicate the interpretation of
610 palaeohydrological $\delta^{2}H_{lipid}$ signatures (Sachse et al., 2012; Sessions, 2016; Huang and
611 Meyers, 2018): higher plant $\delta^{2}H_{lipid}$ are influenced by factors such as humidity,
612 evapotranspiration rates, light, vegetation assemblage and plant physiological
613 differences (e.g., Smith and Freeman, 2006; Hou et al., 2008; Liu and Yang, 2008;
614 Yang et al., 2009; Kahmen et al., 2013), whilst algal $\delta^{2}H_{lipid}$ are influenced by metabolic
615 processes, growth rate and phase, nutrients and temperature (e.g., Schouten et al.,
616 2006; Sachse and Sachs, 2008; Wolhow et al., 2009; Zhang et al., 2009). Salinity also
617 influences D/H fractionation of both plant and algal lipids, facilitating the application of
618 $\delta^{2}H_{lipid}$ as a palaeosalinity proxy (discussed in Section 5).

619 Palaeohydrological $\delta^{2}H_{lipid}$ reconstructions developed from terrestrial and marine
620 sediment archives (e.g., Sauer et al., 2001; Xie et al., 2000; Huang et al., 2004;
621 Schefuß et al., 2005) have provided insight into diverse aspects of the Quaternary
622 climate system and its impacts on palaeohydrology. Applications have included
623 reconstructions of changes in the ITCZ and ENSO (e.g., Atwood and Sachs, 2014;
624 Massa et al., 2021), the South Pacific Convergence Zone (e.g., Maloney et al., 2022),
625 the Southern Annular Mode (e.g., van der Bilt, 2022); monsoonal activity (e.g, Seki et
626 al., 2009; Basu et al., 2019), seismic activity (e.g,, Norström et al., 2018), insolation

627 forcing (e.g., Lupien et al., 2022) and meltwater dynamics (e.g., Aichner et al., 2022).
628 By comparing terrestrial and aquatic *n*-alkane δ^2H signatures, variations in
629 evapotranspiration of lake environments (e.g., Sachse et al., 2004, 2006), climate-
630 driven lake level changes (e.g., Günther et al., 2016; Saini et al., 2017; Aichner et al.,
631 2019) and seasonality of precipitation (e.g., Kjellman et al., 2020; Katrantsiotis et al.,
632 2021) have been determined. Another approach to disentangling the impact of lake
633 water evaporation from precipitation changes is coupling δ^2H and $\delta^{18}O$ reconstructions,
634 as demonstrated using δ^2H of *n*-alkanes and of $\delta^{18}O$ sugar biomarkers to develop a
635 Late Glacial–Holocene palaeohydrological reconstruction from Himalayan Nepal (Hepp
636 et al., 2015). Reconstructed palaeohydrology from δ^2H_{lipid} have also provided climatic
637 contexts for human evolution (as reviewed by Patalano et al., 2021) and human
638 settlements (e.g., Sharifi et al., 2015; Balascio et al., 2020).

639 Care is needed to disentangle changes in *n*-alkane δ^2H that are driven by biological
640 fractionation or vegetation change rather than hydroclimate (e.g., Liu et al., 2006;
641 Wang et al., 2013; Griepentrog et al., 2019). This can be effectively achieved by
642 reconstructing vegetation change using pollen, biomarker distributions, leaf wax $\delta^{13}C$,
643 or sedaDNA. At Meerfelder Maar, western Europe, the influences of vegetation change
644 and hydroclimate were assessed using *n*-alkane distributions, pollen, and *n*-alkane
645 δ^2H, demonstrating that cooler and wetter conditions were established ~2.8 ka BP
646 (Rach et al., 2017). Contrasting late Holocene $\delta^2H_{dinosterol}$ hydroclimate reconstructions
647 from paired lakes in the western tropical Pacific showcases the importance of multi-site
648 and multi-proxy data to distinguish between climate and other limnological drivers of
649 hydrological change (Maloney et al., 2022). By combining *n*-alkane and *n*-acid
650 distributions with *n*-alkane $\delta^{13}C$ and δ^2H, both vegetation ($\delta^{13}C_{31}$ and $\delta^{13}C_{33}$) and
651 precipitation (δ^2H_{C29}) were recorded and could be separated (Wang et al., 2013).
652 Under arid conditions in the Qinling Mountains, China, a strong correlation between
653 altitude and δ^2H_{lipid} (but not $\delta^{13}C_{lipid}$) highlights the potential to reconstruct and evaluate
654 palaeoelevation and its interaction with local hydroclimate (Liu, 2021). These studies
655 demonstrate both the complexity but also the valuable and detailed environmental
656 issue which can be recovered using CSIA.

657 Where temperature and hydroclimate reconstructions are available from the same
658 archive, the synchroneity or links between both larger and smaller-scale climate
659 drivers can be interrogated (e.g., Berke et al., 2014; Tierney et al., 2008; Muñoz et al.,
660 2020; Stockhecke et al., 2021). In Lake Victoria, Africa, coherence between leaf wax
661 δ^2H hydroclimate and GDGT-inferred temperature records (Section 3) provided clear
662 evidence for orbitally forced tropical climate since the Late Pleistocene, and
663 highlighted the role of ENSO-related teleconnections in shaping climatic events such
664 as the Younger Dryas (Figure 5) (Berke et al., 2012b). In Lake Elsinore (California),
665 abrupt changes recorded by leaf wax δ^2H in the late glacial (32-20 ka) were
666 independent of GDGT-inferred temperature shifts and were attributed to changes in
667 storm tracks (Feakins et al., 2019). In a marine sediment core offshore Sumatra, leaf
668 wax δ^2H challenged previous views of increased precipitation over the Indo-Pacific
669 Warm Pool during the Last Glacial Maximum, which was attributed to regional
670 differences in deglacial sea level and coastline configuration (Niedermeyer et al.,
671 2014). In turn, new Holocene oscillations in the Indian Ocean precipitation could be
672 linked to rainfall in East Africa via a “precipitation dipole”, rather than by ENSO
673 (Niedermeyer et al., 2014). These examples are important for demonstrating that we
674 can extend our understanding of the late glacial climate instability beyond ice and
675 ocean dynamics, to include hydroclimate and atmospheric variability, especially in the
676 low latitudes.

677

678 **5. Reconstructing salinity using lake and marine sediments**

679 Palaeosalinity reconstructions in the oceans and in lakes may provide an indication of
680 changes in circulation (e.g. through changing water masses or currents) or
681 hydroclimate (e.g. where enhanced freshwater inputs or increased evaporation can
682 lead to lake salinity changes). In estuarine or coastal settings, salinity variations may
683 also reflect changes in river discharge or the relative contribution of marine and
684 freshwater as influenced by local changes in relative sea level. In this section we
685 outline both biomarker distributions and CSIA which have detailed changes in salinity
686 either in marine (Section 5.1) or lacustrine (Section 5.2) settings.

687

688 ***5.1 Sea-surface salinity as an indicator of circulation or sea-level changes***

689 During the early U^{K}_{37}'-SST calibration work (Section 3.1), a potential salinity or polar
690 water mass influence over the abundance of the haptophyte algae $C_{37:4}$ alkenone was
691 determined (Rosell-Melé, 1998; Bendle et al., 2005), noting that this alkenone is not
692 part of the U^{K}_{37}' index (Table 1). Subsequently, high $C_{37:4}$ values have been used to
693 track expansion of (sub)polar water masses in the Atlantic, Pacific, and Southern
694 Oceans across glacial-interglacial and million-year timescales (McClymont et al.,
695 2008b; Martinez-Garcia et al., 2010). Elevated $C_{37:4}$ alkenone abundances (low
696 salinity) have identified meltwater from Heinrich event icebergs reaching the Iberian
697 Peninsula (Martrat et al., 2007), and glacial meltwater reaching the North-east Pacific
698 (Sanchez-Montes et al., 2020). Although not specific salinity markers, terrestrial-
699 derived biomarkers in the iceberg-rafted debris-rich Heinrich layers (Madureira et al.,
700 1997; Rosell-Mele et al., 1997; van der Meer, 2007) confirmed the release of IRD and
701 meltwater to the North Atlantic Ocean. Alternatively, large inputs of heavily altered
702 carotenoids to southern Greenland, in the absence of IRD, suggested that an outburst
703 flood occurred during the last interglacial (Nicholl et al., 2012).

704 More direct records of sea-surface salinity draw on the impact of changing salinity on
705 D/H fractionation in seawater and during biosynthesis (e.g. Sauer et al., 2001;
706 Englebrecht and Sachs, 2005; Schouten et al., 2006). Cultured haptophyte algae show
707 that $\delta^2H_{alkenone}$ records salinity change (Engelbrecht and Sachs, 2005; Schouten et al.,
708 2006), and may even be used to identify the source regions of alkenones transported
709 to sediment drift sites (Englebrecht and Sachs, 2005). An early application in the
710 eastern tropical Pacific used instrumental records to show that $\delta^2H_{alkenone}$ fluctuations
711 recorded rainfall and river discharge in Columbia, and revealed reduced runoff during
712 the last glacial compared to the Holocene (Pahnke et al., 2007). Combined $\delta^2H_{alkenone}$
713 and dinoflagellate cyst analysis showed substantial freshening of the Black Sea over
714 the last ~3000 years, and refuted a hypothesis that salinity changes were responsible
715 for changes to the haptophyte assemblage (van der Meer et al., 2008). In the South-
716 east Atlantic, a decoupling of SST and salinity across multiple deglaciations has been
717 recognised, whereby salinity ($\delta^2H_{alkenone}$) increased earlier than ocean warming (U^{K}_{37}'
718 index); both changes pre-date the onset of deglaciation and may even play a role in
719 triggering or facilitating ocean circulation change during glacial-interglacial transitions
720 (Kasper et al., 2014; Petrick et al., 2015). In the Mediterranean Sea, $\delta^2H_{alkenone}$
721 confirmed a large drop in surface salinity at the onset of a Last Interglacial sapropel,
722 supporting the hypothesis that these organic-rich layers were the result of precession-
723 driven monsoon rains disrupting the circulation (van der Meer et al., 2007). As for leaf
724 wax δ^2H (Section 4.2), care is needed to assess whether salinity change is the primary
725 signal being recorded by sedimentary δ^2H_{lipid}, since it could also be impacted by factors
726 including variations in growth rate (Wolhowe et al., 2009) and the algal species/genera
727 (Schouten et al., 2006; van der Meer et al., 2008; Nelson and Sachs, 2014).

728 In coastal systems, salinity change can be a reflection of relative sea-level change. A
729 fall in $C_{37:4}$ abundance (increased salinity) was used to identify relative sea-level rise in
730 a Scottish isolation basin following the last deglaciation (Bendle et al., 2009). The

relative contribution of mangrove species biomarkers (e.g., taraxerol) to inter-tidal sediments has also been explored as an alternative indicator of sea-level change (Versteegh et al., 2004; Koch et al., 2011), but local influences on sedimentation patterns and biomarker degradation require further investigation (He et al., 2018; Sefton, 2020). Both *n*-alkane and taraxerol δ^2H in mangrove systems show potential for isolating a biological response to changes in salinity (Ladd and Sachs, 2015). A salinity impact on mangrove water-use efficiency was also indicated by *n*-alkane $\delta^{13}C$ in Australia (Ladd and Sachs, 2013). A challenge in low-latitude settings is to isolate a sea-level driven salinity change from a hydroclimate impact on precipitation or seawater δ^2H (e.g. Pahnke et al., 2007; Tamalavage et al., 2020). However, by combining pollen analysis with plant wax distributions and δ^2H from a mangrove system in the Bahamas, the time-varying influences of changes in vegetation assemblage and precipitation could be disentangled during the Holocene (Tamalavage et al., 2020). Multi-proxy analyses thus show great potential for evaluating the relative influences of vegetation change, hydroclimate, and sea-level driven salinity variability in mangrove environments.

5.2 Lake salinity as an indicator of hydrological change

As observed in the marine environment (Section 5.1), high abundances of the haptophyte-algae $C_{37:4}$ alkenone have been recorded with low salinity in modern calibration studies of saline lakes (Liu et al., 2008, 2011; Song et al., 2016; He et al., 2020) and in comparisons between lake reconstructions and instrumental data (He et al., 2013). Qualitative palaeosalinity reconstructions using $C_{37:4}$ abundance in lake sediments have reconstructed late Holocene moisture fluctuations on the Northern Tibetan Plateau linked to solar irradiance (He et al., 2013), and identified the transition between marine and lake environments associated with ice-shelf expansion in North-east Greenland (Smith et al., 2023). However, not all lakes have recorded the $C_{37:4}$ alkenone (e.g., Toney et al., 2010), and seasonal biases in alkenone production may influence the reconstructions (He et al., 2020). Combined analysis of alkenone distributions and phylogenetic analysis in a suite of saline Chines lakes (Yao et al., 2022) indicates that $C_{37:4}$ alkenone may reflect changing haptophyte groups rather than salinity, since the detected groups occupied different ecological niches. The presence of another salinity-sensitive indicator, the alkenone $C_{38:3Me}$, was detected during times of haptophyte assemblage changes consistent with fresher surface waters in a Pleistocene record from Lake Van, Turkey (Randlett et al., 2014). Palaeosalinity indices, such as the RIK_{37} (ratio of isomeric ketones of C_{37} chain length) $index_{37}$ (ratio of isomeric ketones of C_{37} chain length) index (Longo et al., 2016)), capture salinity-driven shifts in haptophyte species composition and are reliable salinity proxies in oligohaline environments (Longo et al., 2016).

Salinity is also reflected in lake water δ^2H and the biosynthesis of algal lipids: field calibration laboratory culture studies have demonstrated that the salinity is inversely related to the D/H fractionation of algal lipids (e.g., Sessions et al., 1999; Schouten et al., 2006; Sachse and Sachs, 2008; Schwab and Sachs, 2011; Ladd and Sachs, 2012; Nelson and Sachs, 2014; Englebrecht and Sachs, 2015; see Section 4.2 for discussions of other controls on δ^2H_{lipids}). Mid-Holocene changes to the Indian Summer Monsoon have been detected using biomarker δ^2H in a saline-alkaline lake in the core 'monsoon zone' of central India (Sarkar et al., 2015): more enriched δ^2H in terrestrial leaf waxes and cyanobacteria, alongside increased abundance of the biomarker tetrahymanol (generated under saline conditions; Romero-Viana et al., 2012) reconstructed increased salinity and a lowering of lake levels after 6 cal ka BP (Sarkar et al. 2015).

Archaeal GDGTs have also been used as palaeosalinity indicators based on ratios of archaeol, a biomarker for hypersaline archaea, and caldarchaeol, a cosmopolitan isoGDGT that is produced across a range of salinity conditions. The Archaeol and Caldarchaeol Ecometric (ACE) index (Turich and Freeman, 2011) has since been used as a qualitative lacustrine palaeosalinity proxy, showing that salinity increased due to a reduced water balance during periods of higher late glacial temperatures in southern California (Feakins et al., 2019). However, a study of 55 lakes in mid-latitude Asia has identified a threshold response in the ACE index, which suggests that it may only be effective in high lake salinity ranges (60,000-100,000 mg L^{-1}) (He et al., 2020).

6. Reconstructing changes in sea ice extent

Early identification of elevated concentrations (>5-10%) of the abundant haptophyte algae $C_{37:4}$ alkenone in high-latitude marine samples suggested that low temperatures and/or low salinity in (sub)polar waters were important (see Section 5.1). Subsequently, DNA analyses have demonstrated that high $C_{37:4}$ abundances can be more specifically linked to sea ice-associated haptophyte algae (Wang et al., 2021b). With further testing, this new evidence offers the potential for both sea ice and SST information to be simultaneously retrieved from alkenone data in the high latitudes.

Two related sea-ice biomarker proxies have been more extensively developed: specific highly branched isoprenoids (HBIs) usually synthesized in spring by particular ice-associated diatoms (see detailed review by Belt, 2018). In the Arctic, the mono-unsaturated alkene containing 25 carbon atoms is used ("IP_{25}", Belt et al., 2007) but this is not present in the Southern Ocean. Instead, the di-unsaturated HBI ("$IPSO_{25}$") is applied (Belt et al., 2016) (Table 3). Extensive evaluation of the HBIs, especially IP_{25}, against diatom proxy data gives confidence in their ability to reconstruct sea-ice changes (Massé et al., 2008; Weckstrom et al., 2013). $IPSO_{25}$ is a relatively specific environmental indicator, reflecting the tendency for its producer *Berkeleya adeliensis*, to live in platelet ice and the bottom layer of land-fast ice (Belt et al., 2016; Riaux-Gobin et al., 2000), and thus shows a strong signal of coastal production (Masse et al., 2011; Rontani et al., 2019). However, since HBIs have also been determined beyond the continental shelf edge, in the Scotia Sea (Collins et al., 2013); further investigation is required to fully evaluate the interpretation of $IPSO_{25}$ beyond the coastal regions.

A challenge for both HBI proxies is how to interpret the sea ice signal when IP_{25} or $IPSO_{25}$ is absent. Absence could reflect compound degradation within the sea ice, water column or sediments (Belt, 2018), although recent work has confirmed IP_{25} in pre-Quaternary sediments (Knies et al., 2014; Clotten et al., 2018). Alternatively, productivity by ice-dwelling diatoms may be minimal or absent under permanent sea ice cover if photosynthesis is restricted (Belt, 2018). To address the latter concern, the relative abundance of IP_{25} or $IPSO_{25}$ can be compared with open-ocean productivity biomarkers (e.g., HBI III or brassicasterol for diatoms, dinosterol for dinoflagellates). Revised "PIP_{25}" or "$PIPSO_{25}$" indices have been proposed to describe this ratio (Table 3): an absence of both the sea-ice and open-ocean biomarkers yields a $PIP(SO)_{25}$ value of zero ("perennial sea ice"), whereas open-ocean only biomarkers yield a $PIP(SO)_{25}$ value of 1; values in between reflect seasonal sea ice presence (Belt & Müller, 2013).

IP_{25} records have been important in assessing the role of sea ice in past climate changes. Relatively short historical sea ice records have been extended (Tesi et al., 2021). By filling in intervals of sparse historical data, abrupt changes in sea ice have been reconstructed during the last millennium (Massé et al., 2008). Millennial-scale fluctuations in spring sea-ice cover occurred to the north of Iceland during the Holocene and the last glacial-interglacial cycle (e.g., Müller et al., 2009; Hoff et al., 2016; Stein et al., 2017; Xiao et al., 2017; Sadatzki et al., 2020), including contrasting

834 sea-ice conditions between the early/mid and late Younger Dryas close to northern
835 Norway (Cabedo-Sanz et al. 2013). Regional differences between the timing of
836 expanded sea-ice cover were proposed to have contributed to millennial-scale
837 variability in deep-water formation across the deglaciation (Figure 6) (Xiao et al.,
838 2017). Longer-term, an increase in Bering Sea sea-ice cover and development of the
839 seasonal advance and retreat of the sea ice margin occurred alongside the mid-
840 Pleistocene transition ~1 Ma, which might have been important for influencing ice-
841 sheet growth and increased deep ocean storage of carbon during glacial stages
842 (Detlef et al., 2018). The transition from the warm Pliocene epoch into the Quaternary
843 also saw an expansion of Arctic sea ice alongside the intensification of northern
844 hemisphere glaciation ~2.7 Ma (Knies et al., 2014; Clotten et al., 2018). Although
845 preservation over long timescales is promising, concerns have also been raised about
846 the inherent instability of HBIs, meaning caution needs to be applied to interpretation
847 of their presence/absence (Sinninghe Damsté et al., 2007).

848 $IPSO_{25}$ records have been integrated within several multi-proxy studies. Expanded
849 seasonal sea ice cover occurred during the last glacial stage in the Scotia Sea (Collins
850 et al., 2013), and millennial-scale evolution of perennial and seasonal sea ice was
851 recorded over the last deglaciation in the Amundsen Sea (Lamping et al., 2020).
852 Multiple $IPSO_{25}$ records detail expansion and retreat of sea ice during the Holocene
853 (Barbara et al., 2010, 2016; Etourneau et al., 2013; Denis et al., 2010; Tesi et al.,
854 2020; Ashley et al., 2021; Johnson et al., 2021). High-resolution analyses of the last
855 ~400 years have shown that $IPSO_{25}$ can identify trends and cyclicity in seasonal and
856 perennial sea ice cover, and links to ocean or atmospheric forcings (e.g., Campagne et
857 al., 2015; Barbara et al., 2016; Vorrath et al., 2020). Differences in Holocene sea-ice
858 histories between sites likely indicates the influence of local and regional circulation
859 systems (Lamping et al., 2020; Vorrath et al., 2020), which are also expressed in the
860 instrumental record (e.g., Parkinson, 2019).

861

862 ## 7. Tracing biological productivity and biogeochemical cycling

863 Biomarker proxies implicitly record the flux of organic matter between different
864 reservoirs of the Earth system. In this section, we outline biomarkers which have been
865 used qualitatively to explore biogeochemical cycles in more detail by either detecting
866 specific environmental conditions (e.g., biomarkers for methanogenic or
867 methanotrophic micro-organisms) or for tracing changes in productivity and
868 degradation (e.g., fluxes of biomarkers linked to specific producers).

869

870 ### *7.1 Reconstructing biological productivity in lakes and the oceans*

871 The source-specific nature of biomarkers allows for groups of producers to be traced in
872 sedimentary systems, and to assess whether their productivity has changed in the past
873 (Tables 2 and 3). When comparing the relative abundances of productivity markers, it
874 is important to assess the potential impacts of bioturbation, remineralisation and
875 degradation of organic matter; these can be rapid and effective in oxic settings and
876 could bias the target productivity signal (e.g., Leavitt, 1993; Arndt et al., 2013; Jessen
877 et al., 2017). Intact pigments are particularly vulnerable to oxidation, UV radiation and
878 associated processes of degradation, and usually have very low preservation in
879 marine sequences (Reuss et al., 2005; McGowan, 2013). Better preservation may be
880 recorded in lake sediments, but still more successfully with anoxic water columns, or
881 with minimal sinking depths and benthic algae coverage (Leavitt, 1993; Hodgson et al.,
882 2005; McGowan, 2013).

883 Pigment analysis has detected lake productivity oscillations in central Italy linked to
884 warm-cold oscillations in the North Atlantic between ~15.0 and 28.0 cal. ka BP

(Chondrogianni et al., 2004), and changes in lake level linked to the onset of the African Humid Period in Ethiopia (Loakes et al., 2018). In East Antarctica, recolonisation and succession of marine flora has been determined as the ice sheet and sea ice interacted through the Holocene (Hodgson et al., 2003). A distinctive pigment is isorenieratene (Table 3), a carotenoid pigment synthesised by green sulfur bacteria, making it a biomarker for a relatively uncommon but specific environment: photic zone euxinia (both anoxic and sulfidic) (Sinninghe Damsté et al., 2001). Isorenieratene has been instrumental in demonstrating that euxinic conditions developed during the Last Interglacial in the Mediterranean Sea associated with the formation of sapropels (Marino et al., 2007). Significantly, the co-recorded proxy data illustrated the role of increased runoff in altering Mediterranean circulation (Section 5.1) (Marino et al., 2007).

It is more common to find pigment degradation products in marine sediments, often alongside lipid biomarkers for other producers or degradation pathways (Table 3). Chlorophyll degradation products, chlorins (Section 2.2), have been used to reconstruct export production i.e., the organic matter which is removed from the surface ocean and stored longer-term in the deep ocean or sediments (e.g. Petrick et al., 2018). Chlorins, alkenones, sterols and diols have reconstructed intensification or shifts in export production across multiple glacial-interglacial cycles linked to coastal upwelling systems (Petrick et al., 2018), highly productive oceanographic fronts (Cartagena-Sierra et al., 2021), sea-ice extent (Fahl and Stein, 1999) and changing nutrient inputs (e.g., Martinez-Garcia et al., 2011; Sanchez-Montes et al., 2022). In the Subantarctic Atlantic Ocean, a consistent pattern of elevated higher plant *n*-alkanes during glacial intervals aligned closely with dust peaks in Antarctic ice cores (Martinez-Garcia et al., 2009). In turn, colder SSTs and higher primary productivity (both reconstructed from alkenones) demonstrated close connections between ocean and atmosphere circulation, nutrient supply and potential glacial-stage CO_2 drawdown by the ocean through the Quaternary (Martinez-Garcia et al., 2011). A recent global-scale analysis of seafloor sediments flags the potential that alkenone concentrations may be dominated by primary productivity, and thus provide a potentially quantitative reconstruction of production over Quaternary timescales (Raja and Rosell-Melé, 2021).

7.2 Reconstructing sediment, organic matter and nutrient cycling

The presence of terrestrial biomarkers in marine sediments can enable an assessment of the links between ocean circulation and environmental change onshore as detailed above, but may also give insights into the transport pathways of terrestrial organic material and identify important connections between nutrient cycles and productivity alongside palaeohydrology. For example, flood events have been identified in estuarine sediments by increases to the C_{31}/C_{17} *n*-alkane ratio (Meyers, 2003), which were consistent with historical records of the Minjiang River, China, since the 1800s CE (Wang et al., 2014). A "terrestrial to aquatic organic matter *n*-alkane ratio" (TAR, Table 3) has been used to record both dust and glacier-derived sediment inputs to the North Atlantic and Gulf of Alaska across multiple glacial-interglacial cycles (Naafs et al., 2012; Lang et al., 2014; Müller et al., 2018) with potential impacts on marine productivity (Müller et al., 2018; Sanchez-Montes et al., 2020). Biomarker fingerprinting of sediments eroded by the circum-Atlantic ice sheets has added to this detail, and determined the asynchroneity of IRD or meltwater release between different ice sheets (e.g. Stein et al., 2009; Rosell-Mele et al., 2011; Naafs et al., 2013; Hefter et al., 2017).

As well as tracing these land-ocean and land-lake transfers of organic matter, and describing or quantifying lake/ocean export productivity (Section 7.1), biomarkers can be used to trace biogeochemical cycling in two ways: (1) the presence of biomarkers generated under specific environmental conditions, e.g., anoxic settings; (2) the

presence of diagenetic products of the original biosynthesised molecule, where the environmental controls on diagenesis are known. Although used to qualitatively describe organic matter formation, transport and reworking, there is emerging potential to consider biomarker concentrations or transformations as a way to quantify carbon burial and biogeochemical interactions including nutrient and oxygen availability.

In peatlands, biomarker tracers of biogeochemical cycling have been explored, due to the close links between peat water table depth, oxygen availability, and the associated generation of greenhouse gases. For example, elevated concentrations of the anaerobic archaea-produced archaeol reflect rising water tables in peat sequences (Pancost et al., 2011) or enhanced methanogenesis during warm periods of the late Pleistocene and Holocene in Siberian permafrost (Bischoff et al., 2013). Methanogens are also likely the main source of isoGDGT-0 in peats (Basiliko et al., 2003, Pancost and Sinninghe Damsté, 2003); by comparing iso-GDGT-0 and archaeol accumulation rates in a 16 kyr old peat sequence from Hani, China, the long-term link between elevated levels of methanogenesis, high temperatures and high summer insolation was demonstrated (Zheng et al., 2019).

Biohopanoids are largely biomarkers of aerobic bacteria (Rohmer et al., 1992; Talbot et al., 2016b), and include relatively simple C_{30} hopanoids (e.g. diploptene), or more complex versions with additional side chains (bacteriohopanepolyols or BHPs; reviewed by Kusch and Rush, 2022). BHPs have a wide range of sources including methanotrophs, heterotrophs and phototrophs (reviewed by Talbot et al. 2016b; Inglis et al., 2018; Kusch and Rush, 2022). Quaternary applications of BHPs in the Congo fan have demonstrated the correlation between elevated aerobic methane oxidation in the wetlands onshore and late Quaternary interglacial climates (Talbot et al., 2014) as well as a longer-term shift ~1 Ma (Spencer-Jones et al., 2017). Variations in archaeol and diploptene $\delta^{13}C$ values suggested links between the strength of the Asian monsoon and fluctuations in atmospheric methane concentrations (Zheng et al., 2014). Low $\delta^{13}C_{diploptene}$ have also traced the presence and small-scale spatial heterogeneity of methane oxidising bacteria (MOB), and therefore methane oxidation, in Alaskan thermokarst lakes (Davies et al., 2016).

Long-term insights into the nitrogen cycle have been developed using the bacteriohopanetetrol stereoisomer (BHT-*x*), a tracer of anaerobic oxidation of ammonium (anammox) (Rush et al., 2014). For example, BHT-x demonstrated the link between higher temperatures and the intensification of oxygen deficiency zones in the Late Pleistocene in the Gulf of Alaska (Zindorf et al., 2020). This study indicated that, unlike redox-sensitive trace metals, BHT-*x* is not impacted by dilution effects of high sedimentation rates. Ammonium oxidation has also been reconstructed using ratios of isoGDGT [2]/[3], indicating the presence of the archaea *Thaumarchaeota:* in the South China Sea, interglacials were shown to be characterised by concurrent increases in ammonium oxidation and $\delta^{15}N$-inferred N_2 fixation (Dong et al., 2019).

Transformation of the original biosynthesised compounds into recognisable products, under specific redox conditions, have also allowed changes in aerobic/anaerobic conditions to be traced in a range of environments. Interlinked changes to pH and water table explained the presence and down-core variations of an unusual hopanoid (the C_{31} 17α,21β(H)-homohopane) in Holocene peats, which is usually only found in thermally mature organic matter (Pancost et al., 2003; McClymont et al., 2008a; Inglis et al., 2018). Transformation of sterols into stanols at the interface between oxic and anoxic conditions (Wakeham, 1989; Naafs et al., 2019) has also been used to qualitatively assess Holocene changes in peat redox conditions and water table depth (Naafs et al., 2019). In a marine sediment core, the different resistance to oxygenation of a plant wax *n*-alcohol and *n*-alkane was exploited to identify bottom current strength and thus duration of organic matter exposure to oxygenated waters across multiple millennial-scale and glacial-interglacial cycles (Martrat et al., 2007).

To assess the impacts of biogeochemical cycles on atmospheric CO_2, the $\delta^{13}C_{alkenone}$ biomarker proxy showed early promise, drawing on the fractionation of stable carbon isotopes during haptophyte photosynthesis (Bidigare et al., 1997). However, recent work has demonstrated that CO_2 uptake by haptophytes is different at low CO_2 concentrations (Badger et al., 2019), which requires careful interpretation of alkenone-based CO_2 reconstructions during the Quaternary.

8. Sedimentary records of humans and animals in Quaternary landscapes

Lipid biomarker analyses of sedimentary archives are increasingly used to characterise the presence, activities and impacts of humans and animals in the landscape, either as independent reconstructions or as complementary evidence in support of archaeological and palaeoecological anthropogenic reconstructions. Biomarkers also offer an alternative approach when levels of preservation are low or where archaeological excavation is not possible due to time, financial or logistical constraints (discussed in Brown et al., 2022). Biomarkers in archaeological remains contain a wealth of information about the origin of artefacts and deposits and their associated use (reviewed by Evershed, 2008); however, here we focus on sedimentary biomarker proxies that provide both direct and indirect evidence for the presence and environmental impacts of human and animals. For more information, we direct readers to the dedicated review of anthropic biomarkers in sediment archives (Dubois and Jacob, 2016).

8.1. Faecal biomarkers as direct sedimentary indicators of human and animals

Faecal steroid biomarkers (5β-stanols, bile acids), which are produced in the digestive tracts of mammals and deposited via excrement into the environment, present an opportunity to directly identify both animals and humans from sedimentary archives (reviewed by Bull et al., 2002). These compounds are well-preserved within sedimentary archives over Holocene timescales (e.g., Simpson et al., 1998; D'Anjou et al., 2012; White et al., 2019; Schroeter et al., 2020; Brown et al., 2021). Different species produce different diagnostic distributions of faecal steroids due to differences in diets, digestive processes and gut bacteria (e.g., Leeming et al., 1996). Steroid ratios have therefore been used to distinguish between source organisms in investigations of modern faeces and archaeological deposits (e.g., Prost et al., 2017; Zocatelli et al., 2017; Shillito et al., 2020; Kemp et al., 2022), including through multivariate statistics analysis (Harrault et al., 2019). The presence of 5β-stanols is not conclusive evidence of faecal deposition, since small amounts can be produced through the reduction of cholesterol sedimentary environments (e.g., Gaskell and Eglinton, 1975; Bethel et al., 1994), however the application of sterol ratios and the tandem analysis of sterols and bile acids can be used to confirm faecal input and improve faecal source assignment (e.g., Prost et al., 2017). Identification of faecal sources are improved by characterising steroid distributions of local reference dung to correct for within species variability of sterol threshold values (Larson et al., 2022) and reference soils to account for in situ sterol transformation (e.g., Bull et al., 2002; Birks et al., 2011).

Interactions between seabirds and their environment have been particularly effective using faecal steroid (reviewed by Duda et al., 2021). Relationships between penguin colonies and vegetation on the West Antarctic Peninsula over the last 2400 years have been retrieved from lake sediments (Wang et al., 2007). Local declines of northern common eider *(Somateria mollissima borealis)* populations in Arctic Canada and Greenland have been linked to changes in sea-ice concentrations during the Little Ice Age (Hargan et al., 2019), and Holocene little auk population changes have been

linked to the availability and stability of open waters (polynyas) in the sea ice (Ribeiro et al., 2021).

New insights into the presence and impacts of humans in past landscapes have occurred where faecal steroids have refined the timings of human arrival and settlement activities in locations such as northern Norway (D'Anjou et al., 2012), the North Atlantic Faroe Islands (Curtin et al., 2021), the Azores Archipelago (Raposeiro et al., 2021); the Pacific Cook Islands (Sear et al., 2020) and New Zealand (Argiriadis et al., 2018). Faecal steroids have also reconstructed the presence of humans and/or livestock (e.g., White et al., 2018; Vachula et al., 2019; McWethy et al., 2020; Elliott Arnold et al., 2021; Keenan et al., 2021; Ortiz et al., 2022), characterised long-term animal husbandry practices and land use (e.g., Mackay et al., 2020; Schroeter et al., 2020; Birk et al., 2021), and the diets of extinct species (e.g., van Geel et al., 2008; Sistiaga et al., 2014). Comprehensive modern characterisation of east African megafauna also illustrates the potential for faecal sterol applications to inform conservation palaeobiology (Kemp et al., 2022).

Robust sedimentary faecal biomarker identifications of human presence in past landscapes are developed in combination with other sedimentary markers of anthropogenic activity such as pollen, charcoal, fire-derived lipid biomarkers (e.g., D'Anjou et al., 2012; Battistel et al., 2016; Section 8.2), and/or domesticated mammal sedaDNA (e.g., Brown et al., 2021, 2022), and are integrated with existing historical and/or archaeologyical context. Current uncertainties associated within-species variability of steroid distributions, contributions from environmentally transformed 5β-stanols, and steroid transportation, storage, secondary deposition and degradation processes (e.g., Birk et al., 2021; Keenan et al., 2021; Davies et al., 2022; Lawson et al., 2022), present a range of opportunities for further analysis to refine steroid identification of faecal sources and enhance their applications as anthropogenic and mammalian tracers in Quaternary science.

8.2. Biomarkers of burning and agricultural activity as indirect indicators of human activity

Pyrogenic biomarkers can enhance understandings of fire histories since their signatures and concentrations record information on the fuel type and conditions during the fire such as burn intensity and moisture content, as demonstrated through modern burning experiments (e.g., Oros and Simoneit, 2001; Karp et al., 2020) and palaeo comparisons with macro- and micro-charcoal (e.g., Elias et al., 2001; Schreuder et al., 2019a).

Polycyclic aromatic hydrocarbons (PAH) are produced during the incomplete combustion of biomass (reviewed by Richter and Howard (2000) and Lima et al. (2005)). PAH compound distributions represent combustion conditions, vegetation fuel type and transport pathways (Karp et al., 2020) and can be used to distinguish between local and regional burning events (e.g., Vachula et al., 2022). Many PAHs can be atmospherically transported across thousands of kilometres, although some compounds, such as benzo[a]pyrene have lower modelled half-life transport distances of ca. 500km (Halsall et al., 2001). PAHs are produced by a wide range of burn temperatures (ca. 200 – 700 °C; Lu et al., 2009), but higher concentrations are produced under high intensity burning temperatures of 400 – 500 °C and during the combustion of woody rather than grassy vegetation (Karp et al., 2020). Palaeo-PAH records may therefore be biased towards wildfires and sensitive to changes in fuel type and/or fire regime. Whilst PAHs can be released from petrogenic sources (e.g., Wakeham et al., 1980), pyrogenic inputs can be identified using relative distributions of PAHs (e.g.,Stogiannidis and Laane, 2015) or through comparisons with other fire proxies (e.g., Ruan et al., 2020; Tan et al., 2020). Long-term records of PAH fire

histories have tracked human settlement and activity in the late Holocene in northern Norway (D'Anjou et al., 2012), East Africa (Battistel et al., 2016) and New Zealand (Argiriadis et al., 2018) and characterised the advent of hominin pyrotechnology in the Middle Palaeolithic (Brittingham et al., 2019). PAHs from lake sediments have also tracked industrial emissions such as combustion of coal (e.g., Meyers, 2003) and other fossil fuels (e.g., Guo et al., 2022); anthropogenic pollution contributions must be considered if using PAHs to reconstruct fire histories over the industrial period.

Levoglucosan and its isomers (mannosan and galactosan) are monosaccharide anhydride (MA) compounds that are specific palaeo-fire proxies (reviewed by Simoneit, 2002 and Bhattarai et al., 2019) since they are exclusively formed during the combustion of cellulose (Simoneit et al., 1999) during burn temperatures of ca. 150 – 350 °C (e.g., Kuo et al., 2008). MAs can travel hundreds to thousands of kilometres transported by wind and rivers (e.g., Mochida et al., 2010; Zennaro et al., 2014). Ratios of levoglucosan, mannosan and galactosan can reveal the type of biomass involved in burning events (e.g., Fabbri et al., 2009; Kirchgeorg et al., 2014) and combustion conditions (e.g., Kuo et al., 2011). Lake sediment comparisons of macroscopic charcoal and MAs from The Mayan Lowlands, Guatemala, demonstrated the advances of combining these fire proxies to enhance understanding of palaeo fire regimes at different spatial scales (Schüpbach et al., 2015). Offshore levoglucosan records have confirmed vegetation changes associated with the late Quaternary megafaunal extinction in Southeastern Australia (Lopes dos Santos et al., 2013b) and demonstrated increased burning linked with vegetation change and human settlement in sub-Saharan Northwest Africa 60-50ka (Schreuder et al., 2019b). MA records from ice cores have been successfully applied to track post-Last Glacial Maximum and Holocene fire intensity and burning type at regional to semi-hemispheric scales (e.g., Zennaro et al., 2014; Battistel et al., 2018; Segato et al., 2021; Chen et al., 2022). Combustion-derived derivatives of lignin phenols, monosaccharide molecules and diterpenoids are also major components of smoke particulate matter and can be detected in sediment archives (Oros and Simoneit, 2001).

Evidence of crop cultivation and processing can characterise the timings of human presence and the types of activities taking place in past landscapes. Although not every cultivar has known specific lipid biomarkers, millacin is a marker of the introduced broomcorn millet in well-defined botanical settings (e.g., Jacob et al., 2008a,b; Bossard et al., 2013). Fluxes of millacin detected in lake sediments have, for example, traced the introduction, intensification and failure of millet cultivation since the Bronze Age in the French Alps, and comparisons with contemporary palaeohydrological reconstructions have demonstrated climatically-driven downturns in millet cultivation in the Hallstatt period (Jacob et al., 2008a). Other cultivar biomarkers include cannabinol, a marker of hemp that can be used to identify processing activities (retting) from sediment archives (e.g., Lavrieux et al., 2013; Schmidt et al., 2020; Rull et al., 2022), and palmitone, a marker of *Colocasia esculenta* Schott (taro) (e.g., Krentcher et al., 2019).

9. Conclusions and future outlook

Biomarkers have emerged as valuable parts of the Quaternary science toolkit, due to both quantitative and qualitative insights into past environmental changes, and because multiple biomarkers (and thus multiple environmental signals) can be recovered from single samples. Analytical developments and improved understanding of the processes underpinning the wide range of biomarker proxies outlined here have also led to data that has been both novel and complementary to more established Quaternary science approaches.

The major impacts of biomarker analyses have so far come from the quantification of temperature changes, and detailed assessments of the interactions between vegetation change and hydroclimate. The results are important in spanning a wide range of timescales, from annual/decadal through to the long-term evolution of Quaternary climates at glacial-interglacial and longer timescales. In considering future climate projections, both the quantitative and qualitative insights gained from biomarker reconstructions have enabled data-model comparison and data-model assimilation to be undertaken across a wide range of timescales, including the pre-Quaternary (Tierney et al., 2020; Masson-Delmotte et al., 2021). In addition to providing valuable palaeoclimatic insights, biomarkers are increasingly being used to directly identify human impacts on the environment both pre-dating and through the Industrial era, thereby providing essential long-term context to advance our understanding of the resilience of ecosystems and societies

Continued efforts to better constrain quantitative calibrations of temperature, salinity, sea ice and precipitation will further enhance our biomarker reconstructions. Community-wide collaborations have been important for advancing our understanding and application of palaeo-environmental proxies and their uncertainties (e.g. Schouten et al., 2013 for TEX_{86}; Belt et al., 2014 for IP_{25}); similar approaches could assist with advancing our understanding of more recently developed or more qualitative biomarker proxies (e.g. anthropogenic markers). With the increasing application of (seda)DNA approaches to identify and understand the biomarker producers (e.g., Wang et al., 2019b; Theroux et al., 2020), more nuanced interpretations of past temperature or other environmental changes are also likely to result from reduced uncertainty estimates and through advances in our understanding of signals related to key producers and their potentially varied responses to factors including seasonality and nutrient availability. There is therefore the potential to add to the rich environmental information provided by both biomarkers and other geochemical and palaeoecological proxies, with new assessments of biogeochemical cycling, sea ice evolution, and human-environment interactions, as well as new data on how that organic matter has been preserved, recycled, and transported through palaeo-environments.

In this review, we have outlined some of the many, diverse ways in which biomarkers have advanced understandings of Quaternary environments. The biomarker toolkit is continually evolving, aided by advances in instrument capabilities which are presenting new opportunities to analyse smaller sample sizes and a greater diversity of Quaternary archives. For example, improvements in detection limits facilitated by high resolution mass spectrometry present opportunities to expand the suite of palaeoenvironmental proxies that can be analysed from a single sample, and extend applications where sample sizes are limited and/or biomarker concentrations may be low (e.g., varved sediments, ice cores and/or highly resolved sedimentary records). In turn, untargeted analysis of environmental mass spectrometry spectral data, such as hierarchical clustering (e.g., Bale et al, 2021) and the application of information theory and molecular networking (e.g., Ding et al., 2021), yields highly detailed molecular information, with the potential to provide unprecedented levels of detail about environmental contributions as well the identification of yet unknown biomarkers, that may prove to be of ecological and environmental significance. In addition, there is great potential to expand compound-specific analyses, which have already yielded detailed insights into past hydroclimate, productivity, and CO_2, by extending the range of biomarkers that can be analysed. A rapidly advancing area of biomarker research is radiocarbon analysis of individual lipids, or groups of lipids, which has already demonstrated that different pools of organic matter are being (re)worked and transported through river systems today (e.g., Galy & Eglinton, 2011; Eglinton et al., 2021; Feng et al., 2013) and in the past (Bliedtner et al., 2020). Biomarker radiocarbon analysis shows great potential to not only enhance our understandings of Quaternary

sedimentary environments and processes, but also to improve chronological controls through compound-specific radiocarbon analysis. Biomarkers have therefore made a wealth of contributions to Quaternary science, and the continued advances in this field of research offer many opportunities to extend our understandings of Earth systems in the past, present, and future.

Acknowledgments and funding

We thank Chris Orton for drafting Figure 1 and 3, Tommaso Tesi for access to data to generate Figure 4 and Melissa Berke for comments on an early draft section. We thank the Leverhulme Trust and European Research Council (ANTSIE, grant no. 864637) for funding support.

References

Aichner, B., Ott, F., Słowiński, M., et al. (2018) Leaf wax *n*-alkane distributions record ecological changes during the Younger Dryas at Trzechowskie paleolake (northern Poland) without temporal delay. *Climate of the Past*, 14(11), pp. 1607–1624. https://doi.org/10.5194/cp-14-1607-2018.https://doi.org/10.5194/cp-14-1607-2018.

Aichner, B., Makhmudov, Z., Rajabov, I., et al. (2019). Hydroclimate in the Pamirs Was Driven by Changes in Precipitation-Evaporation Seasonality Since the Last Glacial Period. Geophys. Res. Lett. 46, 13972–13983. https://doi.org/10.1029/2019GL085202

Aichner, B., Wünnemann, B., Callegaro., A. et al. (2022) Asynchronous responses of aquatic ecosystems to hydroclimatic forcing on the Tibetan Plateau. *Commun Earth Environ* **3**, 3. https://doi.org/10.1038/s43247-021-00325-1

Andersson, R.A., Kuhry, P., Meyers, P., et al. (2011) Impacts of paleohydrological changes on n-alkane biomarker compositions of a Holocene peat sequence in the Eastern European Russian Arctic. Organic Geochemistry 42, 1065– 1075. https://doi.org/10.1016/j.orggeochem.2011.06.020https://doi.org/10.1016/j.orggeochem.2011.06.020

Argiriadis, E., Battistel, D., McWethy, et al., (2018) Lake sediment fecal and biomass burning biomarkers provide direct evidence for prehistoric human-lit fires in New Zealand. Sci Rep 8, 12113. https://doi.org/10.1038/s41598-018-30606-3

Arndt, S., Jørgensen, B.B., LaRowe, D.E., (2013) Quantifying the degradation of organic matter in marine sediments: A review and synthesis. Earth-Science Reviews 123, 53–86. https://doi.org/10.1016/j.earscirev.2013.02.008

Ashley, K.E., McKay, R., Etourneau, J., (2021) Mid-Holocene Antarctic sea-ice increase driven by marine ice sheet retreat. Clim. Past 17, 1–19. https://doi.org/10.5194/cp-17-1-2021

Atwood, A.R. and Sachs, J.P. (2014) Separating ITCZ- and ENSO-related rainfall changes in the Galápagos over the last 3 kyr using D/H ratios of multiple lipid biomarkers. *Earth and Planetary Science Letters*, 404, pp. 408–419. https://doi.org/10.1016/j.epsl.2014.07.038.

Avsejs, L.A., Nott, C.J., Xie, S., *et al.* (2002) 5-n-Alkylresorcinols as biomarkers of sedges in an ombrotrophic peat section. *Organic Geochemistry*, 33(7), pp. 861–867. https://doi.org/10.1016/S0146-6380(02)00046-3.

1244 Badger, M. P. S., Chalk, T. B., Foster, G. L., (2019) Insensitivity of alkenone carbon
1245 isotopes to atmospheric CO_2 at low to moderate CO_2 levels. Clim. Past, 15, 539–
1246 554. https://doi.org/10.5194/cp-15-539-2019, 2019)

1247 Baker, A., Blyth, A.J., Jex, C.N., (2019) Glycerol dialkyl glycerol tetraethers (GDGT)
1248 distributions from soil to cave: Refining the speleothem paleothermometer.
1249 Organic Geochemistry 136, 103890.
1250 https://doi.org/10.1016/j.orggeochem.2019.06.011

1251 Bakku, R. K., Araie, H., Hanawa, Y., (2018) Changes in the accumulation of alkenones
1252 and lipids under nitrogen limitation and its relation to other energy storage
1253 metabolites in the haptophyte alga Emiliania huxleyi CCMP 2090. *Journal of*
1254 *Applied Phycology*, 30(1), pp. 23–36. https://doi.org/10.1007/s10811-017-1163-x.

1255 Bale, NJ,. Ding, S,. Hopmans, EC,. et al. (2021) Lipidomics of Environmental Microbial
1256 Communities. I: Visualization of Component Distributions Using Untargeted
1257 Analysis of High-Resolution Mass Spectrometry Data. Front. Microbiol,
1258 12:659302. https://doi.org/10.3389/fmicb.2021.659302

1259 Balascio, N.L., Anderson, R.S., D'Andrea, W.J., (2020) Vegetation changes and plant
1260 wax biomarkers from an ombrotrophic bog define hydroclimate trends and
1261 human-environment interactions during the Holocene in northern Norway. The
1262 Holocene 30, 1849–1865. https://doi.org/10.1177/0959683620950456

1263 Barbara, L., Crosta, X., Leventer, A., et al. (2016) Environmental responses of the
1264 Northeast Antarctic Peninsula to the Holocene climate variability. East Antarctic
1265 Peninsula climate history. Paleoceanography 31, 131–147.
1266 https://doi.org/10.1002/2015PA002785

1267 Barbara, L., Crosta, X., Massé, G., et al. (2010) Deglacial environments in eastern
1268 Prydz Bay, East Antarctica. Quaternary Science Reviews 29, 2731–2740.
1269 https://doi.org/10.1016/j.quascirev.2010.06.027

1270 Basiliko, N., Yavitt, J.B., Dees, P.M., et al. (2003) Methane biogeochemistry and
1271 methanogen communities in two northern peatland ecosystems, New York State.
1272 Geomicrobiology Journal, v. 20, p. 563–577. https://doi.org/10.1080/713851165.

1273 Basu, S., Sanyal, P., Pillai, A.A.S., et al. (2019) Response of grassland ecosystem to
1274 monsoonal precipitation variability during the Mid-Late Holocene: Inferences
1275 based on molecular isotopic records from Banni grassland, western India. PLoS
1276 ONE 14, e0212743. https://doi.org/10.1371/journal.pone.0212743

1277 Battistel, D., Argiriadis, E., Kehrwald, N., et al. (2016) Fire and human record at Lake
1278 Victoria, East Africa, during the Early Iron Age: Did humans or climate cause
1279 massive ecosystem changes? The Holocene, Vol. 27(7) 997–1007.
1280 https://doi.org/10.1177/0959683616678466

1281 Battistel, D., Kehrwald, N. M., Zennaro1, P., et al. (2018) High-latitude Southern
1282 Hemisphere fire history during the midto late Holocene (6000–750 BP). Clim.
1283 Past, 14, 871–886. https://doi.org/10.5194/cp-14-871-2018

1284 Bechtel, A., Smittenberg, R. H., Bernasconi, S. M., et al (2010) 'Distribution of
1285 branched and isoprenoid tetraether lipids in an oligotrophic and a eutrophic
1286 Swiss lake: Insights into sources and GDGT-based proxies', Organic
1287 Geochemistry, 41(8), pp. 822–832. Available at:
1288 https://doi.org/10.1016/j.orggeochem.2010.04.022.

1289 Belt, S.T., (2018) Source-specific biomarkers as proxies for Arctic and Antarctic sea
1290 ice. Organic Geochemistry 125, 277–298.
1291 https://doi.org/10.1016/j.orggeochem.2018.10.002

1292 Belt, S.T., Massé, G., Rowland, S. J., *et al.* (2007) A novel chemical fossil of palaeo
1293 sea ice: IP25. *Organic Geochemistry*, 38(1), pp. 16–27.
1294 https://doi.org/10.1016/j.orggeochem.2006.09.013.

1295 Belt, S.T. and Müller, J. (2013) The Arctic sea ice biomarker IP25: a review of current
1296 understanding, recommendations for future research and applications in palaeo
1297 sea ice reconstructions. Quaternary Science Reviews 79, 9–25.
1298 https://doi.org/10.1016/j.quascirev.2012.12.001

1299 Belt, S. T., Brown, T. A., Ampel, L., et al. (2014) An inter-laboratory investigation of the
1300 Arctic sea ice biomarker proxy IP_{25} in marine sediments: key outcomes and
1301 recommendations, Clim. Past, 10, 155–166. https://doi.org/10.5194/cp-10-155-
1302 2014

1303 Belt, S.T., Cabedo-Sanz, P., Smik, L., *et al.* (2015) Identification of paleo Arctic winter
1304 sea ice limits and the marginal ice zone: Optimised biomarker-based
1305 reconstructions of late Quaternary Arctic sea ice. *Earth and Planetary Science*
1306 *Letters*, 431, pp. 127–139. https://doi.org/10.1016/j.epsl.2015.09.020.

1307 Belt, S.T., Smik, L., Brown, T.A., et al. (2016) Source identification and distribution
1308 reveals the potential of the geochemical Antarctic sea ice proxy IPSO25. Nat
1309 Commun 7, 12655. https://doi.org/10.1038/ncomms12655

1310 Bendle, J., Rosell-Melé, A. and Ziveri, P. (2005) Variability of unusual distributions of
1311 alkenones in the surface waters of the Nordic seas. *Paleoceanography*, 20(2).
1312 https://doi.org/10.1029/2004PA001025.

1313 Bendle, J.A.P., Rosell-Melé, A., Cox, N.J., et al. (2009) Alkenones, alkenoates, and
1314 organic matter in coastal environments of NW Scotland: Assessment of potential
1315 application for sea level reconstruction: Biomarkers in coastal environments.
1316 Geochem. Geophys. Geosyst. 10(12). https://doi.org/10.1029/2009GC002603

1317 Bendle, J. A., Weijers, J. W. H., Maslin, M. A., *et al.* (2010) Major changes in glacial
1318 and Holocene terrestrial temperatures and sources of organic carbon recorded in
1319 the Amazon fan by tetraether lipids. *Geochemistry, Geophysics, Geosystems*,
1320 11(12). https://doi.org/10.1029/2010GC003308.

1321 Berke, M.A., Johnson, T.C., Werne, J.P., (2012a) Molecular records of climate
1322 variability and vegetation response since the Late Pleistocene in the Lake Victoria
1323 basin, East Africa. Quaternary Science Reviews 55, 59–74.
1324 https://doi.org/10.1016/j.quascirev.2012.08.014

1325 Berke, M.A., Johnson, T.C., Werne, J.P., et al. (2012b) A mid-Holocene thermal
1326 maximum at the end of the African Humid Period. Earth and Planetary Science
1327 Letters 351–352, 95–104. https://doi.org/10.1016/j.epsl.2012.07.008

1328 Berke, M.A., Johnson, T. C., Werne, J. P., *et al.* (2014) Characterization of the last
1329 deglacial transition in tropical East Africa: Insights from Lake Albert.
1330 Palaeogeography, Palaeoclimatology, Palaeoecology, 409, pp. 1–8.
1331 https://doi.org/10.1016/j.palaeo.2014.04.014.

1332 Bethell, P. H., Goad, L., Evershed, J., et al. (1994) The study of molecular markers of
1333 human activity: the use of coprostanol in the soil as an indicator of human faecal
1334 material. Journal of Archaeological Science 21 (5), 619–632.
1335 https://doi.org/10.1006/jasc.1994.1061

1336 Bhattacharya, T., Tierney, J.E., Addison, J.A., et al. (2018) Ice-sheet modulation of
1337 deglacial North American monsoon intensification. Nature Geosci 11, 848–852.
1338 https://doi.org/10.1038/s41561-018-0220-7

1339 Bhattacharya, S., Kishor, H., Ankit, Y., et al. (2021) Vegetation History in a Peat
1340 Succession Over the Past 8,000 years in the ISM-Controlled Kedarnath Region,
1341 Garhwal Himalaya: Reconstruction Using Molecular Fossils. Front. Earth Sci. 9,
1342 703362. https://doi.org/10.3389/feart.2021.703362

1343 Bhattarai, H., Saikawa, E., Wan, X., et al. (2019) Levoglucosan as a tracer of biomass
1344 burning: Recent progress and perspectives. Atmospheric Research 220, 20–33.
1345 https://doi.org/10.1016/j.atmosres.2019.01.004

1346 Bianchi, T.S. and Canuel, E.A. (2011) Chemical Biomarkers in Aquatic Ecosystems, in
1347 *Chemical Biomarkers in Aquatic Ecosystems*. Princeton University Press.
1348 https://doi.org/10.1515/9781400839100

1349 Bingham, E.M., McClymont, E.L., Väliranta, M., et al. (2010) Conservative composition
1350 of n-alkane biomarkers in Sphagnum species: Implications for palaeoclimate
1351 reconstruction in ombrotrophic peat bogs. Organic Geochemistry 41, 214–220.
1352 https://doi.org/10.1016/j.orggeochem.2009.06.010

1353 Birk, J.J., Dippold, M., Wiesenberg G.L.B., *et al.* (2012) Combined quantification of
1354 faecal sterols, stanols, stanones and bile acids in soils and terrestrial sediments
1355 by gas chromatography–mass spectrometry. *Journal of Chromatography A*,
1356 1242, pp. 1–10. https://doi.org/10.1016/j.chroma.2012.04.027.

1357 Birk, J.J., Reetz, K., Sirocko, F., et al., (2021) Faecal biomarkers as tools to
1358 reconstruct land-use history in maar sediments in the Westeifel Volcanic Field,
1359 Germany. Boreas 51, 637–650. https://doi.org/10.1111/bor.12576

1360 Bischoff, J., Mangelsdorf, K., Gattinger, A., et al., (2013) Response of methanogenic
1361 archaea to Late Pleistocene and Holocene climate changes in the Siberian Arctic:
1362 methanogenic response to climate changes. Global Biogeochem. Cycles 27,
1363 305–317. https://doi.org/10.1029/2011GB004238

1364 Bliedtner, M., von Suchodoletz, H., Schäfer, I., et al. (2020) Age and origin of leaf wax
1365 n-alkanes in fluvial sediment–paleosol sequences and implications for
1366 paleoenvironmental reconstructions. Hydrol. Earth Syst. Sci., 24, 2105–2120,
1367 https://doi.org/10.5194/hess-24-2105-2020.

1368 Blyth, A.J., Farrimond, P. and Jones, M. (2006) An optimised method for the extraction
1369 and analysis of lipid biomarkers from stalagmites. *Organic Geochemistry*, 37(8),
1370 pp. 882–890. https://doi.org/10.1016/j.orggeochem.2006.05.003.

1371 Blyth, A.J., Asrat, A., Baker, A., et al. (2007) A new approach to detecting vegetation
1372 and land-use Change using high-resolution lipid biomarker records in stalagmites.
1373 Quat. res. 68, 314–324. https://doi.org/10.1016/j.yqres.2007.08.002

1374 Blyth, A.J., Hartland, A., Baker, A., (2016) Organic proxies in speleothems – New
1375 developments, advantages and limitations. Quaternary Science Reviews 149, 1–
1376 17. https://doi.org/10.1016/j.quascirev.2016.07.001

1377 Blyth, A.J. and Watson, J.S. (2009) Thermochemolysis of organic matter preserved in
1378 stalagmites: A preliminary study. Organic Geochemistry 40, 1029–1031.
1379 https://doi.org/10.1016/j.orggeochem.2009.06.007

1380 Bossard, N., Jacob, J., Le Milbeau, C., et al. (2013) Distribution of miliacin (olean-18-
1381 en-3β-ol methyl ether) and related compounds in broomcorn millet (Panicum
1382 miliaceum) and other reputed sources: Implications for the use of sedimentary
1383 miliacin as a tracer of millet. Organic Geochemistry 63, 48–55.
1384 https://doi.org/10.1016/j.orggeochem.2013.07.012

1385 Boon, J.J., Dupont, L., De Leeuw, J.W., (1986) Characterization of a peat bog profile
1386 by Curie Point pyrolysis-mass spectrometry combined with multivariant analysis

and by pyrolysis gas chromatography–mass spectrometry. In: Fuchsman, C.H. (Ed.), Peat and Water. Elsevier Applied Science Publishers Ltd., pp. 215–219.

Bowen, G.J. and Revenaugh, J. (2003) Interpolating the isotopic composition of modern meteoric precipitation. *Water resources research*, 39(10). https://doi.org/10.1029/2003WR002086

Brassell, S., Eglinton, G., Marlowe, I. et al., (1986) Molecular stratigraphy: a new tool for climatic assessment. Nature 320, 129–133. https://doi.org/10.1038/320129a0

Bray, E.E., Evans, E.D., (1961) Distribution of n-paraffins as a clue to recognition of source beds. Geochimica et Cosmochimica Acta 22, 2–15. https://doi.org/10.1016/0016-7037(61)90069-2

Brittingham, A., Hren, M.T., Hartman, G., et al. (2019) Geochemical Evidence for the Control of Fire by Middle Palaeolithic Hominins. Sci Rep 9, 15368. https://doi.org/10.1038/s41598-019-51433-0

Brown, A.G., Fonville, T., van Hardenbroek, M., et al. (2022) New integrated molecular approaches for investigating lake settlements in north-western Europe. Antiquity 96, 1179–1199. https://doi.org/10.15184/aqy.2022.70

Brown, A.G., Van Hardenbroek, M., Fonville, T., et al (2021) Ancient DNA, lipid biomarkers and palaeoecological evidence reveals construction and life on early medieval lake settlements. Sci Rep 11, 11807. https://doi.org/10.1038/s41598-021-91057-x

Bull, I.D., Lockheart, M.J., Elhmmali, M.M., et al. (2002) The origin of faeces by means of biomarker detection. Environment International 27, 647–654. https://doi.org/10.1016/S0160-4120(01)00124-6

Bush, R.T. and McInerney, F.A. (2013) Leaf wax n-alkane distributions in and across modern plants: Implications for paleoecology and chemotaxonomy. Geochimica et Cosmochimica Acta 117, 161–179. https://doi.org/10.1016/j.gca.2013.04.016

Cabedo-Sanz, P., Belt, S.T, Knies, J.,et al. (2013) Identification of contrasting seasonal sea ice conditions during the Younger Dryas, Quaternary Science Reviews, 79, 74-86, https://doi.org/10.1016/j.quascirev.2012.10.028.

Campagne, P., Crosta, X., Houssais, M.N., et al. (2015) Glacial ice and atmospheric forcing on the Mertz Glacier Polynya over the past 250 years. Nat Commun 6, 6642. https://doi.org/10.1038/ncomms7642

Capron, E., Govin, A., Feng, R., (2017) Critical evaluation of climate syntheses to benchmark CMIP6/PMIP4 217 ka Last Interglacial simulations in the high-latitude regions. Quaternary Science Reviews 168, 137-160. https://doi.org/10.1016/j.quascirev.2017.04.019

Carr, A.S., Boom, A., Chase, B.M. *et al.* (2015) Holocene sea level and environmental change on the west coast of South Africa: evidence from plant biomarkers, stable isotopes and pollen. J Paleolimnol **53**, 415–432. https://doi.org/10.1007/s10933-015-9833-7.

Cartagena-Sierra, A., Berke, M.A., Robinson, R.S., et al. (2021) Latitudinal Migrations of the Subtropical Front at the Agulhas Plateau Through the Mid-Pleistocene Transition. Paleoceanog and Paleoclimatol 36(7), https://doi.org/10.1029/2020PA004084

Castañeda, I.S., Mulitza, S., Schefuß, E., et al. (2009a) Wet phases in the Sahara/Sahel region and human migration patterns in North Africa. Proc. Natl. Acad. Sci. U.S.A. 106, 20159–20163. https://doi.org/10.1073/pnas.0905771106

Castañeda, I.S., Werne, J.P., Johnson, T.C., et al. (2009b) Late Quaternary vegetation history of southeast Africa: The molecular isotopic record from Lake Malawi. Palaeogeography, Palaeoclimatology, Palaeoecology, 275, 100-112, doi: 10.1016/j.palaeo.2009.02.008.

Castañeda, I.S. and Schouten, S.(2011) A review of molecular organic proxies for examining modern and ancient lacustrine environments. Quaternary Science Reviews 30, 2851–2891. https://doi.org/10.1016/j.quascirev.2011.07.009

Castañeda, I.S., Werne, J.P., Johnson, T.C., (2007) Wet and arid phases in the southeast African tropics since the Last Glacial Maximum. Geology, 35 (9): 823–826. doi: https://doi.org/10.1130/G23916A.1.

Chen, N., Bianchi, T. S., McKee, B. A., et al. (2001) Historical trends of hypoxia on the Louisiana shelf: application of pigments as biomarkers. Organic Geochemistry, 32(4), 543-561. https://doi.org/10.1016/S0146-6380(00)00194-7

Chen, A., Yang, L., Kang, H., *et al.* (2022) Southern hemisphere fire history since the late glacial, reconstructed from an Antarctic sediment core. *Quaternary Science Reviews*, 276, p. 107300. https://doi.org/10.1016/j.quascirev.2021.107300.

Chondrogianni, C., Ariztegui, D., Rolph, T., et al. (2004) Millennial to interannual climate variability in the Mediterranean during the Last Glacial Maximum. Quaternary International 122, 31–41. https://doi.org/10.1016/j.quaint.2004.01.029

Clotten, C., Stein, R., Fahl, K., et al. (2018) Seasonal sea ice cover during the warm Pliocene: Evidence from the Iceland Sea (ODP Site 907). Earth and Planetary Science Letters 481, 61–72. https://doi.org/10.1016/j.epsl.2017.10.011

Collins, L.G., Allen, C.S., Pike, J., et al. (2013) Evaluating highly branched isoprenoid (HBI) biomarkers as a novel Antarctic sea-ice proxy in deep ocean glacial age sediments. Quaternary Science Reviews 79, 87–98. https://doi.org/10.1016/j.quascirev.2013.02.004

Conte, M.H., Sicre, M.-A., Rühlemann, C., et al. (2006) Global temperature calibration of the alkenone unsaturation index (UK^{37}) in surface waters and comparison with surface sediments: alkenone unsaturation index. Geochem. Geophys. Geosyst. 7. https://doi.org/10.1029/2005GC001054

Craig, H. and Gordon, L.I. (1965) Deuterium and oxygen 18 variations in the ocean and marine atmosphere. Proceedings of a Conference on Stable Isotopes in Oceanographic Studies and Paleotemperatures, V. Lischi & Figli, Pisa, Spoleto, Italy (1965), pp. 9-130.

Cranwell, P.A. (1973) Chain-length distribution of n-alkanes from lake sediments in relation to post-glacial environmental change. *Freshwater Biology*, 3(3), pp. 259–265. https://doi.org/10.1111/j.1365-2427.1973.tb00921.x.

Cranwell, P.A., Eglinton, G., Robinson, N., (1987) Lipids of aquatic organisms as potential contributors to lacustrine sediments—II. Organic Geochemistry 11, 513–527. https://doi.org/10.1016/0146-6380(87)90007-6

Cuddington, K. and Leavitt, P.R., (1999) An individual-based model of pigment flux in lakes: implications for organic biogeochemistry and paleoecology. Can. J. Fish. Aquat. Sci. 56, 1964–1977. https://doi.org/10.1139/f99-108

Curtin, L., D'Andrea, W.J., Balascio, N.L., et al (2021) Sedimentary DNA and molecular evidence for early human occupation of the Faroe Islands. Commun Earth Environ 2, 253. https://doi.org/10.1038/s43247-021-00318-0

1480 D'Andrea, W.J. and Huang, Y., (2005) Long chain alkenones in Greenland lake
1481 sediments: Low δ13C values and exceptional abundance. Organic Geochemistry
1482 36, 1234–1241. https://doi.org/10.1016/j.orggeochem.2005.05.001

1483 D'Andrea, W.J., Huang, Y., Fritz, S.C., et al. (2011) Abrupt Holocene climate change
1484 as an important factor for human migration in West Greenland. Proc. Natl. Acad.
1485 Sci. U.S.A. 108, 9765–9769. https://doi.org/10.1073/pnas.1101708108

1486 D'Andrea, W.J., Theroux, S., Bradley, R.S., et al. (2016) Does phylogeny control U 37
1487 K -temperature sensitivity? Implications for lacustrine alkenone
1488 paleothermometry. Geochimica et Cosmochimica Acta 175, 168–180.
1489 https://doi.org/10.1016/j.gca.2015.10.031

1490 D'Anjou, R.M., Bradley, R.S., Balascio, N.L., et al. (2012) Climate impacts on human
1491 settlement and agricultural activities in northern Norway revealed through
1492 sediment biogeochemistry. Proc. Natl. Acad. Sci. U.S.A. 109, 20332–20337.
1493 https://doi.org/10.1073/pnas.1212730109

1494 Daniels, W.C., Castañeda, I.S., Salacup, J.M., (2021) Archaeal lipids reveal climate-
1495 driven changes in microbial ecology at Lake El'gygytgyn (Far East Russia) during
1496 the Plio-Pleistocene. J. Quaternary Sci, 37: 900-914.
1497 https://doi.org/10.1002/jqs.3347

1498 Davies, K.L., Pancost, R.D., Edwards, M.E., et al. (2016) Diploptene d^{13}C values from
1499 contemporary thermokarst lake sediments show complex spatial variation.
1500 Biogeosciences 13, 2611–2621. https://doi.org/10.5194/bg-13-2611-2016

1501 Davies, A.L., Harrault, L., Milek, K., et al. (2022) A multiproxy approach to long-term
1502 herbivore grazing dynamics in peatlands based on pollen, coprophilous fungi and
1503 faecal biomarkers. Palaeogeography, Palaeoclimatology, Palaeoecology 598,
1504 111032. https://doi.org/10.1016/j.palaeo.2022.111032

1505 Dearing Crampton-Flood, E., Tierney, J.E., Peterse, F., et al. (2020) BayMBT: A
1506 Bayesian calibration model for branched glycerol dialkyl glycerol tetraethers in
1507 soils and peats. Geochimica et Cosmochimica Acta 268, 142–159.
1508 https://doi.org/10.1016/j.gca.2019.09.043

1509 De Bar, M. W., Stolwijk, D. J., McManus, J. F., et al. (2018) A Late Quaternary climate
1510 record based on long-chain diol proxies from the Chilean margin. Clim. Past, 14,
1511 1783–1803. https://doi.org/10.5194/cp-14-1783-2018

1512 De Bar, M.W., Weiss, G., Yildiz, C., et al. (2020) Global temperature calibration of the
1513 Long chain Diol Index in marine surface sediments. Organic Geochemistry 142,
1514 103983. https://doi.org/10.1016/j.orggeochem.2020.103983

1515 De Jonge, C., Hopmans, E.C., Zell, C.I., et al. (2014) Occurrence and abundance of 6-
1516 methyl branched glycerol dialkyl glycerol tetraethers in soils: Implications for
1517 palaeoclimate reconstruction. Geochimica et Cosmochimica Acta 141, 97-112,
1518 https://doi.org/10.1016/j.gca.2014.06.013

1519 De Jonge C., Stadnitskaia A., Streletskaya I. D., et al. (2015) Impact of riverine
1520 suspended particulate matter on the branched glycerol dialkyl glycerol tetraether
1521 composition of lakes: The outflow of the Selenga River in Lake Baikal (Russia).
1522 Organic Geochemistry 83, 241-252.
1523 https://doi.org/10.1016/j.orggeochem.2015.04.004

1524 Denis, D., Crosta, X., Barbara, L., et al. (2010) Sea ice and wind variability during the
1525 Holocene in East Antarctica: insight on middle–high latitude coupling. Quaternary
1526 Science Reviews 29, 3709–3719. https://doi.org/10.1016/j.quascirev.2010.08.007

1527 Denis, E.H., Toney, J.L., Tarozo, R., et al. (2012) Polycyclic aromatic hydrocarbons
1528 (PAHs) in lake sediments record historic fire events: Validation using HPLC-

fluorescence detection. Organic Geochemistry 45, 7–17. https://doi.org/10.1016/j.orggeochem.2012.01.005

De Rosa, M., Esposito, E., Gambacorta, A., *et al.* (1980) Effects of temperature on ether lipid composition of Caldariella acidophila. *Phytochemistry*, 19(5), pp. 827–831. https://doi.org/10.1016/0031-9422(80)85120-X.

Detlef, H., Belt, S.T., Sosdian, S.M., et al. (2018) Sea ice dynamics across the Mid-Pleistocene transition in the Bering Sea. Nat Commun 9, 941. https://doi.org/10.1038/s41467-018-02845-5

Diefendorf, A.F. and Freimuth, E.J. (2017) Extracting the most from terrestrial plant-derived n-alkyl lipids and their carbon isotopes from the sedimentary record: A review. Organic Geochemistry 103, 1–21. https://doi.org/10.1016/j.orggeochem.2016.10.016

Ding S,. Bale NJ,. Hopmans EC,. et al. (2021) Lipidomics of Environmental Microbial Communities. II: Characterization Using Molecular Networking and Information Theory. *Front. Microbiol.* 12:659315. https://doi.org/10.3389/fmicb.2021.659315

Dong, L., Li, Z., & Jia, G. (2019) Archaeal ammonia oxidation plays a part in late Quaternary nitrogen cycling in the South China Sea. *Earth and Planetary Science Letters*, **509**, 38– 46. https://doi.org/10.1016/j.epsl.2018.12.023

Dubois, N., and Jacob, J., (2016) Molecular Biomarkers of Anthropic Impacts in Natural Archives: A Review. Frontiers in Ecology and Evolution, 4. https://doi.org/10.3389/fevo.2016.00092

Duda, M.P., Hargan, K. E., Michelutti, N., et al. (2021) Reconstructing Long-Term Changes in Avian Populations Using Lake Sediments: Opening a Window Onto the Past. Frontiers in Ecology and Evolution, 9. https://doi.org/10.3389/fevo.2021.698175

Eglinton, G. and Calvin, M. (1967) Chemical Fossils. Sci Am 216, 32–43. https://doi.org/10.1038/scientificamerican0167-32

Eglinton, G., Hamilton, R.J., (1967) Leaf Epicuticular Waxes: The waxy outer surfaces of most plants display a wide diversity of fine structure and chemical constituents. Science 156, 1322–1335. https://doi.org/10.1126/science.156.3780.1322

Eglinton, T.I., Aliwihare, L.I., Bauer, J.E., (1996) Gas Chromatographic Isolation of Individual Compounds from Complex Matrices for Radiocarbon Dating. Anal. Chem., 68, 904-912. https://doi.org/10.1021/ac9508513

Eglinton, T.I., Galv, V.V., Hemingway, J.D. et al., (2021) Climate control on terrestrial biospheric carbon turnover. Proc. Nat. Acad. Sci., 118 (8) e2011585118. https://doi.org/10.1073/pnas.2011585118.

Eley, Y.L. and Hren, M.T. (2018) Reconstructing vapor pressure deficit from leaf wax lipid molecular distributions. Scientific Reports, 8(1), 3967. https://doi.org/10.1038/s41598-018-21959-w.

Elias, V. O., Simoneit, B. R. T., Cordeiro, R. C., et al. (2001) Evaluating levoglucosan as an indicator of biomass burning in Carajɑs, Amazônia: a comparison to the charcoal record. Geochim. Cosmochim. Acta 65, 267–272. https://doi.org/10.1016/S0016-7037(00)00522-6.

Englebrecht, A.C. and Sachs, J.P. (2005) Determination of sediment provenance at drift sites using hydrogen isotopes and unsaturation ratios in alkenones. *Geochimica et* Cosmochimica Acta, 69(17), 4253–4265. https://doi.org/10.1016/j.gca.2005.04.011.

1576 Epstein, B.L., D'Hondt, S. and Hargraves, P.E. (2001) The possible metabolic role of
1577 C37 alkenones in Emiliania huxleyi. Organic Geochemistry, 32(6), 867–875.
1578 https://doi.org/10.1016/S0146-6380(01)00026-2.

1579 Erdem, Z., Lattaud, J., van Erk, M. R., *et al.* (2021) Applicability of the Long Chain Diol
1580 Index (LDI) as a Sea Surface Temperature Proxy in the Arabian Sea.
1581 *Paleoceanography and* Paleoclimatology, 36(12), 4255
1582 https://doi.org/10.1029/2021PA004255.

1583 Etourneau, J., Collins, L.G., Willmott, V., et al. (2013) Holocene climate variations in
1584 the western Antarctic Peninsula: evidence for sea ice extent predominantly
1585 controlled by changes in insolation and ENSO variability. Clim. Past 9, 1431–
1586 1446. https://doi.org/10.5194/cp-9-1431-2013

1587 Evershed, R.P., (2008) Organic residue analysis in archaeology: the archaeological
1588 biomarker revolution. Archaeometry 50, 895–924. https://doi.org/10.1111/j.1475-
1589 4754.2008.00446.x

1590 Fabbri, D., Torri, C., Simoneit, B.R.T., et a. (2009) Levoglucosan and other cellulose
1591 and lignin markers in emissions from burning of Miocene lignites. Atmospheric
1592 Environment, 43 (14), 2286-2295.
1593 https://doi.org/10.1016/j.atmosenv.2009.01.030

1594 Fahl, K. and Stein, R. (1999) Biomarkers as organic-carbon-source and environmental
1595 indicators in the Late Quaternary Arctic Ocean: problems and perspectives.
1596 Marine Chemistry 63, 293–309. https://doi.org/10.1016/S0304-4203(98)00068-1

1597 Feakins, S.J., Wu, M.S., Ponton, C., et al (2019) Biomarkers reveal abrupt switches in
1598 hydroclimate during the last glacial in southern California. Earth and Planetary
1599 Science Letters 515, 164–172. https://doi.org/10.1016/j.epsl.2019.03.024

1600 Feng, X., Vonk, J.E., van Dongen, B.E., (2013) Differential mobilization of terrestrial
1601 carbon pools in Eurasian Arctic river basins. Proc. Natl. Acad. Sci. U.S.A. 110,
1602 14168–14173. https://doi.org/10.1073/pnas.1307031110

1603 Ficken, K.J., Li, B., Swain, D.L., et al. (2000) An n-alkane proxy for the sedimentary
1604 input of submerged/floating freshwater aquatic macrophytes. Organic
1605 Geochemistry 31, 745–749. https://doi.org/10.1016/S0146-6380(00)00081-4

1606 Fietz, S., Huguet, C., Bendle, J., et al. (2012) Co-variation of crenarchaeol and
1607 branched GDGTs in globally-distributed marine and freshwater sedimentary
1608 archives. Global and Planetary Change 92–93, 275–
1609 285.https://doi.org/10.1016/j.gloplacha.2012.05.020

1610 Foster, L.C., Pearson, E. J., Juggins, S., *et al.* (2016) Development of a regional
1611 glycerol dialkyl glycerol tetraether (GDGT)–temperature calibration for Antarctic
1612 and sub-Antarctic lakes. *Earth and Planetary Science Letters*, 433, 370–379.
1613 https://doi.org/10.1016/j.epsl.2015.11.018.

1614 Galy, V. and Eglinton, T. (2011) Protracted storage of biospheric carbon in the
1615 Ganges–Brahmaputra basin. *Nature Geoscience*, 4(12), 843–847.
1616 https://doi.org/10.1038/ngeo1293.

1617 Gaskell, S.J. and Eglinton, G. (1975) Rapid hydrogenation of sterols in a contemporary
1618 lacustrine sediment. *Nature*, 254(5497), 209–211.
1619 https://doi.org/10.1038/254209b0.

1620 Griepentrog, M., De Wispelaere, L., Bauters, M., *et al.* (2019) Influence of plant growth
1621 form, habitat and season on leaf-wax n-alkane hydrogen-isotopic signatures in
1622 equatorial East Africa. *Geochimica et Cosmochimica Acta*, 263, 122–139.
1623 https://doi.org/10.1016/j.gca.2019.08.004.

Günther, F., Thiele, A., Biskop, S., et al. (2016) Late quaternary hydrological changes at Tangra Yumco, Tibetan Plateau: a compound-specific isotope-based quantification of lake level changes. J Paleolimnol 55, 369–382. https://doi.org/10.1007/s10933-016-9887-1

Guo, F., Gao, M., Dong, J., *et al.* (2022) The first high resolution PAH record of industrialization over the past 200 years in Liaodong Bay, northeastern China. *Water Research*, 224, p. 119103. https://doi.org/10.1016/j.watres.2022.119103.

Hargan, K.E., Gilchrist, H.G., Clyde, N.M.T., et al. (2019) Multicentury perspective assessing the sustainability of the historical harvest of seaducks. Proc. Natl. Acad. Sci. U.S.A. 116, 8425–8430. https://doi.org/10.1073/pnas.1814057116

Harning, D.J., Curtin, L., Geirsdóttir, Á., et al. (2020) Lipid Biomarkers Quantify Holocene Summer Temperature and Ice Cap Sensitivity in Icelandic Lakes. Geophys. Res. Lett. 47. https://doi.org/10.1029/2019GL085728

Harrault, L., Milek, K., Jardé, E., et al. (2019) Faecal biomarkers can distinguish specific mammalian species in modern and past environments. PLoS ONE 14, e0211119. https://doi.org/10.1371/journal.pone.0211119

Harris, P.G. and Maxwell, J.R. (1995) A novel method for the rapid determination of chlorin concentrations at high stratigraphic resolution in marine sediments. Organic Geochemistry 23, 853–856. https://doi.org/10.1016/0146-6380(95)80007-E

Harris, P.G., Zhao, M., Rosell-Melé, A., et al. (1996) Chlorin accumulation rate as a proxy for Quaternary marine primary productivity. Nature 383, 63–65. https://doi.org/10.1038/383063a0

He, D., Bernd, R.T., Simoneit, J.B., *et al.* (2018) Early diagenesis of triterpenoids derived from mangroves in a subtropical estuary. *Organic Geochemistry*, 125, 196–211. https://doi.org/10.1016/j.orggeochem.2018.09.005.

He, Y., Zhao, C., Wang, Z., et al. (2013) Late Holocene coupled moisture and temperature changes on the northern Tibetan Plateau. Quaternary Science Review, 80 (2013), 47-57. https://doi.org/10.1016/j.quascirev.2013.08.017.

He, Y., Wang, H., Meng, B., et al. (2020) Appraisal of alkenone- and archaeal ether-based salinity indicators in mid-latitude Asian lakes. Earth Planet. Sc. Lett., 538, Article 116236. https://doi.org/10.1016/j.epsl.2020.116236

Hedges, J.I., Ertel, J.R., Leopold, E.B. (1982) Lignin geochemistry of a Late Quaternary sediment core from Lake Washington. Geochimica et Cosmochimica Acta 46, 1869–1877. https://doi.org/10.1016/0016-7037(82)90125-9

Hefter, J., Naafs, B.D.A., Zhang, S., (2017) Tracing the source of ancient reworked organic matter delivered to the North Atlantic Ocean during Heinrich Events. Geochimica et Cosmochimica Acta 205, 211–225. https://doi.org/10.1016/j.gca.2017.02.008

Heidke, I., Scholz, D., Hoffmann, T., (2019) Lignin oxidation products as a potential proxy for vegetation and environmental changes in speleothems and cave drip water – a first record from the Herbstlabyrinth, central Germany. Clim. Past 15, 1025–1037. https://doi.org/10.5194/cp-15-1025-2019

Hepp, J., Tuthorn, M., Zech, R., *et al.* (2015) Reconstructing lake evaporation history and the isotopic composition of precipitation by a coupled δ18O–δ2H biomarker approach. *Journal of Hydrology*, 529, pp. 622–631. https://doi.org/10.1016/j.jhydrol.2014.10.012.

1671 Herbert, T.D., Peterson, L.C., Lawrence, K.T., et al. (2010) Tropical Ocean
1672 Temperatures Over the Past 3.5 Million Years. Science 328, 1530–1534.
1673 https://doi.org/10.1126/science.1185435

1674 Hodgson, D.A., Wright, S. W., Tyler, P.A., *et al.* (1998) Analysis of fossil pigments from
1675 algae and bacteria in meromictic Lake Fidler, Tasmania, and its application to lake
1676 management. *Journal of Paleolimnology*, 19(1), pp. 1–22.
1677 https://doi.org/10.1023/A:1007909018527.

1678 Hodgson, D.A., McMinn, A., Kirkup, H., et al. (2003) Colonization, succession, and
1679 extinction of marine floras during a glacial cycle: A case study from the Windmill
1680 Islands (east Antarctica) using biomarkers: late Quaternary marine floras.
1681 Paleoceanography 18. https://doi.org/10.1029/2002PA000775

1682 Hodgson, D.A., Vyverman, W., Verleyen, E., et al. (2005) Late Pleistocene record of
1683 elevated UV radiation in an Antarctic lake. Earth and Planetary Science Letters
1684 236, 765–772. https://doi.org/10.1016/j.epsl.2005.05.023

1685 Hoff, U., Rasmussen, T.L., Stein, R., et al. (2016) Sea ice and millennial-scale climate
1686 variability in the Nordic seas 90 kyr ago to present. Nat Commun 7, 12247.
1687 https://doi.org/10.1038/ncomms12247

1688 Holtvoeth, J., Whiteside, J.H., Engels, S., et al. (2019) The paleolimnologist's guide to
1689 compound-specific stable isotope analysis – An introduction to principles and
1690 applications of CSIA for Quaternary lake sediments. Quaternary Science Reviews
1691 207, 101–133. https://doi.org/10.1016/j.quascirev.2019.01.001

1692 Hopmans, E.C., Weijers, J.W.H., Schefuß, E., et al. (2004) A novel proxy for terrestrial
1693 organic matter in sediments based on branched and isoprenoid tetraether lipids.
1694 Earth and Planetary Science Letters 224, 107–116.
1695 https://doi.org/10.1016/j.epsl.2004.05.012

1696 Huang, Y., Shuman, B., Wang, Y., et al. (2004) Hydrogen isotope ratios of individual
1697 lipids in lake sediments as novel tracers of climatic and environmental change: a
1698 surface sediment test. Journal of Paleolimnology 31, 363–375.
1699 https://doi.org/10.1023/B:JOPL.0000021855.80535.13

1700 Huang, Y., Shuman, B., Wang, Y., (2006) Climatic and environmental controls on the
1701 variation of C3 and C4 plant abundances in central Florida for the past 62,000
1702 years. Palaeogeography, Palaeoclimatology, Palaeoecology 237, 428–435.
1703 https://doi.org/10.1016/j.palaeo.2005.12.014

1704 Huang, X., Wang, C., Zhang, J., et al. (2011) Comparison of free lipid compositions
1705 between roots and leaves of plants in the Dajiuhu Peatland, central China,
1706 Geochem. J., 45, 365–373. https://doi.org/10.2343/geochemj.1.0129, 2011.

1707 Huguet, C., Routh, J., Fietz, S., et al. (2018) Temperature and Monsoon Tango in a
1708 Tropical Stalagmite: Last Glacial-Interglacial Climate Dynamics. Sci Rep 8, 5386.
1709 https://doi.org/10.1038/s41598-018-23606-w

1710 Inglis, G.N., Naafs, B.D.A., Zheng, Y., et al. (2018) Distributions of geohopanoids in
1711 peat: Implications for the use of hopanoid-based proxies in natural archives.
1712 Geochimica et Cosmochimica Acta 224, 249–261.
1713 https://doi.org/10.1016/j.gca.2017.12.029

1714 Inglis, G.N., and Tierney, J.E., (2020) The TEX86 Paleotemperature Proxy, 1st ed.
1715 Cambridge University Press. https://doi.org/10.1017/9781108846998

1716 Inglis, G.N., Bhattacharya, T., Hemingway, J.D., et al. (2022) Biomarker Approaches
1717 for Reconstructing Terrestrial Environmental Change. Annu. Rev. Earth Planet.
1718 Sci. 50, 369–394. https://doi.org/10.1146/annurev-earth-032320-095943

Innes, H.E., Bishop, A.N., Head, I.M., *et al.* (1997) Preservation and diagenesis of hopanoids in Recent lacustrine sediments of Priest Pot, England. Organic Geochemistry, 26(9), pp. 565–576. https://doi.org/10.1016/S0146-6380(97)00017-X.

Jacob, J., Disnar, J.-R., Arnaud, F., et al. (2008a) Millet cultivation history in the French Alps as evidenced by a sedimentary molecule. Journal of Archaeological Science 35, 814–820. https://doi.org/10.1016/j.jas.2007.06.006

Jacob, J., Disnar, J.-R., Bardoux, G., et al. (2008b) Carbon isotope evidence for sedimentary miliacin as a tracer of Panicum miliaceum (broomcorn millet) in the sediments of Lake le Bourget (French Alps). Organic Geochemistry 39, 1077–1080. https://doi.org/10.1016/j.orggeochem.2008.04.003

Jaffé, R., Mead, R., Hernandez, M.E., (2001) Origin and transport of sedimentary organic matter in two subtropical estuaries: a comparative, biomarker-based study. Organic Geochemistry 32 (4), 507-526. https://doi.org/10.1016/S0146-6380(00)00192-3

Jeffrey, S.W., Mantoura, R.F.C. and Wright, S.W. (1997, Eds.) Phytoplankton pigments in oceanography (1997, Eds.): 261-282.

Jessen, G.L., Lichtschlag, A., Ramette, A., et al. (2017) Hypoxia causes preservation of labile organic matter and changes seafloor microbial community composition (Black Sea). Sci. Adv. 3(2), e1601897. https://doi.org/10.1126/sciadv.1601897

Jetter, R., Kunst, L., & Samuels, A. L. (2006). Composition of plant cuticular waxes. Annual plant reviews volume 23: Biology of the plant cuticle, 145-181.

Johnson, K.M., McKay, R.M., Etourneau, J., et al. (2021) Sensitivity of Holocene East Antarctic productivity to subdecadal variability set by sea ice. Nat. Geosci. 14, 762–768. https://doi.org/10.1038/s41561-021-00816-y

Kahmen, A., Schefuß, E. and Sachse, D. (2013) Leaf water deuterium enrichment shapes leaf wax n-alkane δD values of angiosperm plants I: Experimental evidence and mechanistic insights. Geochimica et Cosmochimica Acta, 111, pp. 39–49. https://doi.org/10.1016/j.gca.2012.09.003.

Kalpana, M.S., Routh, J., Fietz, S., et al. (2021) Sources, Distribution and Paleoenvironmental Application of Fatty Acids in Speleothem Deposits From Krem Mawmluh, Northeast India. Front. Earth Sci. 9, 687376. https://doi.org/10.3389/feart.2021.687376

Karp, A.T., Holman, A.I., Hopper, P., et al. (2020) Fire distinguishers: Refined interpretations of polycyclic aromatic hydrocarbons for paleo-applications. Geochimica et Cosmochimica Acta 289, 93–113. https://doi.org/10.1016/j.gca.2020.08.024

Kasper, S., van der Meer, M.T.J., Mets, A., et al. (2014) Salinity changes in the Agulhas leakage area recorded by stable hydrogen isotopes of C_{37}-alkenones during Termination I and II. Clim. Past 10, 251–260. https://doi.org/10.5194/cp-10-251-2014

Katrantsiotis, C., Norström, E., Rienk, H., et al. (2021) Seasonal variability in temperature trends and atmospheric circulation systems during the Eemian (Last Interglacial) based on n-alkanes hydrogen isotopes from Northern Finland. Quaternary Science Reviews, 273, p. 107250. https://doi.org/10.1016/j.quascirev.2021.107250.

Keenan, B., Imfeld, A., Johnston, K., *et al.* (2021) Molecular evidence for human population change associated with climate events in the Maya lowlands.

Quaternary Science Reviews, 258, p. 106904. https://doi.org/10.1016/j.quascirev.2021.106904.

Keenan, B., Imfeld, A., Gélinas, Y., et al. (2022) Understanding controls on stanols in lake sediments as proxies for palaeopopulations in Mesoamerica. J Paleolimnol 67, 375–390. https://doi.org/10.1007/s10933-022-00238-9

Kehelpannala, C., Rupasinghe, TWT., Hennessy, T., et al (2020) A comprehensive comparison of four methods for extracting lipids from Arabidopsis tissues. Plant Methods. 2020 Dec 3;16(1):155. https://doi.org/10.1186/s13007-020-00697-z.

Kemp, A.C., Vane, C.H., Kim, A.W., (2022) Fecal steroids as a potential tool for conservation paleobiology in East Africa. Biodivers Conserv 31, 183–209. https://doi.org/10.1007/s10531-021-02328-y

Killops, S.D. and Killops, V.J. (2013) Introduction to Organic Geochemistry (2nd Edition), Wiley-Blackwell, 408pp.

Kim, J.-H., van der Meer, J., Schouten, S.,et al. (2010) New indices and calibrations derived from the distribution of crenarchaeal isoprenoid tetraether lipids: Implications for past sea surface temperature reconstructions. Geochimica et Cosmochimica Acta 74, 4639-4654. https://doi.org/10.1016/j.gca.2010.05.027

Kirchgeorg, T., Schüpbach, S., Kehrwald,N., *et al.* (2014) Method for the determination of specific molecular markers of biomass burning in lake sediments. *Organic Geochemistry*, 71, pp. 1–6. https://doi.org/10.1016/j.orggeochem.2014.02.014.

Kjellman, S.E., Schomacker, A., Thomas, E.K., *et al.* (2020) Holocene precipitation seasonality in northern Svalbard: Influence of sea ice and regional ocean surface conditions. *Quaternary Science Reviews*, 240, p. 106388. https://doi.org/10.1016/j.quascirev.2020.106388.

Knies, J., Cabedo-Sanz, P., Belt, S.T., et al. (2014) The emergence of modern sea ice cover in the Arctic Ocean. Nat Commun 5, 5608. https://doi.org/10.1038/ncomms6608

Koch, B.P., Souza Filho, P.W.M., Behling, H., et al. (2011) Triterpenols in mangrove sediments as a proxy for organic matter derived from the red mangrove (Rhizophora mangle). Organic Geochemistry 42, 62–73. https://doi.org/10.1016/j.orggeochem.2010.10.007

Kornilova, O. and Rosell-Melé, A. (2003) Application of microwave-assisted extraction to the analysis of biomarker climate proxies in marine sediments. Organic Geochemistry 34, 1517–1523. https://doi.org/10.1016/S0146-6380(03)00155-4

Krentscher, C., Dubois, N., Camperio, G., et al. (2019) Palmitone as a potential species-specific biomarker for the crop plant taro (Colocasia esculenta Schott) on remote Pacific islands. Organic Geochemistry 132, 1-10. https://doi.org/10.1016/j.orggeochem.2019.03.006

Kuo, L.-J., Herbert, B.E. and Louchouarn, P. (2008) Can levoglucosan be used to characterize and quantify char/charcoal black carbon in environmental media? *Organic Geochemistry*, 39(10), pp. 1466–1478. https://doi.org/10.1016/j.orggeochem.2008.04.026.

Kuo, L.-J., Louchouarn, P., Herbert, B.E., (2011) Influence of combustion conditions on yields of solvent-extractable anhydrosugars and lignin phenols in chars: Implications for characterizations of biomass combustion residues. Chemosphere 85, 797–805. https://doi.org/10.1016/j.chemosphere.2011.06.074

1814 Kusch, S and Rush, D.(2022) Revisiting the precursors of the most abundant natural
1815 products on Earth: A look back at 30+ years of bacteriohopanepolyol (BHP)
1816 research and ahead to new frontiers. Organic Geochemistry 172, 104469.
1817 https://doi.org/10.1016/j.orggeochem.2022.104469

1818 Kusch, S., Winterfeld, M., Mollenhauer, G., et al (2019) Glycerol dialkyl glycerol
1819 tetraethers (GDGTs) in high latitude Siberian permafrost: Diversity, environmental
1820 controls, and implications for proxy applications. Organic Geochemistry 136,
1821 103888. https://doi.org/10.1016/j.orggeochem.2019.06.009

1822 Ladd, N, S. and Sachs, J.P. (2012) Inverse relationship between salinity and n-alkane
1823 δD values in the mangrove Avicennia marina. Organic Geochemistry, 48, pp. 25–
1824 36. https://doi.org/10.1016/j.orggeochem.2012.04.009.

1825 Ladd, S.N. and Sachs, J.P. (2015) Influence of salinity on hydrogen isotope
1826 fractionation in Rhizophora mangroves from Micronesia, Geochimica et
1827 Cosmochimica Acta 168, 206-221. https://doi.org/10.1016/j.gca.2015.07.004.

1828 Lamb, H. H. (1977) Climatic History and the Future (Climate: Present, Past and
1829 Future, vol. 2; Methuen.

1830 Lamping, N., Müller, J., Esper, O., et al (2020) Highly branched isoprenoids reveal
1831 onset of deglaciation followed by dynamic sea-ice conditions in the western
1832 Amundsen Sea, Antarctica. Quaternary Science Reviews 228, 106103.
1833 https://doi.org/10.1016/j.quascirev.2019.106103

1834 Lang, D.C., Bailey, I., Wilson, P.A., et al. (2014) The transition on North America from
1835 the warm humid Pliocene to the glaciated Quaternary traced by eolian dust
1836 deposition at a benchmark North Atlantic Ocean drill site. Quaternary Science
1837 Reviews 93, 125–141. https://doi.org/10.1016/j.quascirev.2014.04.005

1838 Larson, E.A., Afolabi, A., Zheng, J., et al.(2022) Sterols and sterol ratios to trace fecal
1839 contamination: pitfalls and potential solutions. Environ Sci Pollut Res Int.
1840 Jul;29(35):53395-53402. https://doi.org/10.1007/s11356-022-19611-2.

1841 Lattaud, J., Balzano, S., Marcel, T.J., *et al.* (2021) Sources and seasonality of long-
1842 chain diols in a temperate lake (Lake Geneva). Organic Geochemistry, 156, p.
1843 104223. https://doi.org/10.1016/j.orggeochem.2021.104223.

1844 Lavrieux, M., Jacob, J., Disnar, J.-R., et al. (2013) Sedimentary cannabinol tracks the
1845 history of hemp retting. Geology 41, 751–754. https://doi.org/10.1130/G34073.1

1846 Leavitt, P.R., (1993) A review of factors that regulate carotenoid and chlorophyll
1847 deposition and fossil pigment abundance. J Paleolimnol 9, 109–127.
1848 https://doi.org/10.1007/BF00677513

1849 Leeming, R., Ball, A., Ashbolt, N., et al (1996) Using faecal sterols from humans and
1850 animals to distinguish faecal pollution in receiving waters. Water Research 30,
1851 2893–2900. https://doi.org/10.1016/S0043-1354(96)00011-5

1852 Li, X., Wang, C., Huang, J., (2011) Seasonal variation of fatty acids from drip water in
1853 Heshang Cave, central China. Applied Geochemistry 26, 341–347.
1854 https://doi.org/10.1016/j.apgeochem.2010.12.007

1855 Liu, W., Yang, H. and Li, L. (2006) Hydrogen isotopic compositions of n-alkanes from
1856 terrestrial plants correlate with their ecological life forms. *Oecologia*, 150(2), 330–
1857 338. https://doi.org/10.1007/s00442-006-0494-0.

1858 Liu, W. and Yang, H. (2008) Multiple controls for the variability of hydrogen isotopic
1859 compositions in higher plant *n*-alkanes from modern ecosystems. Global Change
1860 Biology, 14: 2166-2177. https://doi.org/10.1111/j.1365-2486.2008.01608.x

1861 Liu, W., Liu, Z., Fu, M., et al. (2008) Distribution of the C37 tetra-unsaturated alkenone
1862 in Lake Qinghai, China: A potential lake salinity indicator. Geochimica et
1863 Cosmochimica Acta 72 (3), 988-997. https://doi.org/10.1016/j.gca.2007.11.016

1864 Liu, W.G., Yang, H., Wang, HY., et al. (2015) Carbon isotope composition of long
1865 chain leaf wax n-alkanes in lake sediments: A dual indicator of paleoenvironment
1866 in the Qinghai-Tibet Plateau. Organic Geochemistry, 83–84, 190–201.
1867 https://doi.org/10.1016/j.orggeochem.2015.03.017.

1868 Liu, W., Liu, Z., Wang, H., *et al.* (2011) Salinity control on long-chain alkenone
1869 distributions in lake surface waters and sediments of the northern Qinghai-Tibetan
1870 Plateau, China. Geochimica et Cosmochimica Acta, 75(7), 1693–1703.
1871 https://doi.org/10.1016/j.gca.2010.10.029.

1872 Liu, J. (2021) Seasonality of the altitude effect on leaf wax n-alkane distributions,
1873 hydrogen and carbon isotopes along an arid transect in the Qinling Mountains.
1874 Science of The Total Environment, 778, 146272.
1875 https://doi.org/10.1016/j.scitotenv.2021.146272.

1876 Liu, J., Zhao, J., He, D., *et al.* (2022) Effects of plant types on terrestrial leaf wax long-
1877 chain n-alkane biomarkers: Implications and paleoapplications. *Earth-Science*
1878 *Reviews*, 235,104248. https://doi.org/10.1016/j.earscirev.2022.104248.

1879 Lima, A.L.C., Farrington, J.W., Reddy, C.M., (2005) Combustion-Derived Polycyclic
1880 Aromatic Hydrocarbons in the Environment—A Review. Environmental Forensics
1881 6, 109–131. https://doi.org/10.1080/15275920590952739

1882 Loakes, K.L., Ryves, D.B., Lamb, H.F., et al (2018) Late Quaternary climate change in
1883 the north-eastern highlands of Ethiopia: A high resolution 15,600 year diatom and
1884 pigment record from Lake Hayk. Quaternary Science Reviews 202, 166–181.
1885 https://doi.org/10.1016/j.quascirev.2018.09.005

1886 Longo, W.M., Theroux, S., Giblin, A.E., et al. (2016) Temperature calibration and
1887 phylogenetically distinct distributions for freshwater alkenones: Evidence from
1888 northern Alaskan lakes. Geochimica et Cosmochimica Acta 180, 177–196.
1889 https://doi.org/10.1016/j.gca.2016.02.019

1890 Loomis, S.E., Russell, J.M., Ladd, B., et al. (2012) Calibration and application of the
1891 branched GDGT temperature proxy on East African lake sediments. Earth and
1892 Planetary Science Letters 357–358, 277-288.
1893 https://doi.org/10.1016/j.epsl.2012.09.031

1894 Loomis, S.E., Russell, J.M., Heureux, A.M., et al. (2014) Seasonal variability of
1895 branched glycerol dialkyl glycerol tetraethers (brGDGTs) in a temperate lake
1896 system. Geochimica et Cosmochimica Acta 144, 173-187.
1897 https://doi.org/10.1016/j.gca.2014.08.027.

1898 Lopes dos Santos, R.A., Spooner, M.I., Barrows, T.T., et al. (2013a) Comparison of
1899 organic ($U^{K'}_{37}$, TEX^{H}_{86} , LDI) and faunal proxies (foraminiferal assemblages) for
1900 reconstruction of late Quaternary sea surface temperature variability from
1901 offshore southeastern Australia: SST from offshore Southeastern Australia.
1902 Paleoceanography 28, 377–387. https://doi.org/10.1002/palo.20035

1903 Lopes dos Santos, R.A., De Deckker, P., Hopmans, E.C., et al. (2013b) Abrupt
1904 vegetation change after the Late Quaternary megafaunal extinction in
1905 southeastern Australia. Nature Geosci 6, 627–631.
1906 https://doi.org/10.1038/ngeo1856

1907 Lu, H., Zhu, L., & Zhu, N. (2009) Polycyclic aromatic hydrocarbon emission from straw
1908 burning and the influence of combustion parameters. Atmospheric
1909 Environment, **43**(4), 978–983. https://doi.org/10.1016/j.atmosenv.2008.10.02

1910 Lupien, R.L., Russell, J.M., Pearson, E.J., et al. (2022) Orbital controls on eastern
1911 African hydroclimate in the Pleistocene. Sci Rep 12, 3170.
1912 https://doi.org/10.1038/s41598-022-06826-z

1913 Mackay, H., Davies, K.L., Robertson, J., et al. (2020) Characterising life in settlements
1914 and structures: Incorporating faecal lipid biomarkers within a multiproxy case
1915 study of a wetland village. Journal of Archaeological Science 121, 105202.
1916 https://doi.org/10.1016/j.jas.2020.105202

1917 Madureira, L.A.S., van Kreveld, S.A., Eglinton, G., et al. (1997) Late Quaternary high-
1918 resolution biomarker and other sedimentary climate proxies in a Northeast
1919 Atlantic Core. Paleoceanography 12, 255–269.
1920 https://doi.org/10.1029/96PA03120

1921 Magill, C.R., Ashley, G.M. and Freeman, K.H. (2013) Ecosystem variability and early
1922 human habitats in eastern Africa. Proceedings of the National Academy of
1923 Sciences, 110(4), 1167–1174. https://doi.org/10.1073/pnas.1206276110.

1924 Maloney, A.E., Richey, J.N., Nelson, D.B., *et al.* (2022) Contrasting Common Era
1925 climate and hydrology sensitivities from paired lake sediment dinosterol hydrogen
1926 isotope records in the South Pacific Convergence Zone. Quaternary Science
1927 Reviews, 281, 107421. https://doi.org/10.1016/j.quascirev.2022.107421.

1928 Mallorquí, N., Arellano, J.B., Borrego, C.M., et al. (2005) Signature pigments of green
1929 sulfur bacteria in lower Pleistocene deposits from the Banyoles lacustrine area
1930 (Spain). J Paleolimnol 34, 271–280. https://doi.org/10.1007/s10933-005-3731-3

1931 Manley, A., Collins, A. L., Joynes, A., *et al.* (2020) Comparing Extraction Methods for
1932 Biomarker Steroid Characterisation from Soil and Slurry. *Water, Air, & Soil*
1933 *Pollution*, 231(10), 524. https://doi.org/10.1007/s11270-020-04871-w.

1934 MARGO Project Members (2005) Constraints on the magnitude and patterns of ocean
1935 cooling at the Last Glacial Maximum. Nature Geosci 2, 127–132.
1936 https://doi.org/10.1038/ngeo411

1937 Marino, G., Rohling, E.J., Rijpstra, W.I.C., et al. (2007) Aegean Sea as driver of
1938 hydrographic and ecological changes in the eastern Mediterranean. Geol 35, 675.
1939 https://doi.org/10.1130/G23831A.1

1940 Martínez-Garcia, A., Rosell-Melé, A., Geibert, W., et al. (2009) Links between iron
1941 supply, marine productivity, sea surface temperature, and CO2 over the last 1.1
1942 Ma. Paleoceanography, 24. http://dx.doi.org/10.1029/2008PA001657

1943 Martínez-Garcia, A., Rosell-Melé, A., McClymont, E.L., et al. (2010) Subpolar Link to
1944 the Emergence of the Modern Equatorial Pacific Cold Tongue. Science 328,
1945 1550–1553. https://doi.org/10.1126/science.1184480

1946 Martínez-Garcia, A., Rosell-Melé, A., Jaccard, S.L., et al (2011) Southern Ocean dust–
1947 climate coupling over the past four million years. Nature 476, 312–315.
1948 https://doi.org/10.1038/nature10310

1949 Martínez-Sosa, P., Tierney, J.E., Stefanescu, I.C., et al (2021) A global Bayesian
1950 temperature calibration for lacustrine brGDGTs.
1951 https://doi.org/10.1594/PANGAEA.931169

1952 Martrat, B., Grimalt, J.O., Shackleton, N.J., et al. (2007) Four Climate Cycles of
1953 Recurring Deep and Surface Water Destabilizations on the Iberian Margin.
1954 Science 317, 502–507. https://doi.org/10.1126/science.1139994

1955 Massa, C., Beilman, D.W., Nichols, J.E., *et al.* (2021) Central Pacific hydroclimate over
1956 the last 45,000 years: Molecular-isotopic evidence from leaf wax in a Hawai'i

peatland. *Quaternary Science Reviews*, 253, 106744. https://doi.org/10.1016/j.quascirev.2020.106744.

Massé, G., Belt, S.T., Crosta, X., et al. (2011) Highly branched isoprenoids as proxies for variable sea ice conditions in the Southern Ocean. Antartic science 23, 487–498. https://doi.org/10.1017/S0954102011000381

Masson-Delmotte, V., Zhai, P., Pirani, A., et al. (2021) Climate Change 2021: The Physical Science Basis. Contribution of Working Group I to the Sixth Assessment Report of the Intergovernmental Panel on Climate Change, Cambridge University Press, Cambridge, United Kingdom and New York, NY, USA, https://doi.org/10.1017/9781009157896.

McClymont, E.L., Rosell-Melé, A., Giraudeau, J., et al. (2005) Alkenone and coccolith records of the Mid-Pleistocene in the south-east Atlantic: Implications for the U^{K}_{37}' index and south African climate. Quaternary Science Reviews 24, 1559-1572. https://doi.org/10.1016/j.quascirev.2004.06.024.

McClymont, E.L., Martínez-Garcia, A., Rosell-Melé, A., (2007) Benefits of freeze-drying sediments for the analysis of total chlorins and alkenone concentrations in marine sediments. Organic Geochemistry 38, 1002–1007. https://doi.org/10.1016/j.orggeochem.2007.01.006

McClymont, E.L., Mauquoy, D., Yeloff, D., et al. (2008a) The disappearance of Sphagnum imbricatum from Butterburn Flow, The Holocene, 18, 991-1002.https://doi.org/10.1177/0959683608093537

McClymont, E.L., Rosell-Melé, A., Haug, G., et al. (2008b) Expansion of subarctic water masses in the north Atlantic and Pacific Oceans and implications for mid-Pleistocene ice-sheet growth. Paleoceanography, 23, PA4214. https://doi.org/10.1029/2008PA001622.

McClymont, E. L., Bingham, E.M., Nott, C.J., et al. (2011) Pyrolysis GC–MS as a rapid screening tool for determination of peat-forming plant composition in cores from ombrotrophic peat. Organic Geochemistry, 42, 1420-1435. https://doi.org/10.1016/j.orggeochem.2011.07.004

McClymont, E.L., Ganeshram, R.S., Pichevin, L.E., et al (2012) Sea-surface temperature records of Termination 1 in the Gulf of California: Challenges for seasonal and interannual analogues of tropical Pacific climate change: Gulf of California termination 1. Paleoceanography 27(2). https://doi.org/10.1029/2011PA002226

McClymont, E.L., Sosdian, S.M., Rosell-Melé, A., et al. (2013) Pleistocene sea-surface temperature evolution: Early cooling, delayed glacial intensification, and implications for the mid-Pleistocene climate transition. Earth-Science Reviews 123, 173–193. https://doi.org/10.1016/j.earscirev.2013.04.006

McClymont, E.L., Bentley, M.J., Hodgson, D.A., et al. (2022) Summer sea-ice variability on the Antarctic margin during the last glacial period reconstructed from snow petrel (*Pagodroma nivea*) stomach-oil deposits. Clim. Past 18, 381–403. https://doi.org/10.5194/cp-18-381-2022

McGowan, S. (2007) Pigments in sediments of aquatic environments. Encyclopedia of Quaternary Science. Elsevier, Amsterdam (2007): 2062-2074.

McGowan, S., Barker, P., Haworth, E.Y., et al. (2012) Humans and climate as drivers of algal community change in Windermere since 1850. *Freshwater Biology*, 57(2), 260–277. https://doi.org/10.1111/j.1365-2427.2011.02689.x

McGowan, S., 2013. Paleolimnology - Pigment Studies, in: Elias, S.A., Mock, C.J. (Eds.), Encyclopedia of Quaternary Science (Second Edition). Elsevier, Amsterdam, pp. 326-338. https://doi.org/10.1016/B0-444-52747-8/00247-7

Meckler, A.N., Vonhof, H., Martínez-García, A., (2021) Temperature Reconstructions Using Speleothems. Elements 17, 101–106. https://doi.org/10.2138/gselements.17.2.101

Meyers, P.A., (2003) Applications of organic geochemistry to paleolimnological reconstructions: a summary of examples from the Laurentian Great Lakes. Organic Geochemistry 34, 261–289. https://doi.org/10.1016/S0146-6380(02)00168-7

Mochida, M., Kawamura, K., Fu, P., *et al.* (2010) Seasonal variation of levoglucosan in aerosols over the western North Pacific and its assessment as a biomass-burning tracer. *Atmospheric Environment*, 44(29), 3511–3518. https://doi.org/10.1016/j.atmosenv.2010.06.017.

Müller, P.J., Kirst, G., Ruhland, G., et al. (1998) Calibration of the alkenone paleotemperature index U37K′ based on core-tops from the eastern South Atlantic and the global ocean (60°N-60°S). Geochimica et Cosmochimica Acta 62, 1757–1772. https://doi.org/10.1016/S0016-7037(98)00097-0

Müller, J., Massé, G., Stein, R., et al. (2009) Variability of sea-ice conditions in the Fram Strait over the past 30,000 years. Nature Geosci 2, 772–776. https://doi.org/10.1038/ngeo665

Müller, J., Romero, O., Cowan, E.A., et al. (2018) Cordilleran ice-sheet growth fueled primary productivity in the Gulf of Alaska, northeast Pacific Ocean. Geology, 46 (4), 307-310. https://doi.org/10.1130/G39904.1.

Muñoz, S.E., Porter, T.J., Bakkelund, A., et al. (2020) Lipid Biomarker Record Documents Hydroclimatic Variability of the Mississippi River Basin During the Common Era. Geophysical Research Letters 47. https://doi.org/10.1029/2020GL087237

Naafs, B.D.A., Hefter, J., Acton, G., et al. (2012) Strengthening of North American dust sources during the late Pliocene (2.7Ma). Earth and Planetary Science Letters 317–318, 8–19. https://doi.org/10.1016/j.epsl.2011.11.026

Naafs, B.D.A., Hefter, J., Grützner, J., et al. (2013) Warming of surface waters in the mid-latitude North Atlantic during Heinrich events: HIGH SSTs DURING HEINRICH EVENTS. Paleoceanography 28, 153–163. https://doi.org/10.1029/2012PA002354

Naafs, B.D.A., Gallego-Sala, A.V., Inglis, G.N., et al. (2017) Refining the global branched glycerol dialkyl glycerol tetraether (brGDGT) soil temperature calibration. Organic Geochemistry 106, 48–56. https://doi.org/10.1016/j.orggeochem.2017.01.009

Naafs, B.D.A., Inglis, G.N., Blewett, J., et al. (2019) The potential of biomarker proxies to trace climate, vegetation, and biogeochemical processes in peat: A review. Global and Planetary Change 179, 57–79. https://doi.org/10.1016/j.gloplacha.2019.05.006

Nakakuni, M., Dairiki, C., Kaur, G., et al. (2017) Stanol to sterol ratios in late Quaternary sediments from southern California: An indicator for continuous variability of the oxygen minimum zone. Organic Geochemistry 111, 126–135. https://doi.org/10.1016/j.orggeochem.2017.06.009

Nelson, D.B. and Sachs, J.P. (2014) The influence of salinity on D/H fractionation in dinosterol and brassicasterol from globally distributed saline and hypersaline

2053 lakes. Geochimica et Cosmochimica Acta, 133, 325–339.
2054 https://doi.org/10.1016/j.gca.2014.03.007.

2055 Ngugi, C.C., Oyoo-Okoth, E., Gichuki, J., et al. (2017) Fingerprints of upstream
2056 catchment land use in suspended particulate organic matter (SPOM) at the river
2057 discharge sites in Lake Victoria (Kenya): insights from element, stable isotope
2058 and lipid biomarker analysis. Aquat Sci 79, 73–87.
2059 https://doi.org/10.1007/s00027-016-0480-5

2060 Nicholl, J., Hodell, D., Naafs, B., et al. (2012) A Laurentide outburst flooding event
2061 during the last interglacial period. Nature Geoscience, 5(12), pp. 901–904.
2062 https://doi.org/10.1038/ngeo1622.

2063 Nichols, J.E., Booth, R.K., Jackson, S.T., et al. (2006) Paleohydrologic reconstruction
2064 based on n-alkane distributions in ombrotrophic peat. Organic Geochemistry 37,
2065 1505–1513. https://doi.org/10.1016/j.orggeochem.2006.06.020

2066 Nichols, J.E., (2010) Procedures for extraction and purification of leaf wax biomarkers
2067 from peats. Mires and Peats, 7, Article 13, 1-7.

2068 Nichols, J.E. and Huang, Y. (2012) Hydroclimate of the northeastern United States is
2069 highly sensitive to solar forcing. Geophys. Res. Lett. 39,
2070 https://doi.org/10.1029/2011GL050720

2071 Niedermeyer, E.M., Sessions, A.L., Feakins, S.J., *et al.* (2014) Hydroclimate of the
2072 western Indo-Pacific Warm Pool during the past 24,000 years. Proceedings of
2073 the National Academy of Sciences, 111(26), 9402–9406.
2074 https://doi.org/10.1073/pnas.1323585111.

2075 Nishihara, M. and Koga, Y. (1987) Extraction and Composition of Polar Lipids from the
2076 Archaebacterium, Methanobacterium thermoautotrophicum : Effective Extraction
2077 of Tetraether Lipids by an Acidified Solvent 1. The Journal of Biochemistry,
2078 101(4), pp. 997–1005. https://doi.org/10.1093/oxfordjournals.jbchem.a121969.

2079 Norström, E., Katrantsiotis, C., Finné, M., et al. (2018) Biomarker hydrogen isotope
2080 composition (δD) as proxy for Holocene hydroclimatic change and seismic
2081 activity in SW Peloponnese, Greece. J. Quaternary Sci., 33(5), 563-574.
2082 https://doi.org/10.1002/jqs.3036.

2083 Ohkouchi, N., Eglinton, T.I., Keigwin, L.D., et al. (2002) Spatial and Temporal Offsets
2084 Between Proxy Records in a Sediment Drift. Science 298(5596), 1224-1227.
2085 https:doi/ord/10.1126/science.1075287

2086 Orem, W.H., Colman, S.M., Lerch, H.E., (1997) Lignin phenols in sediments of Lake
2087 Baikal, Siberia: application to paleoenvironmental studies. Organic Geochemistry
2088 27, 153–172. https://doi.org/10.1016/S0146-6380(97)00079-X

2089 Oros, D.R. and Simoneit, B.R.T. (2001) Identification and emission factors of
2090 molecular tracers in organic aerosols from biomass burning Part 1. Temperate
2091 climate conifers. Applied Geochemistry 16, 1513–1544.
2092 https://doi.org/10.1016/S0883-2927(01)00021-X

2093 Ortiz, J.E., Gallego, J.L.R., Torres, T., et al. (2010) Palaeoenvironmental
2094 reconstruction of Northern Spain during the last 8000calyr BP based on the
2095 biomarker content of the Roñanzas peat bog (Asturias). Organic Geochemistry,
2096 41(5),454-466, https://doi.org/10.1016/j.orggeochem.2010.02.003.

2097 Ourisson, G., Albrecht, P., & Rohmer, M., (1979) The hopanoids: palaeochemistry and
2098 biochemistry of a group of natural products. Pure and Applied Chemistry, 51(4),
2099 709-729. https://doi.org/10.1351/pac197951040709.

2100 Pahnke, K., Sachs, J. P., Keigwin, L., (2007) Eastern tropical Pacific hydrologic
2101 changes during the past 27,000 years from D/H ratios in
2102 alkenones. Paleoceanography, 22, PA4214. doi:10.1029/2007PA001468.

2103 Pancost, R.D., Baas, M., van Geel, B. et al. (2002) Biomarkers as proxies for plant
2104 inputs to peats: an example from a sub-boreal ombrotrophic bog. Organic
2105 Geochemistry 33(7), 675–690. https://doi.org/10.1016/S0146-6380(02)00048-7.

2106 Pancost, R.D., and Sinninghe Damsté, J.S., (2003) Carbon isotopic compositions of
2107 prokaryotic lipids as tracers of carbon cycling in diverse settings: Chemical
2108 Geology, v. 195, p. 29–58. https://doi.org/10.1016/S0009-2541(02)00387-X.

2109 Pancost, R.D., Baas, M., van Geel, B., et al. (2003) Response of an ombrotrophic bog
2110 to a regional climate event revealed by macrofossil, molecular and carbon
2111 isotopic data. The Holocene 13, 921–932.
2112 https://doi.org/10.1191/0959683603hl674rp

2113 Pancost, R.D., McClymont, E.L., Bingham, E.M., et al. (2011) Archaeol as a
2114 methanogen biomarker in ombrotrophic bogs. Organic Geochemistry 42, 1279–
2115 1287. https://doi.org/10.1016/j.orggeochem.2011.07.003

2116 Parkinson, C.L., (2019) A 40-y record reveals gradual Antarctic sea ice increases
2117 followed by decreases at rates far exceeding the rates seen in the Arctic. Proc.
2118 Natl. Acad. Sci. U.S.A. 116, 14414–14423.
2119 https://doi.org/10.1073/pnas.1906556116

2120 Past Interglacials Working Group of PAGES (2016) Interglacials of the last
2121 800,000 years. Rev. Geophys., 54, 162– 219.
2122 https://doi.org/10.1002/2015RG000482.

2123 Patalano, R., Roberts, P., Boivin, N., et al (2021) Plant wax biomarkers in human
2124 evolutionary studies. Evolutionary Anthropology,
2125 30: 385– 398. https://doi.org/10.1002/evan.21921

2126 Pearson, E.J., Juggins, S., Farrimond, P., (2008) Distribution and significance of long-
2127 chain alkenones as salinity and temperature indicators in Spanish saline lake
2128 sediments. Geochimica et Cosmochimica Acta 72, 4035–4046.
2129 https://doi.org/10.1016/j.gca.2008.05.052

2130 Pérez-Angel, L. C., Sepúlveda, J., Molnar, P., et al. (2020) Soil and air temperature
2131 calibrations using branched GDGTs for the Tropical Andes of Colombia: Toward
2132 a pan-tropical calibration. *Geochemistry, Geophysics, Geosystems*, 21,
2133 e2020GC008941. https://doi.org/10.1029/2020GC008941

2134 Peters, K.E., Walters, C.C., Moldowan, J.M., (2005) The biomarker guide, 2nd ed.
2135 Cambridge University Press, Cambridge, UK ; New York.
2136 https://doi.org/10.1017/S0016756806212056

2137 Peterse, F., van der Meer, J., Schouten, J., *et al.* (2012) Revised calibration of the
2138 MBT–CBT paleotemperature proxy based on branched tetraether membrane
2139 lipids in surface soils. *Geochimica et Cosmochimica Acta*, 96, 215–229.
2140 https://doi.org/10.1016/j.gca.2012.08.011.

2141 Peterse, F., Martínez-Garcia, A., Xhou, B., *et al.* (2014) Molecular records of
2142 continental air temperature and monsoon precipitation variability in East Asia
2143 spanning the past 130,000 years. *Quaternary Science Reviews*, 83, 76–82.
2144 https://doi.org/10.1016/j.quascirev.2013.11.001.

2145 Petrick, B.F., McClymont, E.L., Marret, F., et al. (2015) Changing surface water
2146 conditions for the last 500 ka in the Southeast Atlantic: Implications for variable
2147 influences of Agulhas leakage and Benguela upwelling: Last 500 ka in the

Southeast Atlantic. Paleoceanography 30, 1153–1167. https://doi.org/10.1002/2015PA002787

Petrick, B., McClymont, E.L., Littler, K., et al. (2018) Oceanographic and climatic evolution of the southeastern subtropical Atlantic over the last 3.5 Ma. Earth and Planetary Science Letters 492, 12–21. https://doi.org/10.1016/j.epsl.2018.03.054

Pitcher, A., Hopmans, E.C., Schouten, S., et al. (2009) Separation of core and intact polar archaeal tetraether lipids using silica columns: Insights into living and fossil biomass contributions, Organic Geochemistry 40(1), 12-19. https://doi.org/10.1016/j.orggeochem.2008.09.008.

Plancq, J., McColl, J.L., Bendle, J.A., et al. (2018) Genomic identification of the long-chain alkenone producer in freshwater Lake Toyoni, Japan: implications for temperature reconstructions. Organic Geochemistry 125, 189–195. https://doi.org/10.1016/j.orggeochem.2018.09.011

Post-Beittenmiller, D. (1996) Biochemistry and Molecular Biology of Wax Production in Plants. Annual Review of Plant Physiology and Plant Molecular Biology, 47(1), 405–430. https://doi.org/10.1146/annurev.arplant.47.1.405.

Powers, L.A., Johnson, T.C., Werne, J.P., et al. (2005) Large temperature variability in the southern African tropics since the Last Glacial Maximum. Geophys. Res. Lett. 32, L08706. https://doi.org/10.1029/2004GL022014

Powers L.A., Werne, J.P., Vanderwoude, A.J., et al. (2010) Applicability and calibration of the TEX86 paleothermometer in lakes. Organic Geochemistry, 41(4), 404-413. https://doi.org/10.1016/j.orggeochem.2009.11.009

Poynter, J.G., Farrimond, P., Robinson, N., et al. (1989) Aeolian-Derived Higher Plant Lipids in the Marine Sedimentary Record: Links with Palaeoclimate, in: Leinen, M., Sarnthein, M. (Eds.), Paleoclimatology and Paleometeorology: Modern and Past Patterns of Global Atmospheric Transport. Springer Netherlands, Dordrecht, 435–462. https://doi.org/10.1007/978-94-009-0995-3_18

Prahl, F.G. and Wakeham, S.G. (1987) Calibration of unsaturation patterns in long-chain ketone compositions for palaeotemperature assessment. Nature 330, 367–369. https://doi.org/10.1038/330367a0

Prost, K., Birk, J.J., Lehndorff, E., et al. (2017) Steroid Biomarkers Revisited – Improved Source Identification of Faecal Remains in Archaeological Soil Material. PLoS ONE 12, e0164882. https://doi.org/10.1371/journal.pone.0164882

Rach, O., Engels, S., Kahmen, A., et al. (2017) Hydrological and ecological changes in western Europe between 3200 and 2000 years BP derived from lipid biomarker δD values in lake Meerfelder Maar sediments. Quaternary Science Reviews 172, 44–54. https://doi.org/10.1016/j.quascirev.2017.07.019

Raja, M. and Rosell-Melé, A. (2021) Appraisal of sedimentary alkenones for the quantitative reconstruction of phytoplankton biomass. Proceedings of the National Academy of Sciences 118 (2) e2014787118. https://doi.org/10.1073/pnas.201478711

Ramdahl, T. (1983) Retene—a molecular marker of wood combustion in ambient air. *Nature*, 306(5943), 580–582. https://doi.org/10.1038/306580a0.

Rampen, S.W., Willmott, V., Kim, J.-H., et al. (2012) Long chain 1,13- and 1,15-diols as a potential proxy for palaeotemperature reconstruction. Geochimica et Cosmochimica Acta 84, 204–216. https://doi.org/10.1016/j.gca.2012.01.024

2194 Rampen, S.W., Datema, M., Rodrigo-Gámiz, M., *et al.* (2014) Sources and proxy
2195 potential of long chain alkyl diols in lacustrine environments. *Geochimica et*
2196 *Cosmochimica Acta*, 144, 59–71. https://doi.org/10.1016/j.gca.2014.08.033.

2197 Randlett, M.-È., Coolen, M.J.L., Stockhecke, M., et al. (2014) Alkenone distribution in
2198 Lake Van sediment over the last 270 ka: influence of temperature and haptophyte
2199 species composition. Quaternary Science Reviews 104, 53–62.
2200 https://doi.org/10.1016/j.quascirev.2014.07.009

2201 Reuss, N., Conley, D.J., Bianchi, T.S. (2005) Preservation conditions and the use of
2202 sediment pigments as a tool for recent ecological reconstruction in four Northern
2203 European estuaries. Marine Chemistry 95 (3–4), 283-302.
2204 https://doi.org/10.1016/j.marchem.2004.10.002.

2205 Riaux-Gobin, C., Tréguer, P., Poulin, M., et al. (2000) Nutrients, algal biomass and
2206 communities in land-fast ice and seawater off Adélie Land (Antarctica). Antarctic
2207 Science 12(2), 160-171. https://doi.org/10.1017/S0954102000000213

2208 Ribeiro, S., Limoges, A., Massé, G., et al. (2021) Vulnerability of the North Water
2209 ecosystem to climate change. Nat Commun 12, 4475.
2210 https://doi.org/10.1038/s41467-021-24742-0

2211 Richter, N., Russell, J.M., Garfinkel, J., et al. (2021) Winter–spring warming in the
2212 North Atlantic during the last 2000 years: evidence from southwest Iceland. Clim.
2213 Past 17, 1363–1383. https://doi.org/10.5194/cp-17-1363-2021

2214 Richter, H. and Howard, J.B. (2000) Formation of polycyclic aromatic hydrocarbons
2215 and their growth to soot—a review of chemical reaction pathways. *Progress in*
2216 *Energy and Combustion Science*, 26(4), 565–608.
2217 https://doi.org/10.1016/S0360-1285(00)00009-5.

2218 Rodrigo-Gámiz, M., García-Alix, A., Jiménez-Moreno, G., et al. (2022) Paleoclimate
2219 reconstruction of the last 36 kyr based on branched glycerol dialkyl glycerol
2220 tetraethers in the Padul palaeolake record (Sierra Nevada, southern Iberian
2221 Peninsula). Quaternary Science Reviews 281, 107434.
2222 https://doi.org/10.1016/j.quascirev.2022.107434

2223 Rohmer, M., Bisseret, P., Neunlist, S., (1992) The hopanoids, prokaryotic triterpenoids
2224 and precursors of ubiquitous molecular fossils. In: Moldowan, J.M., Albrecht, P.,
2225 Philp, R.P. (Eds.), Biological Markers in Sediments and Petroleum. Prentice Hall,
2226 London, pp. 1–17.

2227 Romero-Viana, L., Kienel, U., Sachse, D., (2012) Lipid biomarker signatures in a
2228 hypersaline lake on Isabel Island (Eastern Pacific) as a proxy for past rainfall
2229 anomaly (1942–2006 AD). Palaeogeography, Palaeoclimatology, Palaeoecology,
2230 350–352. 49-61. https://doi.org/10.1016/j.palaeo.2012.06.011.

2231 Ronkainen, T., McClymont, E.L., Väliranta, M., et al. (2013) The n-alkane and sterol
2232 composition of living fen plants as a potential tool for palaeoecological studies.
2233 Organic Geochemistry 59, 1–9. https://doi.org/10.1016/j.orggeochem.2013.03.005

2234 Ronkainen, T., Väliranta, M., Mcclymont, E., et al. (2015) A combined biogeochemical
2235 and palaeobotanical approach to study permafrost environments and past
2236 dynamics. J. Quaternary Sci. 30, 189–200. https://doi.org/10.1002/jqs.2763

2237 Rontani, J.-F., Smik, L., Belt, S.T., (2019) Autoxidation of the sea ice biomarker proxy
2238 IPSO25 in the near-surface oxic layers of Arctic and Antarctic sediments. Organic
2239 Geochemistry 129, 63–76. https://doi.org/10.1016/j.orggeochem.2019.02.002

2240 Rosell-Melé, A., (1998) Interhemispheric appraisal of the value of alkenone indices as
2241 temperature and salinity proxies in high-latitude locations. Paleoceanography 13,
2242 694–703. https://doi.org/10.1029/98PA02355

Rosell-Melé, A., Maslin, M.A., Maxwell, J.R., et al. (1997) Biomarker evidence for "Heinrich" events. Geochimica et Cosmochimica Acta 61, 1671–1678. https://doi.org/10.1016/S0016-7037(97)00046-X

Rosell-Melé, A. and McClymont, E.L. (2007) Chapter Eleven Biomarkers as Paleoceanographic Proxies, in C. Hillaire–Marcel and A. De Vernal (eds) *Developments in Marine Geology*. Elsevier (Proxies in Late Cenozoic Paleoceanography), 441–490. https://doi.org/10.1016/S1572-5480(07)01016-0.

Rosell-Melé, A., Balestra, B., Kornilova, O., et al. (2011) Alkenones and coccoliths in ice-rafted debris during the Last Glacial Maximum in the North Atlantic: implications for the use of $U^{K}_{37}{}'$ as a sea surface temperature proxy: J. Quaternary Sci. 26, 657–664. https://doi.org/10.1002/jqs.1488

Rousseau, L., Keraudren, B., Pèpe, C., et al. (1995) Sterols as biogeochemical markers in pliocene sediments and their potential application for the identification of marine facies. Quaternary Science Reviews 14, 605–608. https://doi.org/10.1016/0277-3791(95)00019-L

Ruan, Y., Mohtadi, M., Dupont, L. M.,et al. (2020) Interaction offire, vegetation, and climate in tropical ecosystems: Amultiproxy study over the past 22,000 years. Global Biogeochemical Cycles,34, e2020GB006677. https://doi.org/10.1029/2020GB006677

Rull, V., Sacristán-Soriano, O., Sànchez-Melsió, A., et al. (2022) Bacterial phylogenetic markers in lake sediments provide direct evidence for historical hemp retting, Quaternary Science Reviews, 295, 107803. https://doi.org/10.1016/j.quascirev.2022.107803.

Rush, D. Sinninghe, J.S., Damsté, S.W., *et al.* (2014) Anaerobic ammonium-oxidising bacteria: A biological source of the bacteriohopanetetrol stereoisomer in marine sediments. Geochimica et Cosmochimica Acta, 140, 50–64. https://doi.org/10.1016/j.gca.2014.05.014.

Russell, J.M., Hopmans, E.C., Loomis, S.E., *et al.* (2018) Distributions of 5- and 6-methyl branched glycerol dialkyl glycerol tetraethers (brGDGTs) in East African lake sediment: Effects of temperature, pH, and new lacustrine paleotemperature calibrations. Organic Geochemistry, 117, 56–69. https://doi.org/10.1016/j.orggeochem.2017.12.003.

Sachse, D., Radke, J., Gleixner, G., (2004) Hydrogen isotope ratios of recent lacustrine sedimentary n-alkanes record modern climate variability. Geochimica et Cosmochimica Acta 68, 4877–4889. https://doi.org/10.1016/j.gca.2004.06.004

Sachse, D., Radke, J., Gleixner, G., (2006) δD values of individual n-alkanes from terrestrial plants along a climatic gradient – Implications for the sedimentary biomarker record. Organic Geochemistry 37, 469–483. https://doi.org/10.1016/j.orggeochem.2005.12.003

Sachse, D. and Sachs, J.P., (2008) Inverse relationship between D/H fractionation in cyanobacterial lipids and salinity in Christmas Island saline ponds. Geochimica et cosmochimica acta 72, 793 806. https://doi.org/10.1016/j.gca.2007.11.022.

Sachse, D., Gleixner, G., Wilkes, H., et al. (2010) Leaf wax n-alkane δD values of field-grown barley reflect leaf water δD values at the time of leaf formation. Geochimica et Cosmochimica Acta 74, 6741–6750. https://doi.org/10.1016/j.gca.2010.08.033

Sachse, D., Billault, I., Bowen, G.J., et al. (2012) Molecular Paleohydrology: Interpreting the Hydrogen-Isotopic Composition of Lipid Biomarkers from

Photosynthesizing Organisms. Annu. Rev. Earth Planet. Sci. 40, 221–249. https://doi.org/10.1146/annurev-earth-042711-105535

Sadatzki, H., Maffezzoli, N., Dokken T.M., (2020) Rapid reductions and millennial-scale variability in Nordic Seas sea ice cover during abrupt glacial climate changes. Proceedings of the National Academy of Sciences 117 (47) 29478-29486. doi: 10.1073/pnas.2005849117

Saini, J., Günther, F,. Aichner, B., *et al.* (2017) Climate variability in the past ~19,000 yr in NE Tibetan Plateau inferred from biomarker and stable isotope records of Lake Donggi Cona. *Quaternary Science Reviews*, 157, 129–140. https://doi.org/10.1016/j.quascirev.2016.12.023.

Sánchez-Montes, M.L., Romero, O.E., Cowan, E.A., et al. (2022) Plio-Pleistocene Ocean Circulation Changes in the Gulf of Alaska and Its Impacts on the Carbon and Nitrogen Cycles and the Cordilleran Ice Sheet Development. Paleoceanog and Paleoclimatol 37. https://doi.org/10.1029/2021PA004341

Sánchez-Montes, M.L., McClymont, E.L., Lloyd, J.M., et al. (2020) Late Pliocene Cordilleran Ice Sheet development with warm northeast Pacific sea surface temperatures. Clim. Past 16, 299–313. https://doi.org/10.5194/cp-16-299-2020

Sarkar, S., Prasad, S., Wilkes, H., et al. (2015) Monsoon source shifts during the drying mid-Holocene: Biomarker isotope based evidence from the core 'monsoon zone' (CMZ) of India. Quaternary Science Reviews 123, 144–157. https://doi.org/10.1016/j.quascirev.2015.06.020

Sauer, P.E., Eglinton, T.I., Hayers, J.M., *et al.* (2001) Compound-specific D/H ratios of lipid biomarkers from sediments as a proxy for environmental and climatic conditions. *Geochimica et Cosmochimica Acta*, 65(2), 213–222. https://doi.org/10.1016/S0016-7037(00)00520-2.

Schefuß, E., Schouten, S., Jansen, J.H.F., et al. (2003) African vegetation controlled by tropical sea surface temperatures in the mid-Pleistocene period. Nature 422, 418–421. https://doi.org/10.1038/nature01500

Schefuß, E., Schouten, S. & Schneider, R., et al. (2005) Climatic controls on central African hydrology during the past 20,000 years. *Nature* **437**, 1003–1006. https://doi.org/10.1038/nature03945

Schmittner, A., Urban, N.M., Shakun, J.D., et al. (2011) Climate Sensitivity Estimated from Temperature Reconstructions of the Last Glacial Maximum. Science, 334(6061), 1385-1388. https://doi.org/10.1126/science.1203513

Schmidt, T., Kramell, A.E., Oehler, F., *et al.* (2020) Identification and quantification of cannabinol as a biomarker for local hemp retting in an ancient sedimentary record by HPTLC-ESI-MS. *Analytical and Bioanalytical Chemistry*, 412(11), 2633–2644. https://doi.org/10.1007/s00216-020-02492-0.

Schouten, S., Hopmans, E.C., Schefuß, E., et al. (2002) Distributional variations in marine crenarchaeotal membrane lipids: a new tool for reconstructing ancient sea water temperatures? Earth and Planetary Science Letters 204, 265–274. https://doi.org/10.1016/S0012-821X(02)00979-2

Schouten, S., Ossebaar, J., Schreiber, K., et al. (2006) The effect of temperature, salinity and growth rate on the stable hydrogen isotopic composition of long chain alkenones produced by *Emiliania huxleyi* and *Gephyrocapsa oceanica.* Biogeosciences 3, 113–119. https://doi.org/10.5194/bg-3-113-2006

Schouten S,. Hopmans EC,. Rosell-Melé A,. et al. (2013) An interlaboratory study of TEX_{86} and BIT analysis of sediments, extracts and standard

2339 mixtures. *Geochemistry, Geophysics, Geosystems*, 14(12), 5263-5285.
2340 https://doi.org/10.1002/2013GC004904

2341 Schreuder, L.T., Donders, T.H., Mets, A., et al. (2019a) Comparison of organic and
2342 palynological proxies for biomass burning and vegetation in a lacustrine sediment
2343 record (Lake Allom, Fraser Island, Australia). Organic Geochemistry 133, 10–19.
2344 https://doi.org/10.1016/j.orggeochem.2019.03.002.

2345 Schreuder, L.T., Hopmans, E.C., Castañeda, I.S., (2019b) Late Quaternary Biomass
2346 Burning in Northwest Africa and Interactions With Climate, Vegetation, and
2347 Humans. Paleoceanography and Paleoclimatology 34, 153–163.
2348 https://doi.org/10.1029/2018PA003467

2349 Schroeter, N., Lauterbach, S., Stebich, M., et al. (2020) Biomolecular Evidence of
2350 Early Human Occupation of a High-Altitude Site in Western Central Asia During
2351 the Holocene. Front. Earth Sci. 8, 20. https://doi.org/10.3389/feart.2020.00020

2352 Schüpbach, S., Kirchgeorg, T., Colombaroli, D., *et al.* (2015) Combining charcoal
2353 sediment and molecular markers to infer a Holocene fire history in the Maya
2354 Lowlands of Petén, Guatemala. *Quaternary Science Reviews*, 115, 123–131.
2355 https://doi.org/10.1016/j.quascirev.2015.03.004.

2356 Schwab, V.F. and Sachs, J.P. (2011) Hydrogen isotopes in individual alkenones from
2357 the Chesapeake Bay estuary. *Geochimica et Cosmochimica Acta*, 75(23),
2358 7552–7565. https://doi.org/10.1016/j.gca.2011.09.031.

2359 Schwark, L., Zink, K. and Lechterbeck, J. (2002) Reconstruction of postglacial to early
2360 Holocene vegetation history in terrestrial Central Europe via cuticular lipid
2361 biomarkers and pollen records from lake sediments. *Geology*, 30(5), 463–466.
2362 https://doi.org/10.1130/0091-7613(2002)030<0463:ROPTEH>2.0.CO;2.

2363 Sear, D.A., Allen, M.S., Hassall, J.D., et al. (2020) Human settlement of East
2364 Polynesia earlier, incremental, and coincident with prolonged South Pacific
2365 drought. Proc. Natl. Acad. Sci. U.S.A. 117, 8813–8819.
2366 https://doi.org/10.1073/pnas.1920975117

2367 Sefton, J., (2020) Evaluating mangrove proxies for quantitative relative sea-level
2368 reconstructions. PhD Thesis, Department of Geography, Durham University,
2369 Durham, U.K.

2370 Segato, D., Villoslada Hidalgo, M. D. C., Edwards, R., et al. (2021) Five thousand
2371 years of fire history in the high North Atlantic region: natural variability and
2372 ancient human forcing. Clim. Past, 17, 1533–1545. https://doi.org/10.5194/cp-17-
2373 1533-2021, 2021.

2374 Seki, O., Meyers, P.A,. Kawamura, K., *et al.* (2009) Hydrogen isotopic ratios of plant
2375 wax n-alkanes in a peat bog deposited in northeast China during the last 16kyr.
2376 *Organic Geochemistry*, 40(6), 671–677.
2377 https://doi.org/10.1016/j.orggeochem.2009.03.007.

2378 Sessions, A.L., Burgoyne, T.W., Schimmelmann, A., et al.(1999) Fractionation of
2379 hydrogen isotopes in lipid biosynthesis. Organic Geochemistry 30, 1193–1200.
2380 https://doi.org/10.1016/S0146-6380(99)00094-7.

2381 Sessions, A.L. (2016) Factors controlling the deuterium contents of sedimentary
2382 hydrocarbons. *Organic Geochemistry*, 96, 43–64.
2383 https://doi.org/10.1016/j.orggeochem.2016.02.012.

2384 Sharifi, A., Pourmand, A., Canuel, E.A., *et al.* (2015) Abrupt climate variability since
2385 the last deglaciation based on a high-resolution, multi-proxy peat record from
2386 NW Iran: The hand that rocked the Cradle of Civilization?. *Quaternary Science*
2387 *Reviews*, 123, 215–230. https://doi.org/10.1016/j.quascirev.2015.07.006.

Shillito, L.-M., Whelton, H.L., Blong, J.C., et al. (2020) Pre-Clovis occupation of the Americas identified by human fecal biomarkers in coprolites from Paisley Caves, Oregon. Sci. Adv. 6, eaba6404. https://doi.org/10.1126/sciadv.aba6404

Shintani, T., Yamamoto, M. and Chen, M.-T. (2011) Paleoenvironmental changes in the northern South China Sea over the past 28,000years: A study of TEX86-derived sea surface temperatures and terrestrial biomarkers. Journal of Asian Earth Sciences, 40(6), 1221–1229. https://doi.org/10.1016/j.jseaes.2010.09.013.

Simoneit, B.R.T., Schauer, J.J., Nolte, C.G., et al. (1999) Levoglucosan, a tracer for cellulose in biomass burning and atmospheric particles, Atmospheric Environment, Vol 33(2), 173-182. https://doi.org/10.1016/S1352-2310(98)00145-9.

Simpson, I.A., Bull, I.D., Dockrill, S.J., *et al.* (1998) Early Anthropogenic Soil Formation at Tofts Ness, Sanday, Orkney. Journal of Archaeological Science, 25(8), 729–746. https://doi.org/10.1006/jasc.1997.0216.

Simoneit, B.R.T. (2002) Biomass burning — a review of organic tracers for smoke from incomplete combustion. Applied Geochemistry, 17(3), 129–162. https://doi.org/10.1016/S0883-2927(01)00061-0.

Sinninghe Damsté, J.S., Hopmans, E.C., Pancost, R.D., *et al.* (2000) Newly discovered non-isoprenoid glycerol dialkyl glycerol tetraether lipids in sediments. Chemical Communications, 0(17), 1683–1684. https://doi.org/10.1039/B004517I.

Sinninghe Damsté, J.S., Schouten, S., van Duin, A.C.T., (2001) Isorenieratene derivatives in sediments: possible controls on their distribution. Geochimica et Cosmochimica Acta 65, 1557–1571. https://doi.org/10.1016/S0016-7037(01)00549-X

Sinninghe Damsté, J.S., Rijpstra, W.I.C., Coolen, M.J.L., et al. (2007) Rapid sulfurisation of highly branched isoprenoid (HBI) alkenes in sulfidic Holocene sediments from Ellis Fjord, Antarctica. Organic Geochemistry 38(1), 128-139. https://doi.org/10.1016/j.orggeochem.2006.08.003

Sinninghe Damsté, J.S., Verschuren, D., Ossebaar, J., et al. (2011) A 25,000-year record of climate-induced changes in lowland vegetation of eastern equatorial Africa revealed by the stable carbon-isotopic composition of fossil plant leaf waxes. Earth and Planetary Science Letters 302, 236–246. https://doi.org/10.1016/j.epsl.2010.12.025

Sinninghe Damsté, J.S., Ossebaar, J., Schouten, S., *et al.* (2012) Distribution of tetraether lipids in the 25-ka sedimentary record of Lake Challa: extracting reliable TEX86 and MBT/CBT palaeotemperatures from an equatorial African lake. Quaternary Science Reviews, 50, 43–54. https://doi.org/10.1016/j.quascirev.2012.07.001.

Sinninghe Damsté, J.S., Weber, Y., Zopfi, J., et al. (2022) Distributions and sources of isoprenoidal GDGTs in Lake Lugano and other central European (peri-)alpine lakes: Lessons for their use as paleotemperature proxies. Quaternary Science Reviews 277, 107352. https://doi.org/10.1016/j.quascirev.2021.107352.

Sistiaga, A., Mallol, C., Galván, B., *et al.* (2014) The Neanderthal Meal: A New Perspective Using Faecal Biomarkers. *PLOS ONE*, 9(6), e101045. https://doi.org/10.1371/journal.pone.0101045.

Smith, F.A. and Freeman, K.H. (2006) Influence of physiology and climate on δD of leaf wax n-alkanes from C3 and C4 grasses. Geochimica et Cosmochimica Acta, 70(5), 1172–1187. https://doi.org/10.1016/j.gca.2005.11.006.

Smith, J. A., Callard, L., Bentley, M. J., et al. (2023) Holocene history of 79° N ice shelf reconstructed from epishelf lake and uplifted glacimarine sediments, The Cryosphere 17(3), 1247-1270, https://doi.org/10.5194/tc-17-1247-2023.

Song, M., Zhou, A., He, Y., et al. (2016) Environmental controls on long-chain alkenone occurrence and compositional patterns in lacustrine sediments, northwestern China. Organic Geochemistry 91, 43-53. https://doi.org/10.1016/j.orggeochem.2015.10.009

Spencer-Jones, C.L., Wagner, T., Talbot, H.M., (2017) A record of aerobic methane oxidation in tropical Africa over the last 2.5 Ma. Geochimica et Cosmochimica Acta 218, 27–39. https://doi.org/10.1016/j.gca.2017.08.042

Spencer-Jones, C.L., McClymont, E.L., Bale, N.J., et al. (2021) Archaeal intact polar lipids in polar waters: a comparison between the Amundsen and Scotia seas. Biogeosciences 18, 3485–3504. https://doi.org/10.5194/bg-18-3485-2021

Stein, R., Hefter, J., Grützner, J., et al. (2009), Variability of surface water characteristics and Heinrich-like events in the Pleistocene midlatitude North Atlantic Ocean: Biomarker and XRD records from IODP Site U1313 (MIS 16–9), Paleoceanography, 24, PA2203, https://doi.org/10.1029/2008PA001639.

Stein, R., Fahl, K., Schade, I., et al. (2017) Holocene variability in sea ice cover, primary production, and Pacific-Water inflow and climate change in the Chukchi and East Siberian Seas (Arctic Ocean). J. Quaternary Sci. 32, 362–379. https://doi.org/10.1002/jqs.2929

Stockhecke, M., Bechtel, A., Peterse, F., *et al.* (2021) Temperature, precipitation, and vegetation changes in the Eastern Mediterranean over the last deglaciation and Dansgaard-Oeschger events. Palaeogeography, Palaeoclimatology, Palaeoecology, 577, 110535. https://doi.org/10.1016/j.palaeo.2021.110535.

Stogiannidis, E. and Laane, R. (2015) Source Characterization of Polycyclic Aromatic Hydrocarbons by Using Their Molecular Indices: An Overview of Possibilities, in D.M. Whitacre (ed.) Reviews of Environmental Contamination and Toxicology. Cham: Springer International Publishing (Reviews of Environmental Contamination and Toxicology), 49–133. https://doi.org/10.1007/978-3-319-10638-0_2.

Sun, S., Meyer, V., Dolman, A., et al. (2020) ^{14}C Blank Assessment in Small-Scale Compound-Specific Radiocarbon Analysis of Lipid Biomarkers and Lignin Phenols. Radiocarbon, 62(1), 207-218. https://doi.org/10.1017/RDC.2019.108

Szymczak-Żyła, M. and Kowalewska, G. (2009) Chloropigments a in sediments of the Gulf of Gdańsk deposited during the last 4000years as indicators of eutrophication and climate change. Palaeogeography, Palaeoclimatology, Palaeoecology 284, 283–294. https://doi.org/10.1016/j.palaeo.2009.10.007

Talbot, H.M., Watson, D.F., Pearson, E.J., et al. (2003) Diverse biohopanoid compositions of non-marine sediments. Organic Geochemistry 34, 1353–1371. https://doi.org/10.1016/S0146-6380(03)00159-1

Talbot, H.M. and Farrimond, P., (2007) Bacterial populations recorded in diverse sedimentary biohopanoid distributions. Organic Geochemistry 38, 1212–1225. https://doi.org/10.1016/j.orggeochem.2007.04.006

Talbot, H.M., Handley, L., Spencer-Jones, C.L., et al. (2014) Variability in aerobic methane oxidation over the past 1.2Myrs recorded in microbial biomarker signatures from Congo fan sediments. Geochimica et Cosmochimica Acta, 133, 387–401. https://doi.org/10.1016/j.gca.2014.02.035.

2484 Talbot, H.M., Bischoff, J., Inglis, G.N., et al. (2016a) Polyfunctionalised bio- and
2485 geohopanoids in the Eocene Cobham Lignite. Organic Geochemistry 96, 77–92.
2486 https://doi.org/10.1016/j.orggeochem.2016.03.006

2487 Talbot, H.M., McClymont, E.L., Inglis, G.N., et al. (2016b) Origin and preservation of
2488 bacteriohopanepolyol signatures in Sphagnum peat from Bissendorfer Moor
2489 (Germany). Organic Geochemistry 97, 95–110.
2490 https://doi.org/10.1016/j.orggeochem.2016.04.011

2491 Tamalavage, A.E., van Hengstum, P. J., Louchouarn, P., *et al.* (2020) Plant wax
2492 evidence for precipitation and vegetation change from a coastal sinkhole lake in
2493 the Bahamas spanning the last 3000 years. Organic Geochemistry, 150, p.
2494 104120. https://doi.org/10.1016/j.orggeochem.2020.104120.

2495 Tan, Z., Wu, C., Han, Y., et al. (2020) Fire history and human activity revealed through
2496 poly cyclic aromatic hydrocarbon (PAH) records at archaeological sites in the
2497 middle reaches of the Yellow River drainage basin, China. Palaeogeography,
2498 Palaeoclimatology, Palaeoecology, 560, 110015,
2499 https://doi.org/10.1016/j.palaeo.2020.110015.

2500 Tareq, S.M., Tanaka, N., Ohta, K,. (2011) Biomarker signature in tropical wetland:
2501 lignin phenol vegetation index (LPVI) and its implications for reconstructing the
2502 paleoenvironment. Science of the Total Environment, 324, 91-103.
2503 https://doi.org/10.1016/j.scitotenv.2003.10.020.

2504 Tesi, T., Belt, S.T., Gariboldi, K., et al. (2020) Resolving sea ice dynamics in the north-
2505 western Ross Sea during the last 2.6 ka: From seasonal to millennial timescales.
2506 Quaternary Science Reviews 237, 106299.
2507 https://doi.org/10.1016/j.quascirev.2020.106299

2508 Tesi, T., Muschitiello, F., Mollenhauer, G., et al. (2021) Rapid Atlantification along the
2509 Fram Strait at the beginning of the 20th century. Sci. Adv. 7, eabj2946.
2510 https://doi.org/10.1126/sciadv.abj2946

2511 Theroux, S., D'Andrea, W.J., Toney, J., et al. (2010) Phylogenetic diversity and
2512 evolutionary relatedness of alkenone-producing haptophyte algae in lakes:
2513 Implications for continental paleotemperature reconstructions. Earth and
2514 Planetary Science Letters, 300, 311–320.
2515 https://doi.org/10.1016/j.epsl.2010.10.009

2516 Theroux, S., Huang, Y., Toney, J.L., et al. (2020) Successional blooms of alkenone-
2517 producing haptophytes in Lake George, North Dakota: Implications for continental
2518 paleoclimate reconstructions. Limnol Oceanogr, 65, 413-425.
2519 https://doi.org/10.1002/lno.11311

2520 Thomas, C. L., Jansen, B., van Loon, E. E., et al. (2001) Transformation of n-alkanes
2521 from plant to soil: a review. SOIL, 7, 785–809. https://doi.org/10.5194/soil-7-785-
2522 2021.

2523 Tierney, J.E., Russell, J.M., Huang, Y., (2010) A molecular perspective on Late
2524 Quaternary climate and vegetation change in the Lake Tanganyika basin, East
2525 Africa. Quaternary Science Reviews 29, 787–800.
2526 https://doi.org/10.1016/j.quascirev.2009.11.030

2527 Tierney, J.E. and Tingley, M.P. (2014) A Bayesian, spatially-varying calibration model
2528 for the TEX86 proxy. Geochimica et Cosmochimica Acta 127, 83–106.
2529 https://doi.org/10.1016/j.gca.2013.11.026

2530 Tierney, J.E. and Tingley, M.P. (2018) BAYSPLINE: A New Calibration for the
2531 Alkenone Paleothermometer. Paleoceanography and Paleoclimatology 33, 281–
2532 301. https://doi.org/10.1002/2017PA003201

Tierney, J.E., Zhu, Z., King, Jo., et al. (2020) Glacial cooling and climate sensitivity revealed. Nature 584, 569-574. https://doi.org/10.1038/s41586-020-2617-x

Tierney, J.E., Poulsen, C.J., Montañez, I.P., et al. (2020) Past climates inform our future. Science 370, eaay3701. https://doi.org/10.1126/science.aay3701.

Toney, J.L., Huang, Y., Fritz, S.C., et al. (2010) Climatic and environmental controls on the occurrence and distributions of long chain alkenones in lakes of the interior United States. Geochimica et Cosmochimica Acta 74, 1563–1578. https://doi.org/10.1016/j.gca.2009.11.021

Trigui, Y., Wolf, D., Sahakyan, L., et al. (2019) First Calibration and Application of Leaf Wax *n*-Alkane Biomarkers in Loess-Paleosol Sequences and Modern Plants and Soils in Armenia. Geosciences, 9(6), 263. https://doi.org/10.3390/geosciences9060263

Turich, C., Freeman, K.H., (2011) Archaeal lipids record paleosalinity in hypersaline systems. Organic Geochemistry, 42 (9), 1147-1157. https://doi.org/10.1016/j.orggeochem.2011.06.002

Vachula, R.S., Russell, J.M., Huang, Y., et al. (2018) Assessing the spatial fidelity of sedimentary charcoal size fractions as fire history proxies with a high-resolution sediment record and historical data. Palaeogeography, Palaeoclimatology, Palaeoecology 508, 166–175. https://doi.org/10.1016/j.palaeo.2018.07.032

Vachula, R. S., Huang, Y., Longo, W. M., et al. (2019). Evidence of Ice Age humans in eastern Beringia suggests early migration to North America. Quaternary Science Reviews, 205, 35-44. https://doi.org/10.1016/j.quascirev.2018.12.003.

Vachula, R.S., Karp, A.T., Denis, E.H., et al. (2022) Spatially calibrating polycyclic aromatic hydrocarbons (PAHs) as proxies of area burned by vegetation fires: Insights from comparisons of historical data and sedimentary PAH fluxes. *Palaeogeography, Palaeoclimatology, Palaeoecology*, 596, 110995. https://doi.org/10.1016/j.palaeo.2022.110995.

van der Bilt, W.G.M., D'Andrea, W.J., Oppedal, L.T., et al. (2022) Stable Southern Hemisphere westerly winds throughout the Holocene until intensification in the last two millennia. Commun Earth Environ 3, 186. https://doi.org/10.1038/s43247-022-00512-8

van der Meer, M.T.J., Baas, M., Rijpstra, W.I.C., et al. (2007) Hydrogen isotopic compositions of long-chain alkenones record freshwater flooding of the Eastern Mediterranean at the onset of sapropel deposition. Earth and Planetary Science Letters 262, 594–600. https://doi.org/10.1016/j.epsl.2007.08.014

van der Meer, M.T.J., Sangiorgi, F., Baas, M., (2008) Molecular isotopic and dinoflagellate evidence for Late Holocene freshening of the Black Sea. Earth and Planetary Science Letters 267(3–4): 426–434. https://doi.org/10.1016/j.epsl.2007.12.001

van Geel, B., Aptroot, A., Baittinger, C., et al. (2008) The ecological implications of a Yakutian mammoth's last meal. Quaternary Research 69(3), 361-376. https://doi.org/10.1016/j.yqres.2008.02.004.

Versteegh, G.J.M., Schefuß, E., Dupont, L., et al. (2004) Taraxerol and Rhizophora pollen as proxies for tracking past mangrove ecosystems. Geochimica et Cosmochimica Acta 68, 411–422. https://doi.org/10.1016/S0016-7037(03)00456-3

Volkman, J.K. (1986) A review of sterol markers for marine and terrigenous organic matter. *Organic Geochemistry*, 9(2), 83–99. https://doi.org/10.1016/0146-6380(86)90089-6.

Vorrath, M.-E., Müller, J., Rebolledo, L., et al. (2020) Sea ice dynamics in the Bransfield Strait, Antarctic Peninsula, during the past 240 years: a multi-proxy intercomparison study. Clim. Past, 16, 2459–2483. https://doi.org/10.5194/cp-16-2459-2020.

Wakeham, S.G., Schaffner, C. and Giger, W. (1980) Polycyclic aromatic hydrocarbons in Recent lake sediments—I. Compounds having anthropogenic origins. *Geochimica et Cosmochimica Acta*, 44(3), 403–413. https://doi.org/10.1016/0016-7037(80)90040-X.

Wakeham, S.G., (1989) Reduction of stenols to stanols in particulate matter at oxic–anoxic boundaries in sea water. Nature 342, 787–790. https://doi.org/10.1038/342787a0

Wakeham, S.G., Hedges, J.I., Lee, C., et al. (1997) Compositions and transport of lipid biomarkers through the water column and surficial sediments of the equatorial Pacific Ocean. *Deep Sea Research Part II: Topical Studies in Oceanography*, 44(9), 2131–2162. https://doi.org/10.1016/S0967-0645(97)00035-0.

Wang, C., Bendle, J.A., Greene, S.E., et al. (2019a) Speleothem biomarker evidence for a negative terrestrial feedback on climate during Holocene warm periods. Earth and Planetary Science Letters 525, 115754. https://doi.org/10.1016/j.epsl.2019.115754

Wang, C., Bendle, J.A., Yang, H., et al. (2021) Global calibration of novel 3-hydroxy fatty acid based temperature and pH proxies. Geochimica et Cosmochimica Acta 302, 101–119. https://doi.org/10.1016/j.gca.2021.03.010

Wang, J., Wang, Y., Wang, X., et al. (2007) Penguins and vegetations on Ardley Island, Antarctica: evolution in the past 2,400 years. Polar Biol 30, 1475–1481. https://doi.org/10.1007/s00300-007-0308-9

Wang, J., Chen, L., Li, L. et al. (2014) Preliminary identification of palaeofloods with the alkane ratio C31/C17 and their potential link to global climate changes. Sci Rep 4, 6502. https://doi.org/10.1038/srep06502

Wang, K. J., Huang, Y., Majaneva, M., et al. (2021b) Group 2i Isochrysidales produce characteristic alkenones reflecting sea ice distribution. Nature Communications, 12(1), 15. https://doi.org/10.1038/s41467-020-20187-z

Wang, K.J., O'Donnell, J.A., Longo, W.M., et al. (2019b) Group I alkenones and Isochrysidales in the world's largest maar lakes and their potential paleoclimate applications. Organic Geochemistry 138, 103924. https://doi.org/10.1016/j.orggeochem.2019.103924

Wang, M., Zheng, Z., Man, M., *et al.* (2017) Branched GDGT-based paleotemperature reconstruction of the last 30,000years in humid monsoon region of Southeast China. *Chemical Geology*, 463, 94–102. https://doi.org/10.1016/j.chemgeo.2017.05.014.

Wang, M., Zong, Y., Zheng, Z., et al. (2018) Utility of brGDGTs as temperature and precipitation proxies in subtropical China. Scientific Reports. 8 (1), 194. https://doi.10.1038/s41598-017-17964-0.

Wang, Y.V., Larsen, T., Leduc, G., *et al.* (2013) What does leaf wax δD from a mixed C3/C4 vegetation region tell us?. *Geochimica et Cosmochimica Acta*, 111, 128–139. https://doi.org/10.1016/j.gca.2012.10.016.

Warnock, J.P., Bauersachs, T., Kotthoff, U., et al. (2018) Holocene environmental history of the Ångermanälven Estuary, northern Baltic Sea. Boreas 47, 593–608. https://doi.org/10.1111/bor.12281

Watson, B.I., Williams, J.W., Russell, J.M., et al. (2018) Temperature variations in the southern Great Lakes during the last deglaciation: Comparison between pollen and GDGT proxies. Quaternary Science Reviews 182, 78–92. https://doi.org/10.1016/j.quascirev.2017.12.011

Weckström, K., Massé, G., Collins, L.G., *et al.* (2013) Evaluation of the sea ice proxy IP25 against observational and diatom proxy data in the SW Labrador Sea. *Quaternary Science Reviews*, 79, 53–62. https://doi.org/10.1016/j.quascirev.2013.02.012.

Weijers, J.W.H., Schouten, S., van den Donker, J.H., *et al.* (2007) Environmental controls on bacterial tetraether membrane lipid distribution in soils. *Geochimica et Cosmochimica Acta*, 71(3), 703–713. https://doi.org/10.1016/j.gca.2006.10.003.

White, A.J., Stevens, L.R., Lorenzi, V., et al. (2018) An evaluation of fecal stanols as indicators of population change at Cahokia, Illinois. Journal of Archaeological Science 93, 129–134. https://doi.org/10.1016/j.jas.2018.03.009

White, A. J., Stevens, L.R, Lorenzi, V., et al. (2019) Fecal stanols show simultaneous flooding and seasonal precipitation change correlate with Cahokia's population decline. Proceedings of the National Academy of Sciences 116 (12) 5461-5466. https://doi.org/10.1073/pnas.1809400116.

White, D.M., Garland, D.S., Beyer, L., et al. (2004) Pyrolysis-GC/MS fingerprinting of environmental samples. Journal of Analytical and Applied Pyrolysis, 71(1), 107-118, DOI:10.1016/S0165-2370(03)00101-3.

Wolhowe, M. D., Prahl, F. G., Probert, I., et al (2009) Growth phase dependent hydrogen isotopic fractionation in alkenone-producing haptophytes, Biogeosciences, 6, 1681–1694. https://doi.org/10.5194/bg-6-1681-2009.

Xiao, X., Zhao, M., Knudsen, K.L., et al. (2017) Deglacial and Holocene sea–ice variability north of Iceland and response to ocean circulation changes. Earth and Planetary Science Letters 472, 14–24. https://doi.org/10.1016/j.epsl.2017.05.006

Xie, S., Nott, C.J., Avsejs, L.A., *et al.* (2000) Palaeoclimate records in compound-specific δD values of a lipid biomarker in ombrotrophic peat. *Organic Geochemistry*, 31(10), 1053–1057. https://doi.org/10.1016/S0146-6380(00)00116-9.

Xie, S., Yi, Y., Huang, J., et al. (2003) Lipid distribution in a subtropical southern China stalagmite as a record of soil ecosystem response to paleoclimate change. Quat. res. 60, 340–347. https://doi.org/10.1016/j.yqres.2003.07.010

Yamamoto, Y., Ajioka, T. and Yamamoto, M. (2016) Climate reconstruction based on GDGT-based proxies in a paleosol sequence in Japan: Postdepositional effect on the estimation of air temperature. Quaternary International, 397, pp. 380–391. https://doi.org/10.1016/j.quaint.2014.12.009.

Yamane, M., Yokoyama, Y., Miyairi, Y., et al. (2014) Compound-Specific ^{14}C Dating of IODP Expedition 318 Core U1357A Obtained Off the Wilkes Land Coast, Antarctica. Radiocarbon, 56(3), 1009-1017. https://doi.org/10.2458/56.17773.

Yang, H., Pagani, M., Briggs, D.E.G. *et al.* (2009) Carbon and hydrogen isotope fractionation under continuous light: implications for paleoenvironmental interpretations of the High Arctic during Paleogene warming. *Oecologia* **160**, 461–470. https://doi.org/10.1007/s00442-009-1321-1

Yang, H., Pancost, R.D., Dang, X., *et al.* (2014) Correlations between microbial tetraether lipids and environmental variables in Chinese soils: Optimizing the

paleo-reconstructions in semi-arid and arid regions. *Geochimica et Cosmochimica Acta*, 126, 49–69. https://doi.org/10.1016/j.gca.2013.10.041.

Yang, Y., Wang, C., Bendle, J.A et al. (2020) A new sea surface temperature proxy based on bacterial 3-hydroxy fatty acids. Organic Geochemistry 141, 103975. https://doi.org/10.1016/j.orggeochem.2020.103975

Yao, Y., Zhao, J., Vachula, R.S., *et al.* (2022) Phylogeny, alkenone profiles and ecology of Isochrysidales subclades in saline lakes: Implications for paleosalinity and paleotemperature reconstructions. Geochimica et Cosmochimica Acta, 317, 472–487. https://doi.org/10.1016/j.gca.2021.11.001.

Zennaro, P., Kehrwald, N., McConnell, J.R., et al. (2014) Fire in ice: two millennia of boreal forest fire history from the Greenland NEEM ice core. Clim. Past 10, 1905–1924. https://doi.org/10.5194/cp-10-1905-2014

Zhang, Z., Zhao, M., Eglinton, G., et al. (2006) Leaf wax lipids as paleovegetational and paleoenvironmental proxies for the Chinese Loess Plateau over the last 170kyr. Quaternary Science Reviews 25, 575–594. https://doi.org/10.1016/j.quascirev.2005.03.009

Zhang, Z., Sachs, J.P. and Marchetti, A. (2009) Hydrogen isotope fractionation in freshwater and marine algae: II. Temperature and nitrogen limited growth rate effects. Organic Geochemistry, 40(3), 428–439. https://doi.org/10.1016/j.orggeochem.2008.11.002.

Zhao, M., Mercer, J.L., Eglinton, G., et al. (2006) Comparative molecular biomarker assessment of phytoplankton paleoproductivity for the last 160kyr off Cap Blanc, NW Africa. Organic Geochemistry 37, 72–97. https://doi.org/10.1016/j.orggeochem.2005.08.022

Zheng, Y., Zhou, W., Meyers, P.A., et al (2007), Lipid biomarkers in the Zoigê-Hongyuan peat deposit: Indicators of Holocene climate changes in West China, Organic Geochemistry, 38(11), 1927-1940. https://doi.org/10.1016/j.orggeochem.2007.06.012

Zheng, Y., Singarayer, J.S., Cheng, P., et al. (2014) Holocene variations in peatland methane cycling associated with the Asian summer monsoon system. Nat Commun 5, 4631. https://doi.org/10.1038/ncomms5631

Zheng, Y., Pancost, R.D., Naafs, B.D.A., *et al.* (2018) Transition from a warm and dry to a cold and wet climate in NE China across the Holocene. Earth and Planetary Science Letters, 493, 36–46. https://doi.org/10.1016/j.epsl.2018.04.019.

Zheng, Y., Fang, Z., Fan, T., et al (2019) Operation of the boreal peatland methane cycle across the past 16 k.y.. Geology 48 (1): 82-86. https://doi.org/10.1130/G46709.1

Zhou, W., Zheng, Y., Meyers, P.A., et al. (2010) Postglacial climate-change record in biomarker lipid compositions of the Hani peat sequence, Northeastern China. Earth and Planetary Science Letters. 294 (1-2), 37-46. https://doi.org/10.1016/j.epsl.2010.02.035.

Zindorf, M., Rush, D., Jaeger, J., et al. (2020) Reconstructing oxygen deficiency in the glacial Gulf of Alaska: Combining biomarkers and trace metals as paleo-redox proxies. Chemical Geology, 558, 119864, 425. https://doi.org/10.1016/j.chemgeo.2020.119864, 2020.

Zocatelli, R., Lavrieux, M., Guillemot, T., et al. (2017) Fecal biomarker imprints as indicators of past human land uses: Source distinction and preservation potential in archaeological and natural archives. Journal of Archaeological Science 81, 79–89. https://doi.org/10.1016/j.jas.2017.03.010

Tables

Table 1. Biomarker proxies for aquatic temperatures. For the equations underpinning the listed indices please see the original publications.

Proxy	Source	Calibration	Uncertainty	Reference
Marine sea-surface temperatures (SSTs)				
$U^{K}_{37'}$	Ratio of long-chain (C_{37}) ketones (alkenones) synthesised by haptophyte algae	Linear core-top calibration, mean annual SST	Includes all three C_{37} alkenones but potential influence of salinity and/or sea ice over $C_{37:4}$	Brassell et al. (1986) Rosell-Mele (1998)
$U^{K}_{37'}$ index	Ratio of long-chain (C_{37}) ketones (alkenones) synthesised by haptophyte algae	Linear, non-linear and Bayesian calibrations, generally to mean annual SST (core-top) or growth temperature (cultures).	Core-top calibration uncertainty 1.5 °C (1σ; linear), 1.4 °C (1σ, <23.4 °C; BAYSPLINE), up to 4.4 °C (1σ, at 29.4 °C; BAYSPLINE). Non-linearity and seasonal bias at high latitudes in Bayesian calibrations.	Linear: Prahl and Wakeham (1987) Linear: Müller et al. (1998) Non-linear: Conte et al. (2006) Bayesian: Tierney and Tingley (2018)
$U^{K}_{38Me'}$ index	Ratio of long-chain (C_{38}) ketones (alkenones) synthesised by haptophyte algae	Linear core-top calibration, mean annual SST	Core-top calibration uncertainty 1.84 °C (including sea ice samples) or 1.30 °C (excluding sea ice samples).	Novak et al. (2022)
TEX_{86} index	Ratio of glycerol dialkyl glycerol tetraethers (GDGTs) synthesised by Thaumarchaeota	Linear, non-linear and Bayesian calibrations, to mean annual SST or to mixed layer temperatures (core-tops).	Potential integration of mixed-layer temperatures not just SST. Non-linear calibrations not recommended due to observed biases.	Linear: Schouten et al. (2002) Non-linear: Kim et al. (2010) Bayesian: Tierney and Tingley (2014), Inglis and Tierney (2020)
Long-chain diol index (LDI)	Ratio of 1,13- and 1,15-long-chain diols, synthesised by marine eustigmatophyte algae in cultures	Linear core-top	3°C (1σ) Not applicable to sediments where salinity <32 psu; some regional-specific non-thermal influences.	Rampen et al. (2012) De Bar et al. (2020)
RAN_{13}	Ratios of the isomers of 3-hydroxy C_{13} fatty acids synthesised by bacteria	Latitudinal transect core-top calibration (NW Pacific)	2.25°C (RMSE)	Yang et al. (2020)
Terrestrial temperature proxies				
$U^{K}_{37'}$ index	Ratio of long-chain (C_{37}) ketones (alkenones)	Multiple calibrations for lake surface water	e.g. Freshwater lakes: 1.3°C (Spring-summer Greenland and Europe).	Greenland lakes: D'Andrea et al. (2011)

	synthesised by haptophyte algae	temperatures, which may be calibrated to air temperatures depending on the location. Seasonal or mean annual.	e.g. Brackish lake cultures: 1.6°C (RMSE) different producers and temperature sensitivities.	Alaskan lakes: Longo et al. (2016) Brackish lakes: Theroux et al. (2020) Reviewed by Castañeda & Schouten (2011)
TEX_{86} index	Ratio of glycerol dialkyl glycerol tetraethers (GDGTs) synthesised by Thaumarchaeota	Multiple calibrations for lake surface water temperatures, which may be calibrated to air temperatures depending on the location. Seasonal or mean annual.	2.1-3.6 °C (RMSE) Mean annual air temperature Potential for production at depth in the lake, rather than a surface water temperature.	Powers et al. (2010) Tierney et al. (2010) Sinninghe Damste et al. (2022) Reviewed by Castañeda & Schouten (2011)
		Cave or surface air temperature	Connection between GDGT and surface air temperature, but some unknown influences occur. Relatively small calibration dataset. needed and recognition of in-cave variables such as location and cave micro-environment.	Blyth et al. (2016) Baker et al. (2019)
MBT and CBT ratios	MBT: ratio of branched GDGTs with varying numbers of methyl groups. CBT: ratio of branched GDGTs with varying numbers of cyclopentyl moieties. Synthesised by (acido)bacteria	MBT related to air temperature and precipitation. Strong impact of pH on CBT enables air temperature to be reconstructed by combining MBT and CBT.	Mean annual air temperature calibrations (RMSE ~5°C) but potential insensitivity <5°C and >20°C. Alternative calibrations needed in (semi) arid soils due to temperature influence on CBT (RMSE 1.83°C).	Weijers et al. (2007) Peterse et al. (2012) Yang et al. (2014)
MBT'_{5Me} index	Ratio of branched GDGTs including the 6-methyl isomers synthesised by (acido)bacterial (note that full range of source organisms remains unknown.	Global soil calibration, recovered from lakes, peats and speleothems	4.8°C (RMSE) in soils. Mean annual air temperature	De Jonge et al. (2014) Baker et al. (2019)
Long-chain diol index (LDI)	Ratio of 1,13- and 1,15-long-chain diols, synthesised by freshwater	Lake surface water temperatures.	Potential temperature influence, but seasonality in production and uncertainty around	Rampen et al. (2014) Lattaud et al. (2021)

	eustigmatophyte algae in cultures		producers limits application.	
RAN_{15} and RAN_{17}	Ratios of the isomers of 3-hydroxy C_{15} and C_{17} fatty acids synthesised by bacteria	Global soil calibration, recovered from lakes and speleothems.	3.5°C RMSE in lakes. Potential influence of pH.	Wang et al. (2021a)

Table 2 (next page) Examples of lipid ratios and compounds used to identify differences in vegetation source and environmental conditions.

Ratio or biomarker	Representation	Interpretation	E.g., Reference
Average chain length (ACL)	Weighted average indication of plant input (*n*-alkanes)	Higher values represent more higher plant inputs, which can be driven by warmer temperatures and/or drier conditions	Poynter et al., (1989) Schefuß et al. (2003) Zhou et al. (2010)
Carbon Preference Index (CPI)	*n*-alkanes with odd over even carbon atom preference, which reflects source material, maturity level and/or contamination.	Higher values can indicate reduced decomposition (e.g., fresher material, colder/drier conditions), lower values can also be driven by petroleum or microbial inputs	Bray and Evans (1961) Zhou et al. (2010)
P(aqueous): (C_{23}+C_{25})/ (C_{23}+C_{25}+C_{29}+C_{31}) *n*-alkanes	Hydrological-submerged vascular compared with terrestrial species	Higher values indicate relatively more submerged plant input and wetter conditions	Ficken et al. (2000)
P(wax): (C_{27}+C_{29}+C_{31})/ (C_{23}+C_{25}+C_{27}+ C_{29}+C_{31}) *n*-alkanes	Hydrological-emerged species compared with total vegetation	Higher values indicated more vascular plant inputs and drier conditions	Zheng et al. (2007)
C_{23}/C_{31} *n*-alkanes	Sphagnum vs higher plants	Higher values indicate relatively more Sphagnum input and wetter conditions	Bingham et al. (2010)
C_{23}/C_{29} *n*-alkanes (peatlands)	Sphagnum vs non-Sphagnum plants	Higher values indicate relatively more Sphagnum input and wetter conditions	Nichols et al. (2006)
C_{29}/C_{33} *n*-alkanes (palaeosols)	Deciduous trees vs grasses and herbs		Trigui et al. (2019)
C_{27}/C_{31} *n*-alkanes (stalagmites)	Grass:tree		Xie et al. (2003) Blyth et al. (2007)
5-*n*-alkylresorcinols	Presence of sedges		Avsejs et al. (2002) McClymont et al. (2008a)
4-isopropenylphenol (peatlands)	Analytical product of Sphagnum acid, specific to Sphagnum	Higher abundance reflects more Sphagnum	Boon et al. (1986) McClymont et al. (2011)
Sterols	Range of markers depending on vegetation type	E.g., lupeol, obtusifoliol, gramisterol from sedge roots in fens	Ronkainen et al. (2013)
Triterpenoids	Range of markers depending on vegetation type	E.g., taraxerol as an indicator of mangroves in tidal sediments or Ericaceae in peatlands, millacin as an indicator of millet	Versteegh et al. (2004) Jacob et al. (2008a,b) Pancost et al. (2002)

Ketones	Range of markers depending on vegetation type	E.g., Palmitone as an indicator of *Colocasia esculenta* (taro).	Krentscher et al. (2019)
Lignin phenols	Terrigenous inputs from vascular parts of plants.	Identify vegetation type and extent, disentangling non-woody woody angiosperms and gymnosperm vegetation. Cannot provide species-level identification. Requires combination with pollen or macrofossil analysis if species-level information needed.	Hedges et al. (1982) Orem et al. (1997) Tareq et al. (2011)
Polycyclic aromatic hydrocarbons (PAHs)	Incomplete combustion of organic matter	Proxy for vegetation burning. Some alkylated PAHs are also formed during thermal maturation and petrogenic processes, however, ratios have been applied to distinguish between (non)pyrogenic sources and identify vegetation type.	Ramdahl et al., 1983. Reviewed by Karp et al. (2020), including ratio details.
Levoglucosan and other monosaccharide anhydride (MA) compounds	Pyrolysis of carbohydrates such as from vegetation.	Wildfire intensity indicator. Ratios of MA indicate the vegetation type involved in the burn and burn conditions. Sometimes only detectable in low abundance. Can be challenging to disentangle local from regional fire histories.	Simoneit et al. (1999) Reviewed by Bhattarai et al., 2019

Table 3: Overview of the key proxies for palaeo-productivity and biogeochemical cycling and sediment transport.

Proxy	Source	Environmental signal	Considerations	E.g., References
Branched vs Isoprenoidal Tetraether (BIT) index from GDGTs	Archaea in soils (brGDGTs) and aquatic settings (isoGDGTs)	Indicator of soil inputs to aquatic systems	Some *in-situ* water column production of branched GDGTs has been identified, complicating interpretations	Hopmans et al. (2004) Bechtel et al. (2010) Fietz et al. (2012)
Terrestrial to aquatic ratio (TAR)	*N*-alkanes from higher plants (long chains) and algae (short chains)	Indicator of plant or soil inputs to aquatic systems	As well as plant inputs, soils and sedimentary rocks may also transport long-chain n-alkanes; multiple potential pathways.	Cranwell (1973) Müller et al., (2014) Sanchez-Montes et al. (2020)
Alkenones	Ketones (alkenones) synthesised by haptophyte algae.	Haptophyte algae productivity signal.	Recent suggestions that alkenone abundance may link directly to total primary productivity, sea ice ($\%C_{37:4}$), or salinity ($\%C_{37:4}$).	Petrick et al. (2018) Cartagena-Sierra et al. (2021) Raja Sanchez and Rosell-Mele (2021) Wang et al. (2021b)
Archaeol	Produced by Anaerobic archaea	Redox changes and methanogensis	Potential to record microbial activity onshore depending on source and transport pathway	Pancost et al. (2011)
Bacteriohopan epolyols (BHPs)	Membrane lipids produced by bacteria.	Microbial processes such as methanogenesis	Potential to record microbial activity onshore depending on source and transport pathway	Talbot et al. (2003) Talbot and Farrimond, (2007)
Chlorins	Algal productivity. Used extensively to reconstruct productivity in ocean sediments.	General phytoplankton productivity marker	Formed from degradation of chlorophyll to more stable tetrapyrrolic pigments. Sedimentary concentration reflects overall export to seafloor.	Harris and Maxwell (1995) Zhao et al. (2006)
Chlorophyll and carotenoid pigments	Mainly aquatic productivity, some inputs from terrestrial plant matter.	Algal production markers. Used to interpret productivity in combination with other markers.	Can be susceptible to degradation, though degradation products can also be productivity markers. Generally, better preserved in lakes than ocean sediments, unless	Leavitt (1993) Hodgson et al. (2003) McGowan (2013)

			near-shore or under anoxic conditions.	
Highly branched isoprenoids (HBIs)	Produced by selected diatoms, including some sea-ice associated species. Arctic: IP25 synthesised by *Haslea* spp. Southern Ocean: IPSO25 synthesised by the sea ice diatom *Berkeleya Adelensis*	General indicators of selected diatom productivity, and for spring sea ice with IP(SO)25.	Combination of IP(SO)25 and associated diatom HBIs or sterols can be used to distinguish between perennial sea ice (no HBIs) and open waters (no IP(SO25)): PIP25: IP25 / (IP25 + phytoplankton marker x c) PIPSO25: IPSO25 / (IP25 + phytoplankton marker x c)	Belt and Muller (2013) Belt et al. (2015, 2016). Vorrath et al. (2020)
isoGDGT-0	Methanogens are likely the dominant producers in peat	Microbial processes such as methanogenesis	Other potential source organisms may conflate the methanogensis signal.	Basiliko et al. (2003) Pancost and Sinninghe Damsté (2003)
Isorenieratene	Algae which can fix in low-light conditions at deep water depths.	Photic zone anoxia, green sulfur bacteria.	Needs suitable environment for preservation.	Sinninghe Damsté et al. (2001) Mallorquí et al. (2005)
Scytonemin	Protective carotenoid production by algae to avoid deleterious effects of harmful UVR.	Indicator of high UVR receipt. Environmental pressure for algae to protect cells during production.	Challenging to decouple UVR limitation from other limiting factors e.g. nutrient availability.	Hodgson et al. (2005)
Sterols (e.g. dinosterol, brassicasterol)	Produced by algae, but also present in some terrestrial material	Can be linked to groups of producers (e.g., dinosterol for dinoflagellates)	Can be degraded in the water column.	Fahl and Stein (1999) Nakakuni et al. (2017)
Compound-specific stable carbon isotopes $\delta^{13}C$ on individual *n*-alkanes, *n*-alkanols and *n*-alkanoic acids	Wide range of sources (Table 1).	Biomarker specific: changes in C_3 to C_4 vegetation; changing productivity or producers.	Can be challenging to interpret in isolation due to producer-specific influences.	(Huang et al. (2006) Tierney et al. (2010) McClymont et al. (2022)

Figures and figure captions

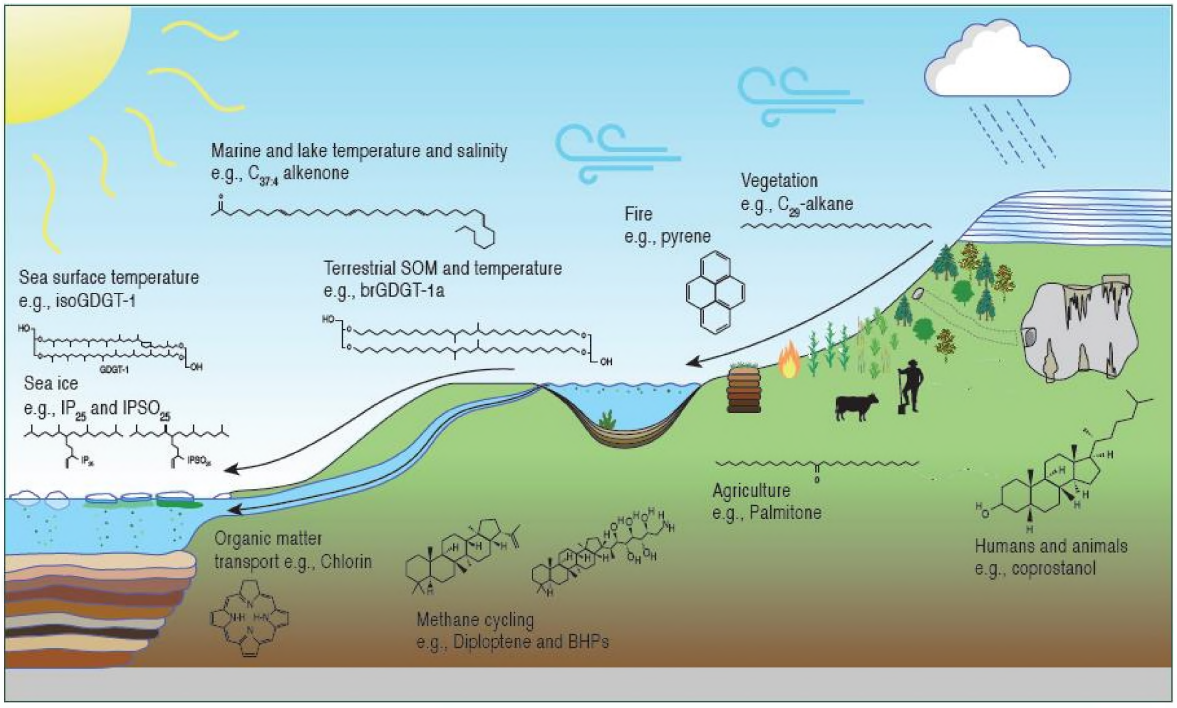

Figure 1. Using biomarkers to trace a wide range of environmental processes. Examples include biomarkers of climate change (e.g., temperature, precipitation, sea ice), ecosystem change (e.g., vegetation cover, productivity dynamics and fire regimes), biogeochemical cycling (e.g., methane production), sediment transport (e.g., soil residence time and land-ocean interactions), and human-environment interactions (e.g., presence of humans and animals and agricultural activity). Biomarkers can be transported between terrestrial ecosystems and to marine environments by rivers, surface water run-off, erosional processes, wind and melting ice. Abbreviations: IP_{25} (Ice Proxy with 25 carbon atoms), $IPSO_{25}$ (Ice Proxy Southern Ocean with 25 carbon atoms), isoGDGT (isoprenoidal glycerol dialkyl tetraether), brGDGT (branched glycerol dialkyl tetraether), BHPs (bacteriohopanepolyols).

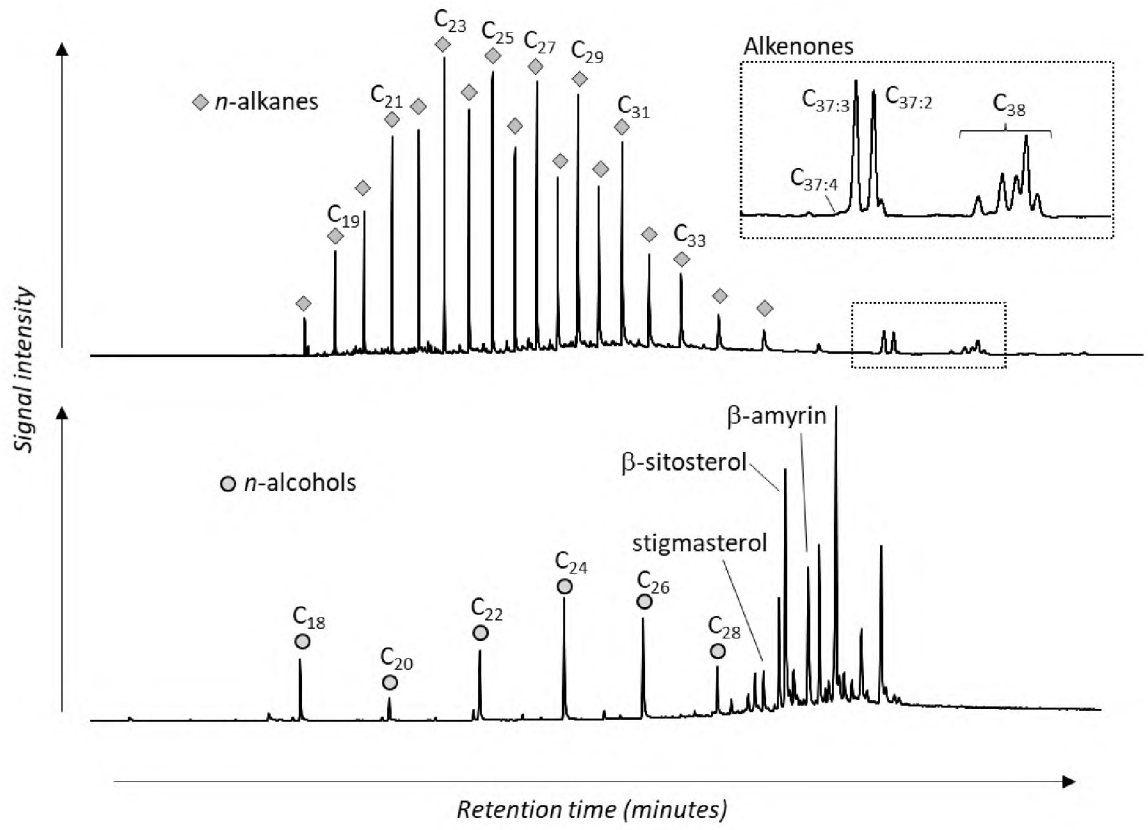

Figure 2: two examples of biomarker distributions containing mixtures of aquatic and vascular plants. Analysis is by chromatography, whereby individual compounds are separated according to their size and chemical structures. The sample is injected at time zero, and the size of the peak corresponds to the abundance of that molecule in the sample. (a) gas chromatogram of the apolar compounds recovered from a lake or marine sediment sample, showing a mixture of aquatic and vascular plant inputs; (b) gas chromatogram of the polar compounds recovered from a peatland sample, showing a mixture of vascular plant inputs.

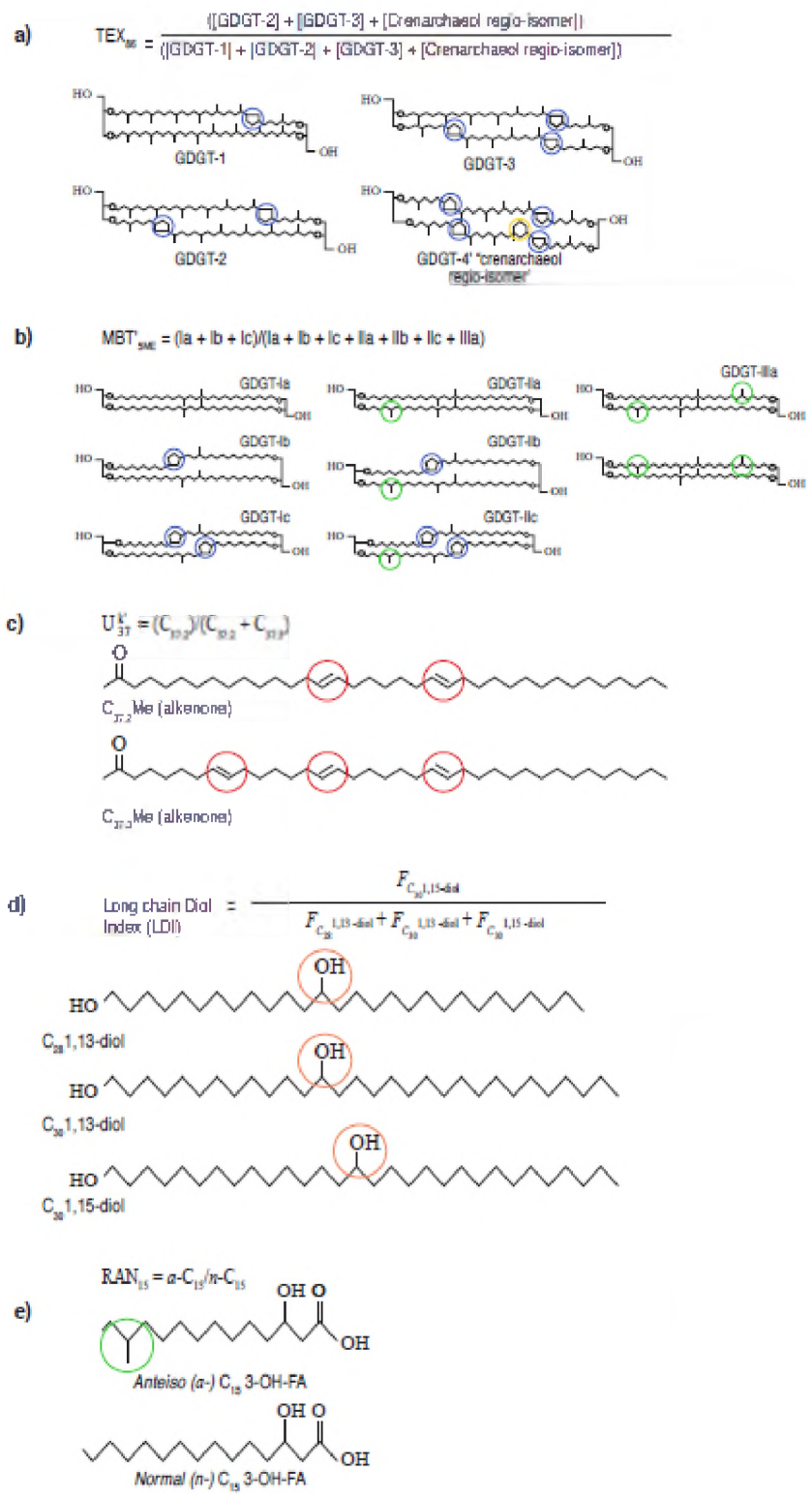

Figure 3: a selection of palaeotemperature biomarkers, detailing the different chemical properties that can be used to identify specific markers and their relationships to biological and environmental variables. (a) TEX_{86} (TetraEther indeX of tetraethers consisting of 86 carbon atoms) temperature proxy is calculated using the relative distributions of isoGDGTs (iso-GDGT-1, iso-GDGT-2 and iso-GDGT-3) and the crenarchaeol regioisomer (Schouten et al., 2002). Blue circles highlight the number of cyclopentane moieties, and the yellow circle

highlights the presence of a cyclohexane ring; (b) MBT'_{5Me} (Methylation of Branched Tetraethers using the 5-methyl isomers) temperature proxy in soils is calculated using relative distributions of 5-methyl brGDGT (de Jonge et al., 2014). Blue circles highlight the presence and number of cyclopentane moieties and green circles highlight the presence and number of methyl groups in the α and/or ω-5 position; (c) U^{K}_{37}' temperature proxy in freshwater and marine environments is calculated using relative distributions of the di- and tri- unsaturated alkenone distributions (Prahl and Wakeham, 1987). The chain lengths of the two alkenones are the same (C_{37} = 37 carbon atoms), but the number of double bonds increases from 2 to 3 (highlighted by red circles); (d) LDI (long chain diol index) temperature proxy in freshwater and marine environments is calculated using relative distributions of C_{28} and C_{30} 1,13- and C_{30} 1,15-alykl diol distributions (Rampen et al., 2012; 2014). Compounds vary in terms of chain lengths (C_{28} = 28 carbons atoms and C_{30} = 30 carbons atoms) and the location of the midchain alcohol group (C_{13} or C_{15}; highlighted by the orange circles); (e) RAN_{15} temperature proxy in soils is calculated using the ratio of anteiso to normal 3-hydroxy C_{15} fatty acid (Wang et al., 2021a). Green circle highlights the methyl-substituent located on the antepenultimate carbon atom.

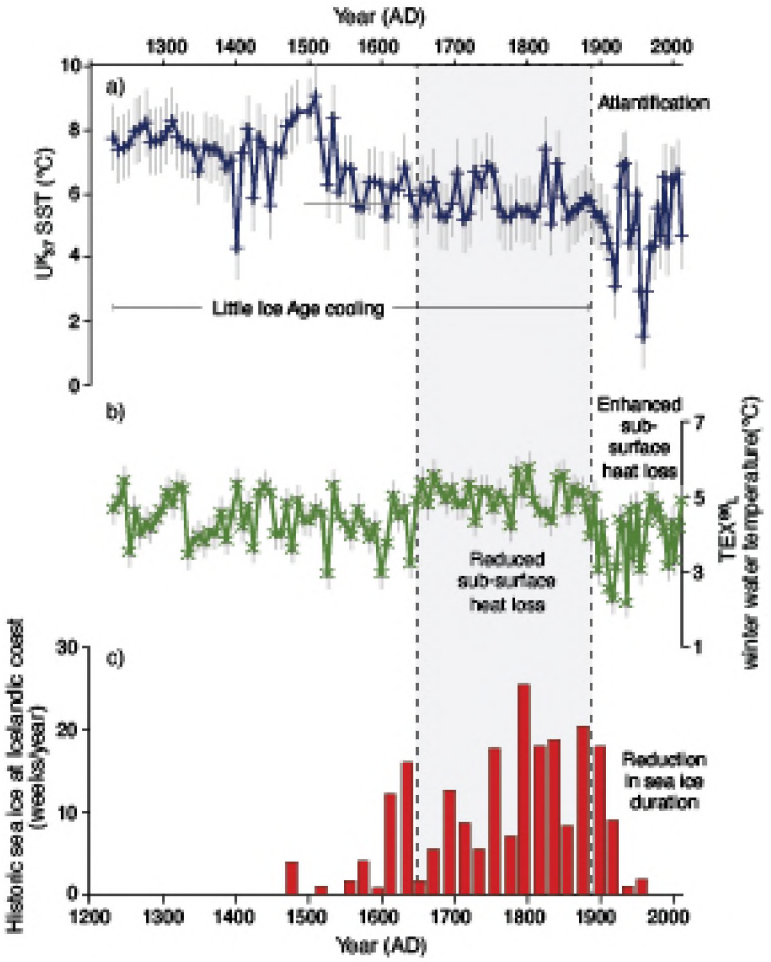

Figure 4: Biomarker insights into changes in late Holocene sea ice and expansion of Atlantic waters ("Atlantification") from reconstructed sea surface temperatures (SST) in the Fram Strait, the largest gateway to the Arctic Ocean (data from Tesi et al., 2021). Surface water and sub-surface water temperature reconstructions are reconstructed from the same sediment core using two different biomarker proxies (U^{K}_{37} and TEX_{86} respectively) and compared with historical records of sea ice persistence. a) U^{K}_{37}-derived SST (standard error is shown in grey vertical lines); b) TEX^{L}_{86}-derived water temperatures (standard error is shown in grey vertical lines); c) Historical records of sea ice presence at Icelandic coasts (weeks/year) (Lamb, 1977).

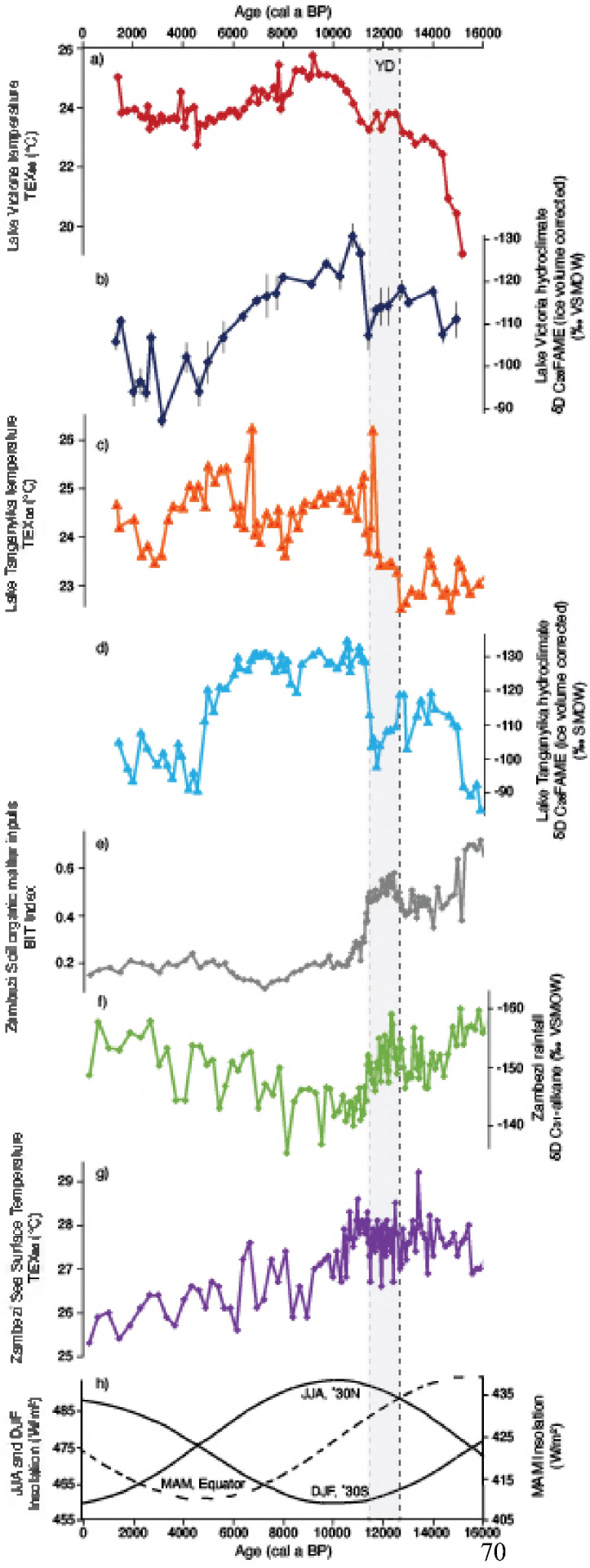

Figure 5: Terrestrial and marine biomarker reconstructions of environmental change in east Africa since the late Pleistocene. a-b) Palaeoclimate reconstructions from Lake Victoria (Berke et al., 2012) a) TEX_{86} palaeotemperatures and b) Palaeoprecipitation record from ice volume corrected δ^2H of the C_{28} leaf wax fatty acid methyl ester (FAME) with error bars (grey lines) representing the mean error of replicated analyses for each sample; C-d) palaeoclimate reconstructions from Lake Tanganyika (Tierney et al., 2008) c) TEX_{86} palaeotemperatures and d) Palaeoprecipitation record from ice volume corrected δ^2H of the C_{28} leaf wax FAME; e-h) Palaeoclimate reconstructions from a marine sediment core off the mouth of the Zambezi River (Schefuß et al., 2011), e) BIT (branched and isoprenoid tetraether) index representing soil organic matter inputs, f) Palaeprecipitation record from δ2H of C_{31} alkane, g) TEX_{86} sea surface temperatures and h) Insolation curves for June–July–August (JJA) and December–January–February (DJF) for Northern (30°N) and Southern (30°S) Hemisphere (solid lines) and March–April–May (MAM) insolation at the equator (dashed line).

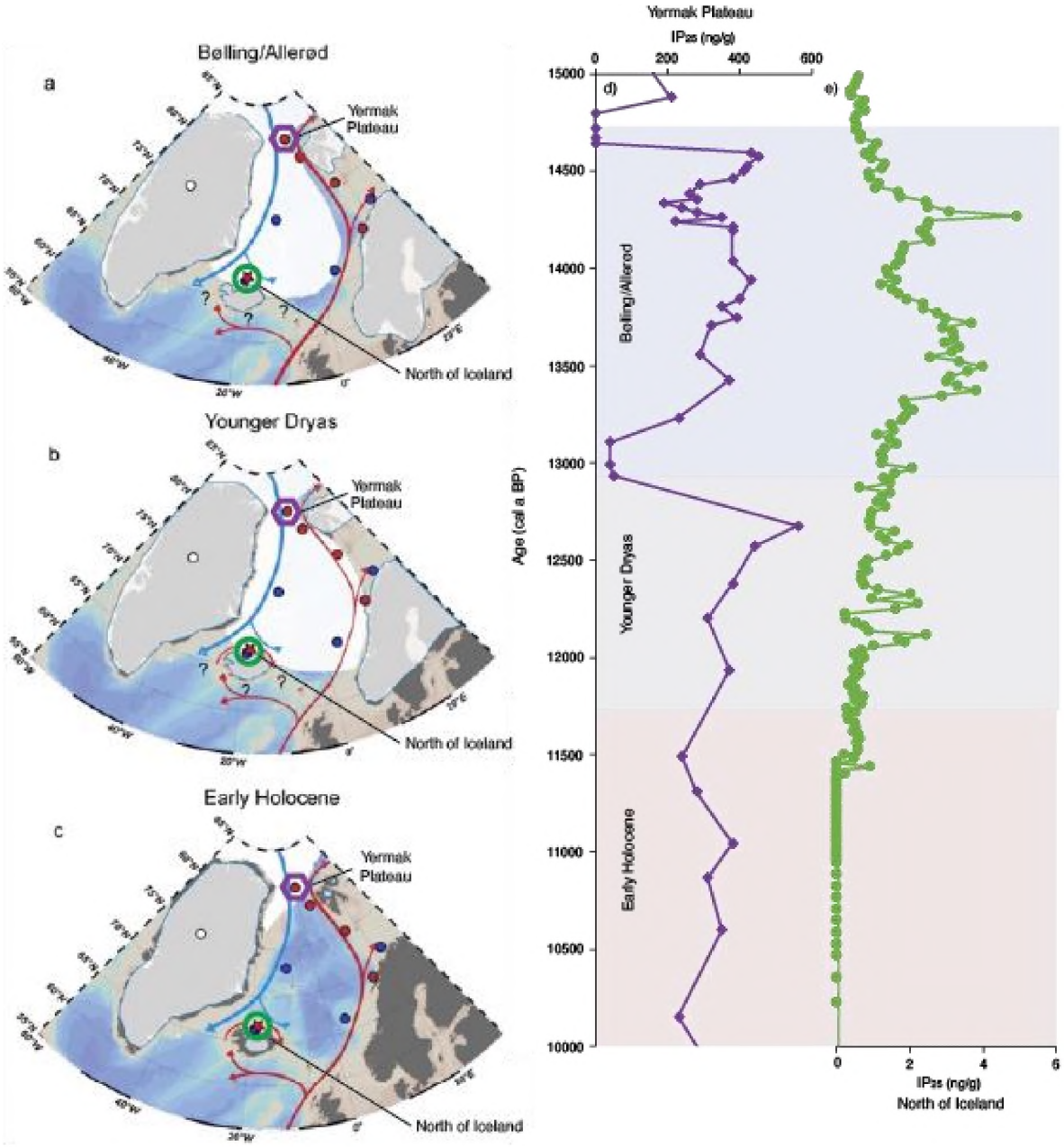

Figure 6. Schematic illustration of biomarker (IP_{25}) inferred changes in spring/summer sea ice extent (white shadings) between a) Bølling/Allerød; b) Younger Dryas and c) Early Holocene (adapted from Xiao et al., 2017, please refer to the original figure for the detailed map key). Atlantic Water advection is represented by red arrows and cold Polar waters from the Arctic Ocean are represented by blue arrows. d-e) Examples of the IP_{25} records used to develop the sea ice maps in a-c). d) Most northerly IP_{25} record of sea ice presence (Yermak Plateau, denoted in purple; Müller et al., 2009) and c) most southerly IP_{25} record of sea ice presence (North of Iceland, denoted in green; Xiao et al., 2017) included in the schematic maps.